THE CHEMILUMINESCENCES AND DEGRADATIONS OF β – LACTAM ANTIBIOTICS AFTER OXIDATION BY POTASSIUM SUPEROXIDE

By

JINGSHUN SUN

A DISSERTATION PRESENTED TO THE GRADUATE SCHOOL
OF THE UNIVERSITY OF FLORIDA IN PARTIAL FULFILLMENT
OF THE REQUIREMENTS FOR THE DEGREE OF
DOCTOR OF PHILOSOPHY

UNIVERSITY OF FLORIDA

1998

Copyright 1998

by

Jingshun Sun

This work is dedicated to my parents, and my wife, Shuang Yang.

ACKNOWLEDGMENTS

I wish to offer my sincere thanks and gratitude to the chairman of my committee, my mentor Dr. John H. Perrin, whose friendship, support and unending patience has made my graduate career a very enjoyable experience.

I thank all of the graduate students in Medicinal Chemistry department for their interest in my work, suggestions and friendship. Thanks go to Dr. James Winefordner, Dr. Ian Tebbett, and Dr. Ray Bergeron for their enthusiasm and consistent support of this project. Special thanks go to Dr. Kenneth Sloan and Dr. Stephen Schulman for their helpful advice and friendship over the last several years.

I would like to thank my family for their love and support especially my parents; they deserve much of the credit for making me the person I am today. Thanks to Jan Kallman and Nancy Rosa who helped to make Florida my home. I would also like to extend my thanks to all faculty, students and stuff at Chemistry department whose assistance is an indispensable part of this achievement. Lastly, I would like to offer my thanks to Shuang Yang for her love, patience and perseverance.

TABLE OF CONTENTS

page

ACKNOWLEDGMENTS iv

LIST OF TABLES viii

LIST OF FIGURES x

ABSTRACT xvii

CHAPTERS

1 INTRODUCTION 1
Reactive Oxygen Species 1
Singlet Oxygen 1
Superoxide Anion 4
Oxygen Toxicity and Diseases 6
Rheumatoid Arthritis 6
Pulmonary Emphysema 7
Ischemic-Reperfusion Tissue Injury 8
Carcinogenesis 8
Aging 9
Neurodegenerative Disorders 10
Chemotherapy 11
Removal of Free Radicals by Superoxide Dismutase and Vitamin E 11
Increasing Formation of Free Radicals 12
Chemiluminescence and β-Lactam Antibiotics 14
β-Lactam Antibiotics 14
Chemiluminescence 15

2 OBJECTIVES 32

3 CHEMILUMINESCENT METHODOLOGY OF STATIC MODE 36

Materials and Apparatus 36
Experimental Methods 37
Preparations of Stock Solutions 38
Preparation of Luminol Solution 38
Preparation of Hydrogen Peroxide Solution 39
Preparation of Saturated Potassium Superoxide Solution 39
Preparation of Phosphate Buffer Solutions 39

4 THE CHEMICAL PROPERTIES OF POTASSIUM SUPROXIDE 47
Comparison Studies 47
Solvent Selection for Potassium Superoxide 48

5 CHEMILUMINESCENCES AND β-LACTAM ANTIBIOTICS 54
Introduction 54
Probe of Maximum Emission Wavelength 55
Discussion 55

6 MECHANISTIC STUDIES 65
The Deuteration Experiment 65
NMR Consideration 69
NMR Spectra of Penicillin G 70
NMR Spectra of Penicillin V 72
Conclusion 74
TLC Analysis 74
Introduction 74
Experimental 75
Results and Discussions 76
HPLC Detection 78
Experimental 78
Results and Discussion 80
Conclusion 80
HPLC/ESI-MS and HPLC/APCI-MS Analysis of the Degradation of Penicillin G Following the Oxidation by Potassium Superoxide 81
Introduction 81
Experimental 84
Results and Discussion 85

7 SUMMARY 120

GLOSSARY 123

APPENDICES

A....124

B....142

C....173

D....186

E....194

REFERENCE 199

BIOGRAPHICAL SKETCH 207

LIST OF TABLES

Table page

Table 1-1: Some deleterious effects of systems generating the superoxide radical.....28

Table 1-2: Neurodegenerative disorders associated with free radicals.....29

Table 1-3: Family of β-lactam antibiotics. 30

Table 1-4: Analytical useful chemiluminescent emitters.....31

Table 3-1: Chemicals and reagents utilized in the static studies of chemiluminescence...41

Table 3-2: Chemical structures and sources of β-lactam antibiotics examined.....42

Table 3-2--continued.....43

Table 3-2—continued 44

Table 3-3: The composition of phosphate buffer solutions. 45

Table 6-1: Effects of deuterium oxide on the intensities of chemiluminescence of penicillin G.....92

Table 6-2: The responds of spraying the three reagents on sample $PGKO_2$ and sample KO_2.....92

Table 6-3: The running time of TLC developments. 92

Table 6-4: The retention times of the reference compounds and sample $PGKO_2$. 93

Table 6-5: The operating conditions of HPLC. 94

Table 6-6: The products of recombination including dimerization after penicillin G reacting with potassium superoxide.....95

Table 6-7: The major products of hydrolysis of penicillin G after interacting with potassium superoxide.....96

Table 6-8: The major products of oxidation of penicillin G after interacting with potassium superoxide.....97

Table 6-9: The six β-lactam antibiotics that emit no chemiluminescence.....98

Table 6-10: The seven β-lactam antibiotics that emit chemiluminescences. 99

LIST OF FIGURES

Figure page

Figure 1-1: Bonding in the diatomic oxygen molecule. 19

Figure 1-2: Potential energy curves for the three low-lying electronic states of molecule oxygen. 20

Figure 1-3: State correlation diagrams for the reactions of the three low-lying states of molecule oxygen with a diene to produce endoperoxide in triplet (T) and singlet (S) states. 21

Figure 1-4: Possible mechanism for formation of oxygen free radical during ischemic reperfusion. 22

Figure 1-5: Parent penicillin. 23

Figure 1-6: Parent cephalosporins. 24

Figure 1-7: Oral beta-lactam antibiotics. 25

Figure 1-8: Nonclassical β-lactam antibiotics. 26

Figure 1-9: Reaction scheme of luminol based chemiluminescence detection. 27

Figure 3-1: Schematic diagram of setup for chemiluminescent measurement in static mode. 46

Figure 4-1: The chemiluminescence of luminol following the oxidation by (a) H_2O_2 and (b) KO_2.. 51

Figure 4-2: The chemiluminescence of luminol reacting with KO_2 in CH_3OH. (a) at starting time, (b) two hours later, (c) three hours later. 52

Figure 4-3: The correlation between time and the chemiluminescent intensities of luminol after repeating the injections of 50 μl of 1:1 CH_3CN-CH_3OH solution containing o.1 M KO_2 into 2.5 ml of 10^{-9} M luminol every 15 minutes. 53

Figure 5-1: The comparison of chemiluminescent intensities of thirteen β-lactam antibiotics following the oxidation by KO_2. 58

Figure 5-2: The calibration curve of penicillin G. 59

Figure 5-3: The calibration curve of dicloxacillin. 60

Figure 5-4: The photocounting chemiluminescent spectrum (intensity vs. wavelength) of penicillin G reacting with superoxide....61

Figure 5-5: The photocounting chemiluminescent spectrum (intensity vs. wavelength) of luminol reacting with hydrogen peroxide....62

Figure 5-6: The typical chemiluminescent spectrum (intensity vs. time) of β-lactam antibioticals. 63

Figure 5-7: The chemiluminescent spectrum (intensity vs. time) of ampicillin. 64

Figure 6-1: The profile of chemiluminescences of penicillin G in different solutions with varied deuterium oxide to water ratios....100

Figure 6-2: ^{1}H-NMR spectrum of potassium penicillin G in D_2O. 101

Figure 6-3: ^{13}C-NMR spectrum of potassium penicillin G in D_2O. 102

Figure 6-4: APT spectrum of potassium penicillin G in D_2O. 103

Figure 6-5: ^{1}H-NMR spectrum of the degradation products of potassium penicillin G in D_2O after the oxidation by solid KO_2. 104

Figure 6-6: ^{13}C-NMR spectrum of the degradation products of potassium penicillin G in D_2O after the oxidation by solid KO_2. 105

Figure 6-7: ^{1}H-NMR spectrum of potassium penicillin V in D_2O. 106

Figure 6-8: ^{13}C-NMR spectrum of potassium penicillin V in D_2O. 107

Figure 6-9: APT spectrum of potassium penicillin V in D_2O. 108

Figure 6-10: ^{1}H-NMR spectrum of the degradation products of potassium penicillin V in D_2O after the oxidation by KO_2. 109

Figure 6-11: ^{13}C-NMR spectrum of the degradation products of potassium penicillin V in D_2O after the oxidation by KO_2. 110

Figure 6-12: The schematic diagrams of TLC assays on sample PG and sample $PGKO_2$. 111

Figure 6-13: the schematic diagrams of preparing the samples for mass spectroscopy by the TLC separations. 112

Figure 6-14: The FAB-mass spectrum of the sample from spot 13. 113

Figure 6-15: The chromatograms of sample PG (a) and sample $PGKO_2$ (b). The buffer system: pH5.66 phosphate buffer containing 0.1% acetonitrile....114

Figure 6-16: Schematic of major processes occurring in electrospray. 115

Figure 6-17: The total chromatograms of sample PG and sample $PGKO_2$. 116

Figure 6-18: The zoom-in chromatogram of the new oxidation products generated by sample $PGKO_2$....117

Figure 6-19: The scheme of generation of sulfoxides after penicillin G reacts with potassium superoxide....118

Figure 6-20: The proposed chemiluminescent mechanism of penicillin G after reacting with potassium superoxide....119

Figure A-1: The positive HPLC/ESI-MS/MS of benzylpenilloic acid....125

Figure A-2: The interpretation of the positive HPLC/ESI-MS/MS of benzylpenilloic acid. 126

Figure A-3: The negative HPLC/ESI-MS/MS of benzylpenilloic acid....127

Figure A-4: The interpretation of the negative HPLC/ESI-MS/MS of benzylpenilloic acid....128

Figure A-5: The positive HPLC/ESI-MS/MS of penicillin G and MS/MS of m/z 335. .129

Figure A-6: The negative of HPLC/ESI-MS/MS of penicillin G and MS/MS of m/z 333....130

Figure A-7: The interpretations of the positive and negative HPLC/ESI-MS/MS of penicillin G....131

Figure A-8: The positive HPLC/ESI-MS/MS of benzylpenillic acid. 132

Figure A-9: The interpretation of the positive HPLC/ESI-MS/MS of benzylpenillic acid. 133

Figure A-10: The positive HPLC/ESI-MS/MS of benzylpenicillenic acid. 134

Figure A-11: The interpretation of the positive HPLC/ESI-MS/MS of benzylpenicillenic acid 135

Figure A-12: The negative HPLC/ESI-MS/MS of benzylpenicillenic acid. 136

Figure A-13: The interpretation of the negative HPLC/ESI-MS/MS of benzylpenicillenic acid 137

Figure A-14: The positive HPLC/ESI-MS/MS of benzylpenicilloic acid. 138

Figure A-15: The interpretation of the positive HPLC/ESI-MS/MS of benzylpenicilloic acid. 139

Figure A-16: The negative HPLC/ESI-MS/MS of benzylpenicilloic acid. 140

Figure A-17: The interpretation of the negative HPLC/ESI-MS/MS of benzylpenicilloic acid. 141

Figure B-1: The positive HPLC/ESI-MS/MS of the sulfoxide of penicillamine dimer. 143

Figure B-2: The interpretation of the positive HPLC/ESI-MS/MS of the sulfoxide of penicillamine dimer. 144

Figure B-3: The negative HPLC/ESI-MS/MS of the sulfoxide of penicillamine dimer. 145

Figure B-4: The interpretation of the negative HPLC/ESI-MS/MS of the sulfoxide of penicillamine dimer. 146

Figure B-5: The positive HPLC/ESI-MS/MS of benzylpenilloic acid sulfoxide. 147

Figure B-6: The interpretation of the positive HPLC/ESI-MS/MS of benzylpenilloic acid sulfoxide. 148

Figure B-7: The negative HPLC/ESI-MS/MS of benzylpenilloic acid sulfoxide. 149

Figure B-8: The interpretation of the negative HPLC/ESI-MS/MS of benzylpenilloic acid sulfoxide. 150

Figure B-9: The positive HPLC/ESI-MS/MS of benzylpenillic acid sulfoxide. 151

Figure B-10: The interpretation of the positive HPLC/ESI-MS/MS of benzylpenillic acid sulfoxide. 152

Figure B-11: The negative HPLC/ESI-MS/MS of benzylpenillic acid sulfoxide. 153

Figure B-12: The interpretation of the negative HPLC/ESI-MS/MS of benzylpenillic acid sulfoxide. 154

Figure B-13: The positive HPLC/ESI-MS/MS of benzylpenicillenic acid sulfoxide.....155

Figure B-14: The interpretation of the positive HPLC/ESI-MS/MS of benzylpenicillenic acid sulfoxide.....156

Figure B-15: The negative HPLC/ESI-MS/MS of benzylpenicillenic acid sulfoxide.....157

Figure B-16: The interpretation of negative HPLC/ESI-MS/MS of benzylpenicillenic acid sulfoxide.....158

Figure B-17: The positive HPLC/ESI-MS/MS of penicillin G sulfoxide. 159

Figure B-18: The interpretation of the positive HPLC/ESI-MS/MS of penicillin G sulfoxide.....160

Figure B-19: The negative HPLC/ESI-MS/MS of penicillin G sulfoxide.....161

Figure B-20: The interpretation of the negative HPLC/ESI-MS/MS of penicillin G sulfoxide.....162

Figure B-21: The positive HPLC/ESI-MS/MS of compound 366a-penicillin G sulfone.....163

Figure B-22: The interpretation of the positive HPLC/ESI-MS/MS of compound 366a-penicillin G sulfone.....164

Figure B-23: The positive HPLC/ESI-MS/MS of compound 366b-isomer of penicillin G sulfone. 165

Figure B-24: The interpretation of the positive HPLC/ESI-MS/MS of compound 366b-isomer of penicillin G sulfone. 166

Figure B-25: The positive HPLC/ESI-MS/MS of compound 366c-isomer of penicillin G sulfone. 167

Figure B-26: The interpretation of the positive HPLC/ESI-MS/MS of compound 366c-isomer of penicillin G sulfone. 168

Figure B-27: The negative HPLC/ESI-MS/MS of compound 366c-isomer of penicillin G sulfone. 169

Figure B-28: The interpretation of the negative HPLC/ESI-MS/MS of compound 366c-isomer of penicillin G sulfone. 170

Figure B-29: The positive HPLC/ESI-MS/MS of benzylpenicilloic acid sulfoxide. 171

Figure B-30: The interpretation of the positive HPLC/ESI-MS/MS of benzylpenicilloic acid sulfoxide. 172

Figure C-1: The positive HPLC/ESI-MS/MS of penicillamine dimer. 174

Figure C-2: The interpretation of the positive HPLC/ESI-MS/MS of penicillamine dimer. 175

Figure C-3: The positive HPLC/ESI-MS/MS of compound 440. 176

Figure C-4: The interpretation of the positive HPLC/ESI-MS/MS of compound 440.... 177

Figure C-5: The positive HPLC/ESI-MS/MS of compound 632. 178

Figure C-6: The interpretation of the positive HPLC/ESI-MS/MS of compound 632.... 179

Figure C-7: The negative HPLC/ESI-MS/MS of compound 632. 180

Figure C-8: The interpretation of the negative HPLC/ESI-MS/MS of compound 632... 181

Figure C-9: The positive HPLC/ESI-MS/MS of compound 642. 182

Figure C-10: The interpretation of the positive HPLC/ESI-MS/MS of compound 642.....183

Figure C-11: The negative HPLC/ESI-MS/MS of compound 642.....184

Figure C-12: The interpretation of the negative HPLC/ESI-MS/MS of compound 642.....185

Figure D-1: The negative HPLC/APCI-MS of benzoic acid. 187

Figure D-2: The interpretation of the negative HPLC/APCI-MS of benzoic acid. 188

Figure D-3: The positive and negative HPLC/ESI-MS/MS of compound 336. 189

Figure D-4: The interpretation of the positive HPLC/ESI-MS/MS of compound 336....190

Figure D-5: The interpretation of the negative HPLC/ESI-MS/MS of compound 336...191

Figure D-6: The positive HPLC/ESI-MS/MS of compound 511. 192

Figure D-7: The interpretation of the positive HPLC/ESI-MS/MS of compound 511....193

Figure E-1: The negative HPLC/ESI-MS/MS of compound 269.....195

Figure E-2: The interpretation of the negative HPLC/ESI-MS/MS of compound 269....196

Figure E-3: The positive HPLC/ESI-MS/MS of compound 353.....197

Figure E-4: The interpretation of the positive HPLC/ESI-MS/MS of compound 353. ...198

Abstract of Dissertation Presented to the Graduate School
of the University of Florida in Partial Fulfillment of the
Requirements for the Degree of Doctor of Philosophy

THE CHEMILUMINESCENCES AND DEGRADATIONS OF β – LACTAM ANTIBIOTICS AFTER OXIDATION BY POTASSIUM SUPEROXIDE

By

Jingshun Sun

August 1998

Chairman: John H. Perrin, PhD
Major Department: Medicinal Chemistry

Penicillin G is investigated as a model to study how thirteen β - lactam antibiotics emit chemiluminescences with different intensities after oxidation with potassium superoxide. The degradation products of aqueous Penicillin G, which reacts with potassium superoxide, are analyzed via direct infusion by HPLC – electrospray ionization (ESI) and atmospheric pressure chemical ionization (APCI) mass spectrometry. A number of products derived from the hydrolysis, oxidation, polymerization and chemiluminescent reaction are identified, and reaction schemes are proposed.

A positive correlation is observed between the chemiluminescences and the autoxidations initiated by the singlet oxygen molecule-$O_2(^1\Delta g)$. Deuteration experiments

reveal that the intensity of the chemiluminescence from Penicillin G in deuterium oxide is approximately ten times as strong as that in neutral water. It is consistent with the longer lifetime of singlet oxygen molecule in deuterium oxide. The results presented here reinforce that singlet oxygen molecules play a crucial role in structural breakage of protein or DNA as well as in the specific disease entities.

CHAPTER 1
INTRODUCTION

Reactive Oxygen Species

A free radical can be defined, as any atom or molecule possessing one or more unpaired electrons. It can be anionic, cationic, or neutral. In biological and other related fields, the major free radical species of interest have been oxygen free radicals. The term oxygen free radicals includes the superoxide anion radical ($O_2^{\cdot-}$), the hydroperoxyl radical ($HO_2^{\cdot}$), the hydroxyl radical ($OH^{\cdot}$), and the peroxide radical ($ROO^{\cdot}$, R = Lipid). Actually these free radicals belong to a group of oxygen molecules called reactive oxygen species because they have stronger oxidizing ability than oxygen itself. Besides the oxygen free radicals these reactive oxygen species consist of hydrogen peroxide (H_2O_2), hypochlorous acid (HOCl), lipid peroxide (LOOH), and singlet oxygen ($^1O_2$).

Singlet Oxygen

When the configuration of the oxygen molecule orbital is described as $KK(2\sigma_g)^2(2\sigma_u)^2(3\sigma_g)^2(1\pi_u)^4(1\pi_g)^4$, the ground state oxygen itself is a biradical, as shown in Figure 1-1. This triplet oxygen has two unpaired electrons, each located in a different π^* antibonding orbital with the same spin quantum number. In accordance with Pauli's principle that a pair of electrons in an atomic of molecular orbital would have antiparallel

spins, this imposes a restriction on the oxidation by the ground state oxygens because the new electrons removed concomitantly from nonradical molecules must be of parallel spin so as to fit into the vacant spaces in the π^* orbitals. The transition metals found at the active site of oxidase and oxygenase enzymes have shown the capability of accepting or donating one electron at a time to increase the reactivity of ground state oxygen and to overcome the spin restriction. Another way of enhancing the reactivity of ground state oxygen is to change the spin direction of one of the two electrons in the π^* orbital. Two higher energy singlet states of oxygen molecule were found by Childe and Mecke [1] (the $^1\Sigma_g^+$ in 1931) and by Herzberg [2] (the $^1\Delta_g$ in 1934). These two forms of the oxygen molecule had an excess energy fraction of a chemical bond, 37.5 and 22.5 Kcal mol^{-1}, respectively, as shown in Figure 1-2.

Singlet $O_2(^1\Sigma_g^+)$ is readily relaxed to $O_2(^1\Delta_g)$ before it has time to react with anything. By definition, delta singlet oxygen is not a free radical. Like oxygen free radicals, however, if singlet oxygen is released in biologic systems, it is capable of rapidly oxidizing many molecules. In *vitro* chemical studies of singlet oxygen show singlet oxygen has the same damaging effects as does the superoxide anion toward various biological structures including nucleic acids, proteins, and lipids [3].

The two principle reactions characteristic of singlet oxygen are cycloaddition and the 'ene' reaction [reaction (1) and (2), respectively]:

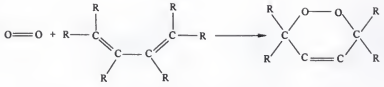

(1)

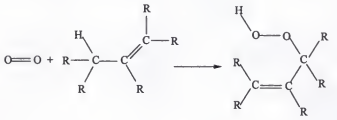

(2)

The formation of endoperoxides shown in reaction (1) requires a conjugated double bond. The formation of hydroperoxides as shown in reaction (2) requires an allylic hydrogen. When the double bonds are surrounded by electron-donating groups, the activation energy for both reactions can be reduced to nearly zero and the rate constant then approaches its maximum value of about 10^8 l mol^{-1} s^{-1} [4]. The formation of dioxetanes in singlet oxygen reactions appears to have a much higher activation energy and is observed chiefly when other pathways are blocked [5,6]. This is consistent with the predictions of the Woodward-Hoffman selection rules for concerted cycloaddition reactions [7]. Such orbital symmetry considerations and more quantitative calculations indicate that the $^1\Delta_g^+$ component is the only one which correlates directly with the ground-state products in reaction (1) [7]. These correlations are illustrated by the potential energy curves shown in Figure 1-3.

Superoxide Anion

Given a single electron the ground state oxygen molecule becomes a superoxide anion (Figure 1-1). It is formed in almost all aerobic cells [8,9,10]. Superoxide chemistry differs greatly regarding whether reactions are carried out in aqueous solution or in organic solvents. In nonpolar environments superoxide is a powerful base, nucleophile, and reducing agent [11,12]. Superoxide can also act as an oxidizing agent, but this ability is only seen with compounds that can donate protons. In aqueous solution, superoxide undergoes the so-called dismutation reaction to form hydrogen peroxide and oxygen. The overall reaction can be written as

$$2O_2^{\cdot} + 2H^+ \longrightarrow H_2O_2 + O_2 \qquad (3)$$

Under physiological conditions, even though uncatalyzed, this reaction can be very fast, i.e. $10^7\ M^{-1}\ S^{-1}$ [13]. The reactivity of superoxide is greatly reduced in water, and dismutation reaction being favored in this media.

The early superoxide theory of oxygen toxicity had been established on the accumulation of evidence showing that superoxide dismutation (SOD) enzymes, which remove superoxide by accelerating the dismutation reaction, are of great importance in allowing organisms to survive in the presence of oxygen and to tolerate the increased oxygen concentrations [8-10, 14, 15]. Since SOD enzymes are specific for superoxide as the substrate, it follows that superoxide must be a toxic species. Indeed, many damaging

effects summarizing in Table 1-1 are associated with superoxide generating systems [16]. However, the damage effects listed in Table 1-1 were produced by superoxide in aqueous solution, moreover, superoxide has proven to be relatively unreactive toward most biological components [17]. Therefore, it seems unlikely that superoxide alone can create such damage.

Historically, it is generally accepted that the superoxide anion radical is not a particularly reactive species but is potentially toxic. It can be transformed into the highly dangerous hydroxyl radical following the metal catalyzed Haber-Weiss reaction [8].

$$H_2O_2 + O_2^{\cdot-} \xrightarrow[\text{catalyst}]{\text{transition metal}} O_2 + OH^- + {}^{\cdot}OH \qquad (4)$$

The hydroxyl radical will react with a wide range of biological molecules in its vicinity.

Inspection of Table 1-1 shows that the metal-dependent Haber-Weiss reaction does not explain all, as there are several damage examples of prevented by SOD but not by catalase. In many other cases, for example the organism *Streptococcus Sanguis*, whose growth appears to be independent of the availability of iron [18] as it contains no heme compounds and lacks catalase and peroxidase, is damaged by exposure to a superoxide-generating system, but this damage is not prevented by scavengers of ·OH. Actually, there is no direct evidence of hydroxyl radical in any superoxide-hydrogen peroxide reacting enzymatic system, and the Haber-Weiss proposal is totally based on the inhibitory effects of SOD enzymes and that of hydroxyl radical scavengers. On the other hand the presence

of singlet oxygen molecule O_2 ($^1\Delta g$) generated in the Haber – Weiss reactions is proved by the characteristic 1268 – nm chemiluminescence emission spectrum of single molecule oxygen [19]. In view of the fact that singlet O_2 ($^1\Delta g$) has a sufficiently long lifetime to diffuse in cells and selectively damage some cell constituents, singlet O_2 ($^1\Delta g$) may be the prime oxidant.

Ironically, it is has been known since 1977 that singlet O_2 ($^1\Delta g$) can be produced either in the non – enzymatic dismutation reaction of superoxide or in the metal catalyzed Haber – Weiss reaction [20]. Singlet O_2 ($^1\Delta g$) has never drawn as much attention as the hydroxyl radical does due to its low concentration and the difficulty of detection.

Oxygen Toxicity and Diseases

Abnormal production of reactive oxygen species have been associated with a number of diseases including rheumatoid arthritis, pulmonary emphysema caused by cigarette smoking, ischemic – reperfusion tissue injury, carcinogenesis, aging, and neurodegeneration disorders such as Alzheimer's Disease, Parkinson's Disease, etc. Conclusive evidence suggests that all cellular components appear to be sensitive to the reactive oxygen species damage, lipids, proteins and nucleic acids being the most susceptible to this injury.

Rheumatoid Arthritis

Rheumatoid arthritis has many characteristics of a free-radical-produced disease. In rheumatoid arthritis, the synovium of the joins is swollen with an inflammatory

infiltrate, and the joint cartilage becomes eroded. Production of synovial fluid, which lubricates the joint, is increased, but its viscosity is decreased because of the breakdown of the polymer hyaluronic acid, which acts as a lubricant. This breakdown may be caused by oxygen free radicals produced by neutrophils that accumulate in large numbers in the affected joints of patients with rheumatoid arthritis [21]. Increased levels of the products of lipid peroxidation reactions are found both in the synovial fluid and in the plasma of patients with active rheumatoid arthritis [22], this indicates the involvement of hydroxyl radical although the exact cause is unknown.

Pulmonary Emphysema

The correlation between pulmonary emphysema and α_1-protease inhibitor deficiency has led to the hypothesis that the lung connective tissue damage is characteristically associated with smoking, and this lung tissue injury results from an impaired ability of protease inhibitors to protect lung elastin from damage caused by leukocyte protease. In human, α_1-protease inhibitor is the major serum antiprotease, and following bronchoalveolar lavage of normal persons, it is responsible for more than 90% of such antielastase activity [23]. Electron spin resonance spectroscopy has shown that cigarette smoke contains a variety of oxygen- and organic- based free radicals [24] and that these free radicals completely prevent α_1-protease inhibitor activity [25]. A recent interesting *in vitro* observation demonstrates that catalase and the antioxidants glutathione and ascorbic acid completely prevent the removal of elastase inhibitory capacity of α_1-protease inhibitor by cigarette smoke.

Ischemic-Reperfusion Tissue Injury

Ischemic-reperfusion tissue injury can occur in several tissues in addition to the heart [26, 27]-for example, the small intestine, gastric mucosa, kidney, liver, and skin. The enzyme xanthine oxidase is widely distributed among these tissues. The intestine, lung, and liver have particularly high levels. The intestinal mucosa is very sensitive to ischemic-reperfusion injury. One hour of regional intestinal ischemia produces a considerable increase in capillary permeability, an effect that is reduced by superoxide dismutase [28]. Biochemical changes during the ischemic period are thought to be the basis for a burst of production of free radicals on reintroduction of molecular oxygenation at reperfusion-Figure 1-4 [29]. As shown in Figure 1-4, during ischemia, adenosine triphosphate (ATP) is metabolized to the substrate hypoxanthine, and the enzyme xanthine dehydrogenase is converted to xanthine oxidase by a protease activated by increased free calcium. On reperfusion, hypoxanthine reacts with molecule oxygen in the presence of xanthine oxidase to form superoxide anion radicals. In the presence of iron salts, superoxide anion radicals can form hydroxyl radicals, which can bring about a number of damages.

Carcinogenesis

Carcinogenesis is thought to occur in two stages. In the initiation stage, a physical, chemical, or biological agent directly causes an irreversible alternation in the molecular structure of DNA of the cell. This alternation is followed by a promotion stage, in which the expression of the genes that regulate cell differentiation and growth is

altered. Oxygen free radicals play a role mostly in the promotion phase of carcinogenesis [30]. Hyperbaric oxygen, superoxide anion radical, and certain organic peroxides are tumor promoters but may also be weak complete carcinogens [31]. In contrast, many antioxidants are antipromoters and anticarcinogens [32]. However, the literature is not extensive enough to fully describe how the molecular structure of DNA is broken down by oxygen free radicals or other unknown oxygen species. Further investigations are needed.

Aging

The universality of aging implies that its cause is basically the same in all species. A free radical hypothesis of aging has been proposed. It suggests that the free radical produced during normal metabolism of the cell over time damages DNA and other macromolecules and leads to degenerative diseases, malignant lesions, and eventual death of the animal [33, 34]. Oxidative DNA damage is rapidly and effectively repaired. The human body is continually repairing oxidized DNA. An estimated several thousand oxidative DNA damage sites are present in the human cell every day, most of which are repaired [35]. A small fraction of unrepaired lesions could cause permanent changes in DNA and might be a major contributor to aging and cancer. The hypothesis that oxygen radicals play a role in aging is supported by the observation that, in general, long-lived species produce fewer endogenous free radicals because of their lower metabolic rate [36]. Long-lived animals also have more superoxide dismutase than do their short-lived counterparts, and animal species with the longest life-spans have the highest levels of

superoxide dismutase [37]. A consequence of the free radical hypothesis of aging is the concept that free radical scavenging agents might be used to prevent aging. Several antioxidants, including vitamin E [38] and butylated hydroxytoluene (BHT) [39] have been tested in animals and have yielded equivocal results. Interestingly, a study of a self-selected group of high dose vitamin E users who were 65 years or older showed an increased mortality associated with consumption of more than 1,000 IU of vitamin E a day [40]. The correlation between life expectancy, life-span, and dietary antioxidant intake in humans remains to be demonstrated.

Neurodegenerative Disorders

The central nervous system (CNS) is particularly vulnerable to free radical damage because of the following anatomical, physiological and biochemical reasons [41]:

1. Relative to its size, there is an increased rate of oxidative metabolic activity.
2. There are relatively low levels of antioxidants (e.g., glutathione) and protective enzyme activity (e.g., glutathione peroxidase, catalase, superoxide dismutase).
3. Abundant readily oxidizable membrane polyunsaturated fatty acids are present.
4. Endogeneous generation of reactive oxygen species via several specific neurochemical reactions are possible.
5. The CNS contains non-replacing neuronal cells, once damaged they may be dysfunctional for life.

6. The CNS neural network is readily disrupted.

The evidence for the role of free radicals in CNS disorders is generally indirect due to their extremely reactivity, as well as due to the general inaccessibility of the brain. *In vivo*, direct biochemical monitoring is impossible, however, numerous experiments still indicate the association between free radicals and several major CNS disorders as shown in Table 1-2.

Chemotherapy

The therapies based on modulation of the formation of free radicals include:

Removal of Free Radicals by Superoxide Dismutase and Vitamin E

Precedents have been made to the possible protection by superoxide dismutase against some kinds of free radical damage in animals. Orgotein, a bovine Cu-Zn superoxide dismutase, has been used as an anti-inflammatory protein drug in veterinary practice [60]. This agent is reported to have beneficial effects in treating rheumatoid arthritis, Duchenne's muscular dystrophy, and radiation-induced cystitis [61, 62, 63], but further double-blind placebo controlled studies are needed to confirm these findings [64]. Human recombinant superoxide dismutase has recently been produced, and trials are planned to evaluate its therapeutic efficacy in myocardial infraction, kidney transplantation, and bronchopulmonary dysplasia in premature infants [65].

Vitamin E had been shown by studies with isolated cells and animals to protect against damage caused by free radicals [66]. Under normal conditions, radical scavenging

by vitamin E is just one of many mechanisms involved in minimizing free radical-related tissue damage. Many of the numerous clinical studies involving large doses of vitamin E have not been adequately controlled, and the therapeutic benefits of vitamin E remain controversial [67].

Increasing Formation of Free Radicals

The main emphasis in treating human disease caused by free radicals is to decrease the formation of free radicals or limit their reaction at critical sites within the body. However, the formation of free radicals might be considered as a useful therapeutic strategy when the desired therapeutic effect is to damage or kill certain cells, but selectivity for the desired site is a priority. The various ions plus short-lived and reactive free radicals formed from the interaction of ionizing radiation and water have shown cell-killing effect [68]. Two major free radicals, hydroxyl radical and the aquated electron (e^-_{aq}), result from the radiolysis of water. The hydrated electron reacts by neucleophilic addition to produce radical anions, it further reacts with molecular oxygen to produce organic peroxide radicals:

$$R + e^-_{aq} \longrightarrow R^{\cdot} \qquad (5)$$

$$R^{\cdot} + O_2 \longrightarrow RO_2^{\cdot} \qquad (6)$$

A surprisingly large number of anticancer drugs in use today, almost half of those approved drugs in the United States, can form free radicals. This fact, considered together with the observation that tumor cells may be deficient in the same enzymes, i.e.

superoxide dismutase and catalase, that normally protect cells from free radical damage, has led to suggestions that free radicals might be involved in the antitumor activity of some of these drugs [69]. The best evidence of a free radical involvement in the cytotoxic effect of an anticancer drug is from the glycopeptide antibiotic bleomycin [70]. Bleomycin binds to DNA and in the presence of ferrous iron and oxygen cleaves DNA. A free radical species, possibly the hydroxyl radical is formed in near vicinity to the DNA and results in its degradation [71].

During the past three decades, the classic transition metal catalyzed Haber-Weiss reaction has met with almost universal acceptance and forms the foundation of this very active research field. Although the interpretation of evidence presented on this subject has been difficult because of the problems in identifying the free radicals, the toxicity of hydroxyl radicals generated by the Haber-Weiss reaction have been blamed for almost every disease caused by reactive oxygen species, and the chemotherapy is exclusively based on modulating the formation of free radicals. That the oxygen free radicals might be involved in human disease is not surprising in view of their existence in many biological systems, which have seemingly evolved elaborate protective mechanisms which normally effectively prevent damage by these radicals. In certain circumstances singlet oxygen has been shown to create similar damages to the hydroxyl radical. Few but strong evidences already support the argument that in some diseases it is singlet oxygen, not the hydroxyl radical which acts as a prime oxidant. This controversy needs to be

clarified in order to better understand the oxygen toxicity and to invent new therapeutic strategy as well as new antioxidants.

Chemiluminescence and β-Lactam Antibiotics

β-Lactam Antibiotics

The β-Lactam structure of penicillin was first proposed by Abraham and Chain in 1943, 14 years after Fleming made his first observations on the antibacterial action of penicillin on a plate seeded with *staphylococci*. It was opposed by those committed to an alternative thiazolidine-oxazolone structure, however, the β-lactam structure was finally established beyond doubt in 1945 when an X-ray crystallographic analysis by Dorothy Hodgkin and Barbara Low came to a successful conclusion[72]. Penicillin was pharmacologically ahead of its time. In the early 1940s, as penicillin research was just getting underway in earnest, the sulfa drugs were a revolutionary new concept in chemotherapy. The discovery of sulfa drugs, which would selectively react with bacteria, was a major innovation in chemotherapy [73]. By 1948 the outstanding value in medicine of benzylpenicillin had been firmly demonstrated, more and more scientists were encouraged to develop new β-lactam antibiotics. Chemical modifications of β-lactam ring and the introduction of specific side chains have led to a new series of compounds with characteristic biological activities. Due to endless efforts, a large family of β-lactam antibiotics is established and still grows rapidly. Representative structures of those drugs are shown in Table 1-3. Many β-lactam antibiotics can be classified into four classes

according to their clinical usefulness and pharmacokinetic properties [74]: (I) parental penicillins (Figure 1-5), (II) parental cephalosporins (Figure 1-6), (III) oral penicillins and cephalosporin (Figure 1-7), (IV) nonclassical β-lactam antibiotics (Figure 1-8). The analytical means for particular β-lactam antibiotics are different because of their diverse chemical, physical, and biological properties. In the case of the analysis of penicillin G, many methods are adopted [75] including titration, colorimetry and UV spectrophotometry, florescence, HPLC, thin layer chromatography, gas-liquid chromatography, electrophoresis, polarography, enzyme electrodes, isotopic assay, biological-based microbiological assay, immunoassay, and enzyme-aided assay (hydrolysis). In 1991, Schulman and Perrin revealed that cephalothin has the ability to prolong and intensify the chemiluminescence derived from the cobalt (II)-luminol-hydrogen peroxide system. It can be used as the basis for the determination of cephalothin in the range of 0.4-400 $\mu g\ ml^{-1}$[76]. Post column chemiluminescent detection after liquid chromatography has also been used to prevent mixing problems and so increase the reproductivity and sensitivity.

Chemiluminescence

Chemiluminescence can be defined as the emission of light as a result of the generation of electronically excited states formed in a chemical reaction. The range of wavelengths of light emitted is suprisingly large-from the near ultravilet to the infra-red. Chemiluminescence is "cold light." The energy is released in the form of light rather than

heat. It has wider variety of color than the bioluminescence of the firefly but is far less efficient. Analysis by chemiluminescence has simple instrumentation, has excellent sensitivity, has very low limits of detection, and has great selectivity and wide dynamic ranges. The efficiency of a luminescent reaction is defined as the number of photons emitted per reacting molecule. The quantum yield is usually written as:

$$\Phi_{CL} = \Phi_R \times \Phi_{ES} \times \Phi_F \quad (7)$$

where Φ_R is the yield of product, Φ_{ES} the number of molecules entering the excited state and Φ_F is the fluorescence quantum yield. High yields of excitation without strong visible emission are possible if Φ_F is very low, as is the case for simple dioxetanes. Phosphorescence is difficult to observe under the conditions of most of the reactions, but in principle Φ_{Phos} can replace Φ_F. Sensitized chemiluminescence results when transfer of energy takes place between chemilulminescent reactants and fluorescent acceptors. The efficiency of this energy transfer (ET) must be taken into account:

$$\Phi_{CL} = \Phi_R \times \Phi_{ES} \times \Phi_{ET} \times \Phi_{F'} \quad (8)$$

where $\Phi_{F'}$ is the fluorescence efficiency of the acceptor, and Φ_{ET} is the efficiency of energy transfer. Addition of fluorescent acceptors can enhance light emission in the case of dioxetanes. The analytically useful chemiluminescent emitters are listed in Table 1-4.

If a target analyte can be determined via HPLC chemiluminescence then it probably has one of three characteristics:

1. it either emits chemiluminescence when mixed with a specific reagent;
2. it catalyzes chemiluminescence between other reagents;
3. it is suppresses chemiluminescence between other reagents.

Since not many pharmaceuticals can give out chemiluminescence, most analysis of HPLC chemiluminescence are based on 2) and 3) reactions, in which luminol (5-amino-2, 3-dihydro-1,4-phthalazinedione), reacts with oxidants like hydrogen peroxide in the presence of a base and a metal catalyst to produce an excited state product (3-aminophthalate, 3-APA) which gives off light at approximately 425 nm. When a compound eluting from the LC column enhances or suppresses this background light, the amount of light increased or decreased will represent the amount of analyte. The reaction system is described in Figure 1-9. Recently Garcia Campana, Baeyens, and Zhao reviewed chemiluminescence detection in capillary electrophoresis [92]. The combination of capillary electrophoresis, which is versatile and robust, and chemiluminescence-based reactions, which are extremely sensitive, is promising for numerous applications in fields such as environmental analysis and medicine. However, it is still not used as a routine technique. Several problems need to be solved, for instance, chemiluminescence lacks selectivity, the emissions of chemiluminescences depend on environmental factors; and the optimization of the volume and geometry of the detection cell and connecting hardware.

In our experiments the investigation of the behavior of the reactive oxygen species has always been the priority. Eleven β–lactam antibiotics have been reacted with potassium superoxide and the oxidation as well as hydrolysis of penicillin G have been examined. The deuteration experiment using penicillin G reinforces the concept that singlet oxygen is generated by superoxide dismutation and that singlet oxygen play an important role in tissue injury and related diseases.

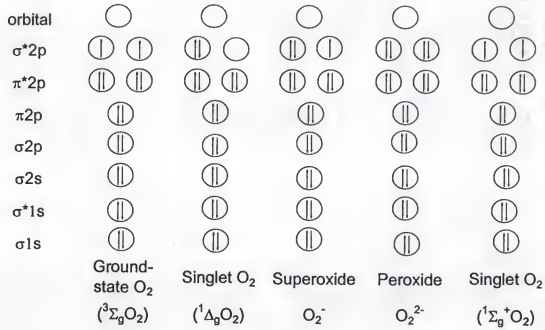

Figure 1-1: Bonding in the diatomic oxygen molecule.

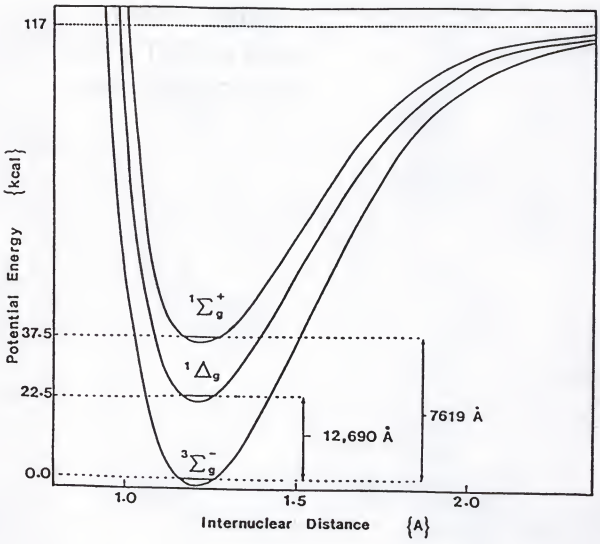

Figure 1-2: Potential energy curves for the three low-lying electronic states of molecular oxygen.

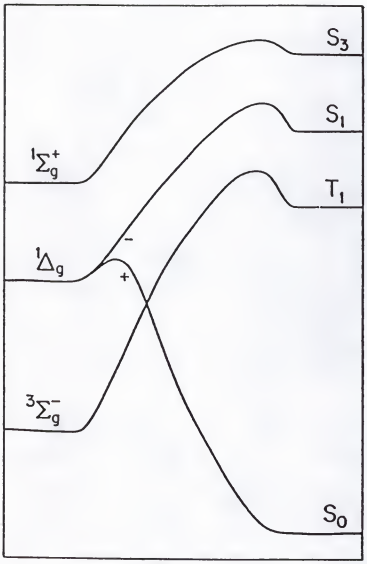

Figure 1-3: State correlation diagrams for the reactions of the three low-lying states of molecule oxygen with a diene to produce endoperoxide in triplet (T) and singlet (S) states.

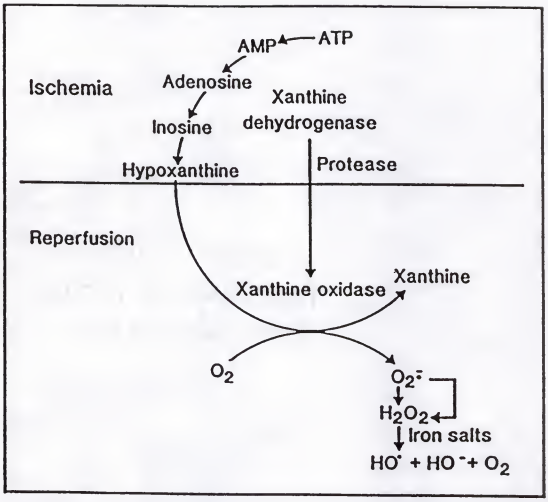

Figure 1-4: Possible mechanism for formation of oxygen free radical during ischemic reperfusion.

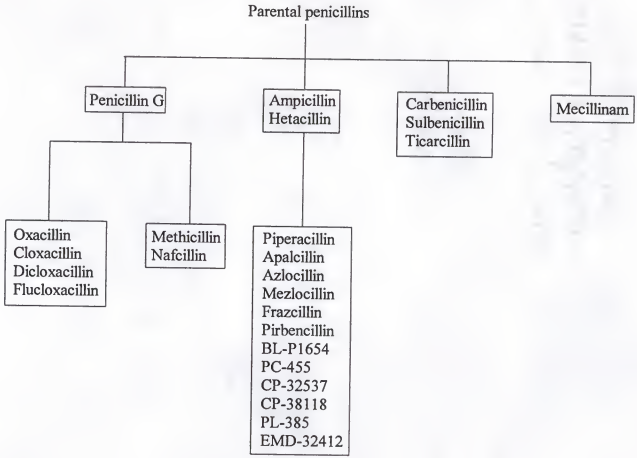

Figure 1-5: Parental penicillins.

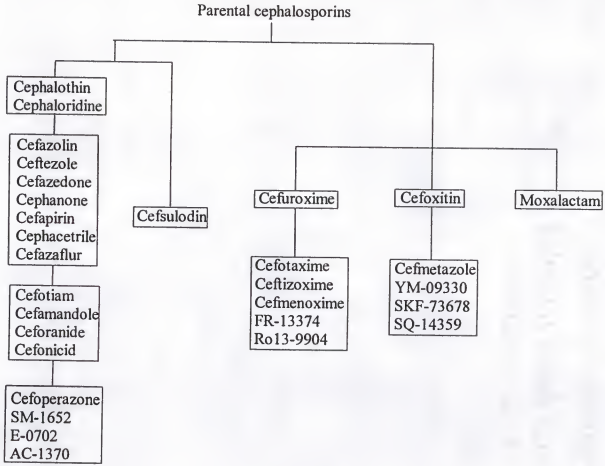

Figure 1-6: Parental cephalosporins.

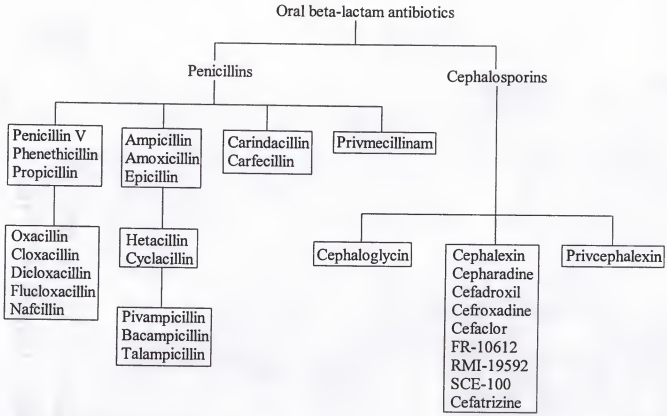

Figure 1-7: Oral beta-lactam antibiotics.

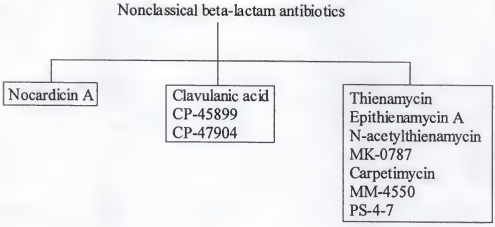

Figure 1-8: Nonclassical β-lactam antibiotics.

In Figure 5, 6, 7, 8 the compounds with similar structures are drawn in the same block.

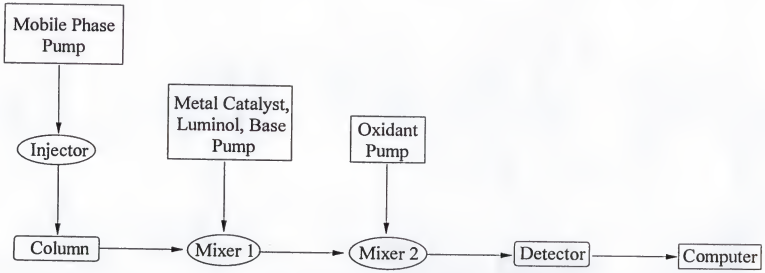

Figure 1-9: Reaction scheme of luminol based chemiluminescence detection.

Table 1-1: Some deleterious effects of systems generating the superoxide radical.

Source of Superoxide	System studied	Damage	Comements
Heart-muscle submitochondrial particles	Activity of NADH-CoQ reductase complex	Activity lost	Damage prevented by SOD. Catalase not protective.
Illuminated FMN	Bacteria	Loss of viability	Protection by SOD
Xanthine + xanthine oxidase	Huamn synovial fluid	Degradation; loss of viscosity	Both SOD and catalase protect
Xanthine + xanthine oxidase	Bateriophage R17	Inactivation	SOD protects partially
Illuminated FMN	Ribonuclease	Losss of activity	SOD protects partially
Illuminated FMN	Calf myoblast cells	Growth abnormality, some cell death.	SOD protects partially
Hypoxanthine-xanthine oxidase	Rat brain membrane (Na^+, K^+)-ATPase	Inactivation	SOD protects partially
Acetaldehyde + xanthine oxidase	Erythrocyte membranes	Lysis	SOD protects
Acetaldehyde + xanthine oxidase	Arachidonic acid	Oxidation	Both SOD and catalase protect
Hypoxanthine-xanthine oxidase	DNA	Degradation, single-strand breaks, attack on sugare moiety.	SOD, $^{\cdot}OH$ scavengers and catalase protect. Iron salts needed.
Autoxidation of dihydroxyfumarate	Rat thymocytes	Inhibition of Na+-dependent amino acid uptake	SOD protects, but not catalse.
Hypoxanthine-xanthine oxidase	Cheek pouch of living hamster (perfused with superoxide-generating system)	Increased permeability of blood vessels, leakage of contents.	SOD protects
Autoxidation of dialuric acid	*Escherichia coli*	Loss of viability	Both SOD and catalase protect
Acetaldehyde + xanthine oxidase	*Staphylococcus aureus*	Loss of viability	SOD, $^{\cdot}OH$ scavengers and catalase protect. Iron salts needed.
Xanthine + xanthine oxidase	Rat lung *in vivo* (instilled into lungs)	Acute lung injury, oedema	SOD protects but not catalase
Xanthine + xanthine oxidase	Rat heart ornithine decarboxylase	Inactivation	SOD protects, also mannitol ($^{\cdot}OH$ scavenger)
Xanthine + xanthine oxidase	Rat heart mitochondria	Lowered P/O ratios and Lower respiratory control	SOD and catalase protect
Xanthine + xanthine oxidase	Rat Heart or liver mitochondria	Inhibition of net Ca^{2+} uptake	SOD protects, also mannitol ($^{\cdot}OH$ scavenger)
Xanthine + xanthine oxidase	Dog heart sarcoplasmic reticulum	Decreased Ca^{2+} uptake	Some protection by SOD and mannitol

Table 1-2: Neurodegenerative disorders associated with free radicals.

Disorders (reference)	Syndrome	Causes	Observation	Comments
Amyotrophic lateral sclerosis (42, 43)	progressive paralysis, causing death within 5 years	degeneration of motor neurons	mutations in the gene encoding the form of CuZnSOD[a]	untreatable, pathogenesis unknown, typically affects adults in midlife
Alzheimer's disease (44, 45, 46, 47)	progressive memory loss, disorientation, striking mute, immobile dementia	cortical atrophy, neurofibrillary tangles, neuritic (senile) plaques, amyloid angiopathy, granulovacuolar degenaration, Hirano bodies	decreased antioxidant levels as well as glutathione synthetase activity, vitamin E inhibition, b amyloid fragments generate free radicals	affects over 2 million Americans, rarely occurs before the age of 50 years
Down's syndrome (48)	mental retardation, accelerated aging	an extra chromosome 21 (trisomy 21)	increased expression of SOD activity	high predisposition to develop Alzheimer's disease
Ischemia and reperfusion (49)	cognitive impairment, ischemic stoke	vascular dementia	increased lipid peroxidation	3% by age of 65 to 74, 50% over 85
Mitochondrial DNA disorders (50,51)	seizures, myoclonus, optic neuropathy, fatigueability, ataxia, vascular headache	mitochondrial DNA mutation	lack protection of histones, extensive oxidative phosphorylation	very diverse group of uncommen conditions
Multiple sclerosis (52,53)	impaired neuronal function	demyelination	increased serum lipid peroxide levels, protein degradation within myelin	affects about 250,000 Americans, twice as common in women as in men, no effective treatment
Parkinson's disease (54, 55, 56, 57, 58, 59)	stooped posture, slowness of voluntary movement, expressionless faces, tremor	dopamine depletion, neuronal loss in substantia nigra	increased lipid peroxidation, abnormal expression of antioxidant enzymes, increased iron content, increased dopamine turnover, induce of Parkinson's disease by toxins	prevalence for both black and white populations after 50 years old in North American, but varies greatly in different countries

[a]copper-zinc superoxide dismutase, which catalzes the conversion of superoxide.

Table 1-3: Family of β-lactam antibiotics.

	Structure
Parental Penicillin	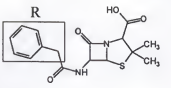 Penicillin G, R= 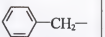
Parental Cepholosporin	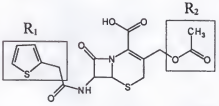 Cephalothin, R_1= 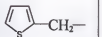 R_2= —$OCOCH_3$
Nonclassical	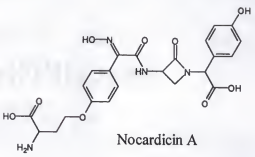 Nocardicin A 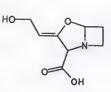 Clavulanic Acid 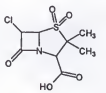 Sulfones 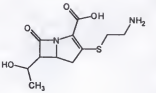 Thienamycin

Table 1-4: Analytical useful chemiluminescent emitters.

Chemiluminescent Emitters	λ_{max} (wavelength Region)	Reference
3-Aminophthalate (from Luminol)	425 nm	77
CH_3Se	750-825 nm	78
CN	383-388 nm	79
HCF	475-750 nm	80
HCHO	350-500 nm	81
HF	670-700 nm	80
HSO	360-380 nm	82
IF	450-800 nm	83
N-methylacridone (from lucigene)	420-500 nm	84
Na	589 nm	85
NO_2	1200 nm	86
OH	306 nm	82
Oxyluciferin (from luciferin)	562 nm	87
$Ru(bpy)_3$	600 nm	88
S_2	275-425 nm	89
SF_2	550-875 nm	90
SO_2	260-480 nm	91

CHAPTER 2
OBJECTIVES

Investigation of the chemiluminescence following the oxidation of β-lactam antibiotics by potassium superoxide will facilitate a better understanding of the involvement of $^1O_2$ in numerous human diseases caused by oxygen toxicity.

Recently more and more people began to realize that the generation of ·OH by transition metal-catalyzed Haber-Weiss reaction is not enough to account for all the damaging effects in the biological components. It is believed that the Haber-Weiss reaction does not occur in biological tissues under normal conditions, but its occurrence during pathological states, e.g. ischaemia, is possible. Even so the Haber-Weiss reaction faces the competition from the Fenton type reaction to produce ·OH. In the meantime, the existence of $^1O_2$ is indicated in the superoxide-generation systems. Mao [93] et al. utilized 2, 2, 6, 6-tetramethyl-4-piperdone as a spin trap of electron spin resonance (ESR) spectroscopy to study the generation of $^1O_2$. They observed the $^1O_2$ spin adduct signal in the incubation of xanthine, xanthine oxidase and H_2O_2, and the depletion of each of the incubation components led to a sharp decrease in $^1O_2$ generation. $^1O_2$ scavengers like sodium azide inhibited $^1O_2$ generation while the ·OH scavenger, ethanol, only slightly decrease the signal intensity. Catalase inhibited $^1O_2$ generation and H_2O_2 enhanced it.

They believe superoxide is capable of generating $^1O_2$ upon reaction with H_2O_2, i.e. the Haber-Weiss reaction. Interestingly they also found that the decomposition of KO_2 generated $^1O_2$, which is consistent with the experimental results obtained by Khan et al. in 1970 [94], 1976 [95], 1981 [96], and 1987 [97]. However, Nilsson and Kearns [98] in 1974 challenged this conclusion with a deuteration study. They adopted the same reacting system as did Khan and injected D_2O rather than H_2O into dry dimethyl sulfoxide (DMSO) containing KO_2, expecting increased intensity of chemiluminescence from the relaxation of $O_2(^1\Delta_g)$ to $^3O_2$ because of the large differences in lifetimes in the two solvents: 2 μsec in H_2O vs. 20 μsec in D_2O. However, no enhancement of chemiluminescent emission was observed, and no oxidation of the $^1O_2$-acceptor tetramethylene (TME) could be detected in this system. Their data suggested that the superoxide anion radical can not be a direct precursor of $^1O_2$. Since no later evidence has been presented, and the deuteration experiment is a very reliable approach to prove the existence of $^1O_2$, the Nilsson and Kearns' study still casts doubt over the possibility of the generation of $^1O_2$ from superoxide.

Indeed, despite a tremendous amount of work, this remains one of the most controversial, confusing, and frustrating areas of research, and the indirect detection of ·OH or other reactive oxygen species based on the scavenger's effects or on the spin trap's signals is one of the major reasons. This is because ·OH and $^1O_2$ are very reactive species, and thus are able to react with many compounds. Therefore, certain compounds can be spin traps for both of them, and some scavengers of ·OH may also be effective for

$^1O_2$. For example, histidine can eliminate $^1O_2$ in addition to the molecular ·OH radical [99].

In the current study based on some similar molecular structures, β-lactam antibiotics are used as models to study how the superoxide-generating system damages DNA molecular and protein structures. The following approaches are made to improve the understanding of oxygen toxicity.

1). Evaluate KO_2's capability as an oxidizer for chemiluminescence. The same amount of KO_2 and H_2O_2 will be used to react with luminol respectively, and under identical experimental conditions to check which gives the stronger chemiluminescence.

2). Study the chemical properties of KO_2 in the liquid phase. A solvent must be found to solubilize KO_2 and allow it to keep its activity as long as possible, because the biological nature of superoxide anion has to be mimicked and handling solid KO_2 is very dangerous.

3). Investigate whether KO_2 can oxidize β-lactam antibiotics with the resultant emissions of chemiluminescence. This will answer the question that how and why oxygen toxicity can damage cell components.

4). Design and carry out new D_2O experiments to clarify the historical controversy.

5). Study the mechanism of chemiluminescence of β-lactam antibiotics. A prediction of chemiluminescences from other compounds is desired.

6). Identify the degradation products and pathways to further confirm the chemiluminescent mechanism and oxygen toxicity.

7). Try to answer the question: which plays the major role in structural breakage of protein and DNA, hydroxyl radical or singlet oxygen?

CHAPTER 3
CHEMILUMINESCENT METHODOLOGY OF STATIC MODE

Materials and Apparatus

The chemiluminescent studies were conducted with a FL-750 Spectrofluorescence Detector (Mcpherson, Acton, MA) in the static mode. The data was collected either by a Servogor 120 flatbed recorder (Norma Goerz Instruments, Elk Grove Village, IL) or by an IBM personal computer XT with Spectra Calc (Galactic Industries Corporation, Salem, NH) as the software and DT 2811 Analog plus Digital Input / Output board (Data Translation Inc., Malbora, MA) as the interface. The sample was weighed accurately to 0.1 mg by a XE-100A Electronic Balance (Denver Instrument Company, Arvada, Colorado). A Fisher Model 10 Accumet pH meter (Fisher Scientific, Pittsburgh, PA) measured the pH values with the sensitivity of 0.01 pH unit (or 1 mv). A Branson ultrasonic cleaner (Branson, Shelton, Conn.) and a Corning PC-351 Hot Plate Stirrer (Corning Inc., Corning, NY) was used to facilitate the dissolution of solutes with low solubilities. The saturated solution of potassium superoxide in 18-crown-6-ether-acetonitrile was centrifuged with a Beckman CPR Centrifuge (Beckman Instruments Inc., Fullerton, CA). The sources and structures of chemicals utilized in these experiments are listed in Table 3-1.

The cell compartment used for the chemiluminescent detection was modified in order to prevent light leakage from the outside of the cell. The needle of a syringe was connected to a curved metal tube, which was immersed in the center of the cuvette. A black rubber stopper with a small hole allowing penetration of the metal tube covered the cuvette holder. Since it can not travel through the curved metal tube, the light does not enter the cuvette on withdrawal of the injection needle. Also a foam box coated with dull black paint inside and outside served as a "dark room" to cover the whole cell department. The setup is described in Figure 3-1. This light proof system was tested by injecting pure water into the cuvette filled with a 10^{-6} M solution of alkaline luminol. Even when the detector was set at its most sensitive status with the High Voltage (HV) of Photomutiplier (PMT) at 1000 volts (Gain = 10.0), Sensitivity at 0.003, and Time Constant at 0.25, no signal was observed. After injecting 3% H_2O_2 into the same solution, the photons collected by PMT was off scale. This proves that in the current system only the light emission inside the cuvette is detected.

Experimental Methods

After the detector and the recorder have been warmed up for several minutes, 2.5 ml of the solution to be detected, was pipetted into the cuvette, and the cuvette was then placed into the cell holder. When the cell holder was capped by the rubber stopper and the "dark box" was sealed, the system was ready for injection. At least three injection were made to get an average of chemiluminescent peak heights or integrated areas with

reasonable reproducibility; usually the Relative Standard Deviation (RSD) was less than 10 %. The cuvette was first washed three times with tap water, then three times with deionized water, finally rinsed with acetone, and dried with pressured air. The quartz fluorescent cuvette was frequently used in these experiments. The UV quartz cuvette can also be used, but the transparent walls must face the PMT window, and no emission filters must be installed so that the PMT collects the total photon emission from the chemiluminescent reactions. Prior to every new experiment the detecting system was validated by a luminol-based chemiluminescent system. A 20 μl, 3% of H_2O_2 was injected into a 2.5 ml, 10^{-3} M of alkaline luminol solution, and a strong, broad peak was detected. The average peak height was 238.5 mv. The experiment parameters were: Gain = 7.10 (710 volts), Sensitivity = 0.1, Time Constant = 0.25, recorder Detecting Scale = 500 mv, recorder Paper Rate = 1 cm/min. The high concentration of reactants and stable signal made this validation very reliable.

Preparations of Stock Solutions

All chemicals and reagents were used as provided without further purification.

Preparation of Luminol Solution

The 0.001 M luminol solution was prepared by the following procedures: 88.58 mg of luminol was weighed and then dissolved in a mixture of about 150 ml deionized water and 6.25 ml of 5 N sodium hydroxide solution with stirring. This solution was transferred into a 250 ml volumetric flask and the volume was adjusted to 250 ml. After

shaking the flask gently to achieve a homogeneous mixture, the stock solution was stored in refrigerator. The high pH of this solution benefited the further dilutions as no additional base was needed to keep luminol in alkaline media.

Preparation of Hydrogen Peroxide Solution

The 3 % H_2O_2 solution was prepared by pipetting 10 ml of 30 % H_2O_2 solution into a 100 ml volumetric flask then adjusted to volume with deionized water.

Preparation of Saturated Potassium Superoxide Solution

The KO_2 was weighed quickly and put into dry acetonitrile, then 18-crown-6-ether was added in excess to solubilize the KO_2 powder. After gentle stirring, the solution was stored overnight in the refrigerator. The acetonitrile solution, containing excess KO_2 and crown ether, was centrifuged at 2500 rpm for 10 minutes at room temperature to leave a saturated solution. Acetonitrile was chosen as the solvent because its polarity enhanced the solubility of ionic species, and also because it is miscible with the aqueous solutions.

Preparation of Phosphate Buffer Solutions

Based on the Henderson-Hasselbalch equation, Table 3-2 was developed to prepare phosphate buffer solutions. To make a buffer with pH range from 3.7 to 9.2, certain amounts of potassium phosphate monobasic and sodium phosphate dibasic were weighed corresponding to the clost pH value in Table 3-2, and dissolved in about 450 ml deionized water. While the solution was stirred by a hot plate stirrer until the dissolution was completed, the pH change was monitored by a pH meter and small amounts of dilute

solutions of sodium hydroxide or hydrochloric acid were added to adjust the pH value to the desired one. Then, the solution was transferred into a 500 ml volumetric flask and made to volume. After gently shaking the solution, the pH value of a small portion of it was measured to confirm the final pH.

All the β-lactam antibiotic solutions were made just before the detection experiments to minimize the effects of hydrolysis, and all the stock solutions were shaken before being utilized.

Table 3-1: Chemicals and reagents utilized in static studies of chemiluminescence.

Class	Chemical or Reagent	Source	Grade
Solvent	Water	Milli-Q[50], Ultra-pure water system. Millipore[a]	Deionized
	Deuterium Oxide	Aldrich[b]	99.9 atom % D
	Methanol	Fisher[d]	HPLC grade
	Reagent Alcohol	Fisher[d]	HPLC grade
	n-Butanol	Fisher[d]	Certified A. C. S.
	Acetone	Fisher[d]	Pesticide grade
	Methylene Chloride	Fisher[d]	Certified A. C. S.
	18-Crown-6-Ether	Aldrich[c]	99%
Acid and Base	85 % Phosphoric Acid	Fisher[d]	Certified A. C. S.
	Hydrochloric Acid (2N)	Fisher[d]	Certified
	Sodium Hydroxide (5N)	Fisher[d]	Certified
Buffer	Potassium Phosphate Monobasic	Fisher[d]	Primary standard
	Sodium Phosphate Dibasic	Fisher[d]	Certified A. C. S.
	Sodium Phosphate Tribasic	Mallinckrodt[e]	Analytical Reagent
	Buffer Solution Concentrate pH4.00	Fisher[d]	Certified
	Buffer Solution Concentrate pH6.00	Fisher[d]	Certified
	Buffer Solution Concentrate pH7.00	Fisher[d]	Certified
	Buffer Solution pH10.00	Fisher[d]	Certified
Oxidant	30 % Hydrogen Peroxide	Fisher[d]	Certified A. C. S.
	Potassium Suproxide	Aldrich[b]	N/A (Powder)

Millipore[a]: Millipore Corp., Bedford, MA.

Aldrich[b]: Aldrich Chemical Company, Inc., Milwaukee, WI 53233.

Aldrich[c]: Aldrich Chemical Company, Milwaukee, WI53201.

Fisher[d]: Fisher Scientific, Fair Lawn, NJ

Mallinckrodt[e]: Mallinckrodt, Inc., Paris, Kenturkey.

Table 3-2: Chemical structures and sources of β-lactam antibiotics examined.

Beta-Lactam Antibiotic	Stucture	Source
Azetidinone		Aldrich[a]
Sulbactam	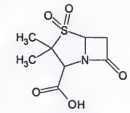	Fluka[b]
Clavulanic Acid	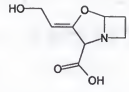	Beecham[c]
Cephalothin	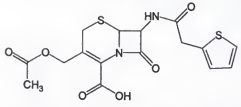	Lilly[d]
Cefotaxime	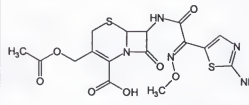	Sigma[e]

Table 3-2--continued

Beta-Lactam Antibiotic	Structure	Source
Penicillin G	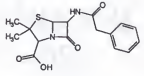	Fluka[b]
Penicillin V	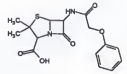	Sigma[e]
Ampicillin	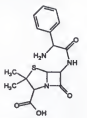	Interchem[f]
Amoxicillin	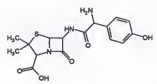	Sigma[e]
Piperacillin	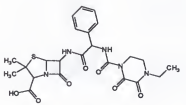	Sigma[e]

Table 3-2—continued

Beta-Lactam Antibiotic	Structure	Source
Dicloxacillin	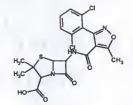	Sigma[e]
Methicillin	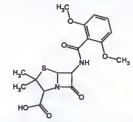	Sigma[e]
Hetacillin	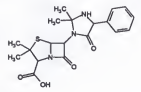	Beecham[c]

Aldrich[a]: Aldrich Chemical Co., Inc. Milwaukee, WI.
Fluka[b]: Fluka Chemical Corp. Milwaukee, WI
Beecham[c]: Smithkline Beecham Pharmaceuticals, Philadelphia, PA.
Lilly[d]: Eli Lilly and Company, Indiapolis, Ind.
Sigma[e]: Sigma Chemical Co., St. Louis, MO.
Interchem[f]: Interchem Corporation, Paramus, NJ.

Table 3-3: The composition of phosphate buffer solutions.

85 % H_3PO_4, ml	KH_2PO_4, g	Na_2HPO_4, g	Na_3PO_4, g	Measured pH
0.99	6.794			2.5
0.61	6.7983			2.75
0.34	6.8023			3.05
0.12	6.8095			3.43
0.05	6.8103			3.7
	6.8133			4.43
	6.7312	0.0453		4.73
	6.463	0.107		5
	6.0688	0.25		5.42
	5.232	0.5488		5.84
	4.6136	1.0166		6.17
	2.7122	1.415		6.56
	1.1775	1.9653		7.06
	0.5317	2.1866		7.48
	0.1553	2.3198		8.04
	0.0256	2.3677		8.77
		2.363		9.21
		2.3614	0.0771	9.59
		2.2292	1.868	10.2
		2.0447	0.4343	10.64
			3.1617	11.79

*The final volume of all buffer solution is 500 ml, and ionic strength is 0.1.

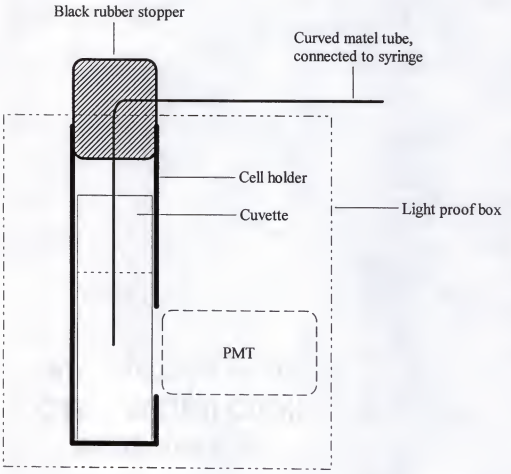

Figure 3-1: Schematic diagram of setup for chemiluminescent measurement in static mode.

CHAPTER 4
THE CHEMICAL PROPERTIES OF POTASSIUM SUPROXIDE

Comparison Studies

Since it is a well-documented oxidant for the chemiluminescent reactions of luminol, H_2O_2 was used as a reference to evaluate KO_2's capability as an oxidizer producing chemiluminescence.

At the same concentration (1 M), 40 µl each of aqueous H_2O_2 solution (a) and KO_2 (b) were reacted with 2.5 ml of 10^{-6} M luminol. The chemiluminescences were recorded by a flatbed recorder. The signal profiles are shown in Figure 4-1. At least three injections were used to obtain the average peak heights for (a) and (b). The intensities in term of peak heights can be calculated as

$$I_a = 53.5 / 100 \times 0.003 \times 100 \text{ mv} = 0.1605 \text{ mv}$$

$$I_b = 70.5 / 100 \times 0.1 \times 500 \text{ mv} = 35.25 \text{ mv}$$

$$I_b / I_a = 35.25 / 0.1605 = 219.6$$

Here, 53.5 is the peak height in centimeters, 100 is the scale height in centimeters which corresponds to the signal scale of 100 mv, and 0.003 is the sensitivity of the photomultiplier tube. Figure 4-1 clearly demonstrates that the chemiluminescence from

the reaction of luminol and KO_2 emitted faster, disappeared faster with greater increased intensity over the reaction with H_2O_2. Using the same experimental parameters, further examinations shown that 5.0×10^{-7} M luminol was detectable with H_2O_2, but 5.0×10^{-11} M with KO_2. The quicker chemiluminescence from the superoxide system seems more desirable for quantition of reactions emitting chemiluminescences, and KO_2 probably has the greater potential to make β-lactam antibiotics chemiluminescent compounds.

These results indicate that the reaction mechanism with KO_2 is different from that with H_2O_2. To increase the chemiluminescence by more than two magnitude, a significant lowering of activity energy is necessary. It seems that the superoxide anion decomposes into other reactive species.

Solvent Selection for Potassium Superoxide

KO_2 solutions with a concentration of 0.1 M were made by dissolving 177.5 mg of KO_2 in 25 ml of various solvents just before the chemiluminescent experiments. These solutions were evaluated using 10^{-5} M luminol injections made every 15 minutes. The experimental parameters were the same as in the comparison experiments, and the stability of chemiluminescent emissions was evaluated.

Clearly, water is not a suitable solvent for KO_2 because of its extremely high reactivity towards KO_2. In CH_3CN, KO_2 was able to oxidize luminol and emit chemiluminescences with similar intensities and peak profiles to KO_2 in H_2O. However, the signal reproducibility was not good. Although CH_3CN is miscible with H_2O, the

mixing status is more variable following injection than is the mixing of the two solutions in water.

CH_3OH was also investigated as a solvent for KO_2. The intensity of chemiluminescence grew abruptly, but disappeared gradually. This is probably due to the relative low rate of releasing KO_2 from CH_3OH into the water. Even though the short-term signals were reproducible, the chemiluminescent emissions of repeated injections decreased significantly over time, as shown in Figure 4-2.

As nonpolar solvents, n-butanol and methylene chloride can barely dissolve KO_2, and no chemiluminescent signal was observed. Furthermore, these solvents are not completely miscible with water.

Unfortunately, all of these solvents can not preserve the activity of KO_2 over two hours. Even when KO_2 was dissolved in the mixed solvents like CH_3CN-CH_3OH, CH_3CN-H_2O, and CH_3OH-H_2O, a similar loss of activity of KO_2 was observed. The typical correlation between the time and chemiluminescent intensity is shown in Figure 4-3.

To increase the solubility of KO_2 in CH_3CN, 18-crown-6-ether was added to give a saturated solution. After standing over night and centrifuged as described in chapter 3, the saturated KO_2 reagent was tested by reacting with luminol. The results were very positive, the chemiluminescent intensity was greatly increased due to the high concentration of KO_2, and the signal was stable for at least 24 hours. More encouragingly, fresh KO_2 and crown ether can be added periodically to keep the KO_2 amount constant,

and the reactivity of this reagent was sustained. The concentration of KO_2 was found to be 0.4386 M as determined by atomic emission spectroscopy (Zeeman 5100, Perkin-Elmer, Norwalk, CT, courtesy to Dr. Bergeron).

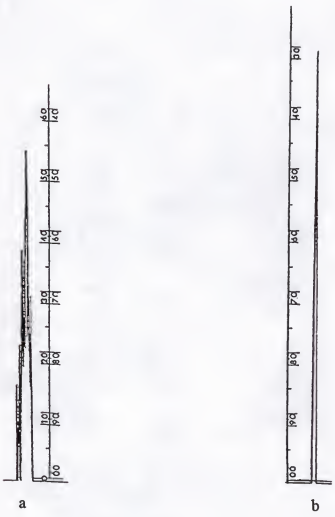

Figure 4-1: The chemiluminescence of luminol following the oxidation by (a) H_2O_2 and (b) KO_2. Experimental parameters: High Voltage (HV) of Photomultiplier Tube (PMT) is 910 volts, Time Constant is 0.25, Suppression Background is set at high, recorder speed is 1 cm/min. Sensitivity of PMT and Signal Scale of recorder is adjusted according to varied intensities. In (a) Sensitivity = 0.003, Signal Scale = 100 mv. In (b) Sensitivity = 0.1, Signal Scale = 500 mv.

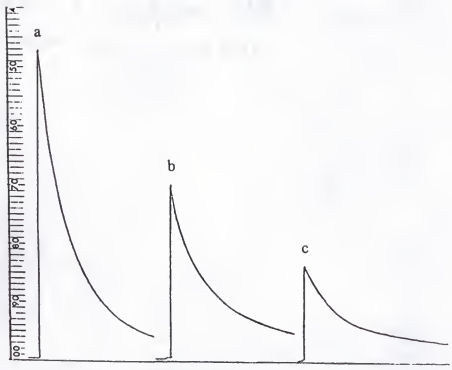

Figure 4-2: The chemiluminescence of luminol reacting with KO_2 in CH_3OH. (a) at starting time, (b) two hours later, (c) three hours later.

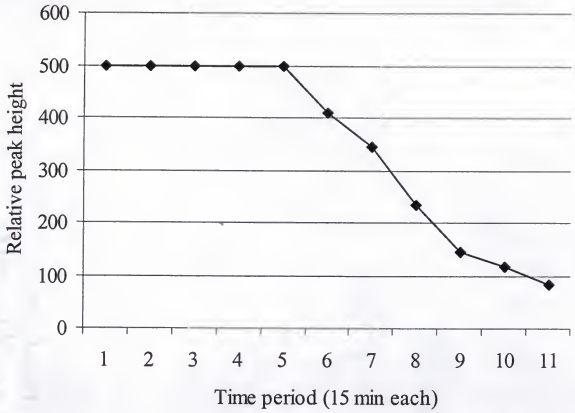

Figure 4-3: The correlation between time and the chemiluminescent intensities of luminol after repeating the injections of 50 µl of 1:1 CH_3CN-CH_3OH solution containing 0.1M K_2O into 2.5 ml of 10^{-9} M luminol every 15 minutes.

CHAPTER 5
CHEMILUMINESCENCES AND β-LACTAM ANTIBIOTIC

Introduction

In the last few years, quantitative studies of β-lactam antibiotics by chemiluminescences were based on either their enhancement [100, 101] or inhibition [102] of the luminol system. In this chapter the chemiluminescent emission following the interaction of KO_2 with 13 β-lactam antibiotics was investigated as a potential analytical tool.

The chemiluminescent intensities of antibiotics were determined at optimized parameters (pH 4.5-7.0. 950 volts across the PMT). 50 ml of saturated KO_2 solution was injected into 2 ml of 1.0 mg/ml antibiotics in 100 ml deionized water. All aqueous antibiotic solutions were prepared just before the detection to minimize the hydrolysis effects. The materials and methods were as described in the chapter 3.

Six of the antibiotics studied gave no measurable signal, while the other seven emitted differently intensified chemiluminescence. The chemiluminescent intensities of the antibiotics are compared in Figure 5-1. The strongest chemiluminescence was observed with penicillin G. The linear dynamic range of 0.01-0.1 mg/ml is shown in Figure 5-2. Dicloxacillin in the concentration range 0.2 to 1.0 mg/ml also gave a linear

relationship, as shown in Figure 5-3. 30 % H_2O_2 had been used to oxidize all the antibiotics but no signal was observed.

Probe of Maximum Emission Wavelength

The maximum emission wavelength of the chemiluminescence following the oxidation of 10 mg/ml penicillin G by the saturated KO_2 reagent was measured at 535 nm by using a SPEX Photocounting Fluorescence Detector Courtesy of Dr. Winefordner. After turning off the excitation source, the fluorescence detector was ready for chemiluminescence determination. The injection of KO_2 was made at emission wavelengths of 400, 450, 520, 530, 540, 600, 700, and 800 nm. The intensity observed at 535 nm was the highest. The chemiluminescenct spectrum between 530-590 nm is shown in Figure 5-4. To validate the detecting system, the spectrum of 10^{-4} M luminol (Figure 5-5) was observed by reacting it with 30% H_2O_2, this data is consistent with the literature [77]. The experiments here demonstrate that the maximum emission from the reaction between penicillin G and KO_2 is at 535 nm.

Discussion

There are some unique characteristics produced by the reactions of β-lactam antibiotics with KO_2. First, in these experiments seven of the thirteen β-lactam antibiotics generated chemiluminescences at pH 4.5-7.0 rather in the more usual alkaline media. It should be remembered that these antibiotics will hydrolyze at extremely acidic or basic pH values [103]. Second, the maximum emission wavelength of chemiluminescence

following the oxidation of penicillin G by KO_2 was observed at 535 nm, which is different from the 425 nm of 3-aminophthalate (from luminol) [77], 275-425 nm range of S_2 [89], 260-480 nm of SO_2 [91]; but is closer to the 420-500 nm range of N-methylacridone (from lucigene) [84] or 562 nm of oxyluciferin (from luciferin) [87]. Third, the chemiluminescences of the emitting antibiotics disappeared very quickly, the typical full width at half maximum (FWHM) was 2 sec (Figure 5-6); the slowest emission, from ampicillin, had a FWHM of 7 sec (Figure 5-7) and probably a diode-array detector is needed to observe the full spectrum.

However, there are still several questions remaining to be answered.

1. When penicillin G was dissolved in an aprotic solvent like CH_3CN, even after oxidation by the KO_2 saturated solution, no chemiluminescent signal was observed. In dry CH_3CN, KO_2 exists in the form of superoxide anion radical. This may indicate that without dismutation reactions with water or other protic solvents, superoxide can not be transferred into the reactive species, and so the question arises what is the reactive species generated from the superoxide dismutation reactions? Since H_2O_2 is not able to generate chemiluminescence after oxidizing any of the β-lactam antibiotics, a possible candidate of this reactive specie is $^1O_2$. Further experiments are conducteded to prove its existence.

2. Why do the six antibiotics including azetidinone, sulbactam, clavulanic acid, methicillin, penicillin V, and cefotaxime not produce chemiluminescence in the reaction? Why do the other seven antibiotics gave chemiluminescences of different intensities? What are the chemiluminescent intermediates and through which pathways do they go?

3. Is it possible that in this reaction the hydroxyl radical has been generated, i.e. is the oxygen toxicity theory based on the Haber-Weiss reaction the right assumption?

To answer these questions, the degradation products of β-lactam antibiotics in the reactions with KO_2 needed to be identified, and a DO_2 experiment needed be designed to prove the existence of $^1O_2$ in the superoxide dismutation reaction.

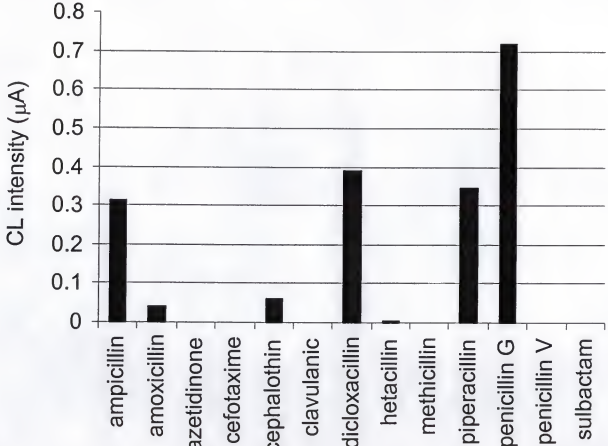

Figure 5-1: The comparison of chemiluminescent intensities of thirteen β-lactam antibiotics following the oxidation by KO_2.

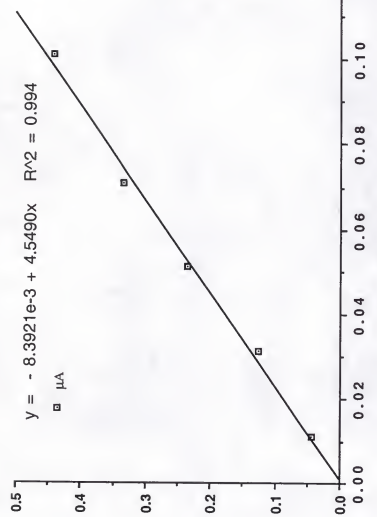

Figure 5-2: The calibration curve of penicillin G.

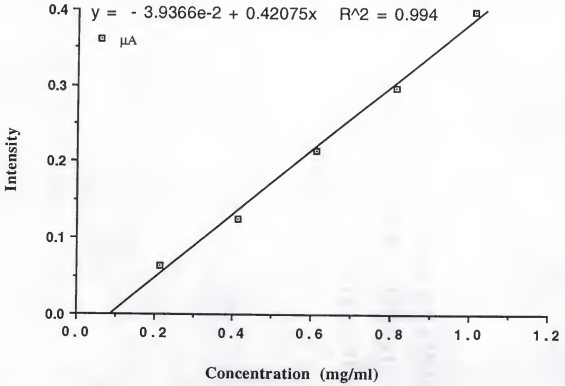

Figure 5-3: The calibration curve of dicloxacillin.

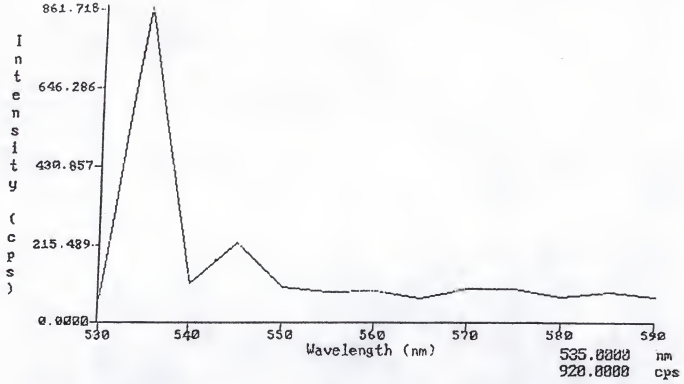

Figure 5-4: The photocounting chemiluminescent spectrum (intensity vs. wavelength) of penicillin G reacting with superoxide.

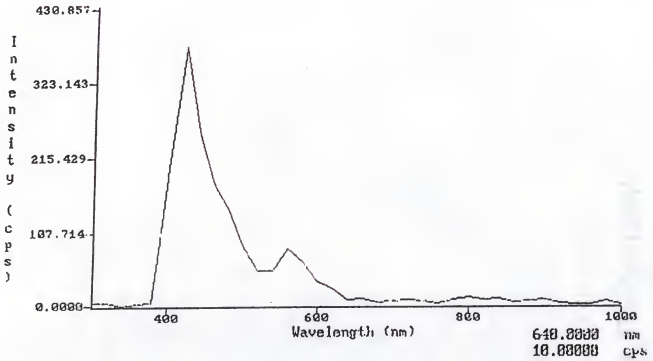

Figure 5-5: The photocounting chemiluminescent spectrum (intensity vs. wavelength) of luminol reacting with hydrogen peroxide.

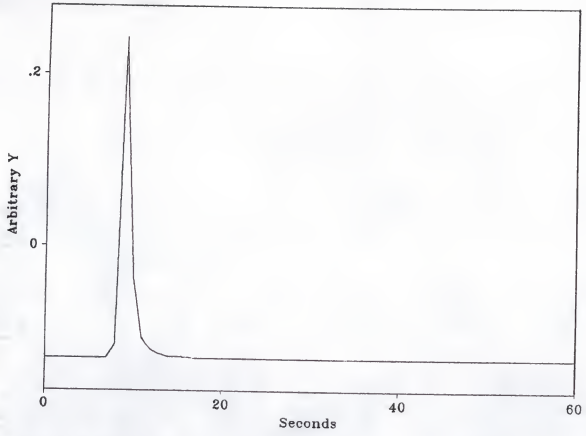

Figure 5-6: The typical chemiluminescent spectrum (intensity vs. time) of β-lactam antibiotics.

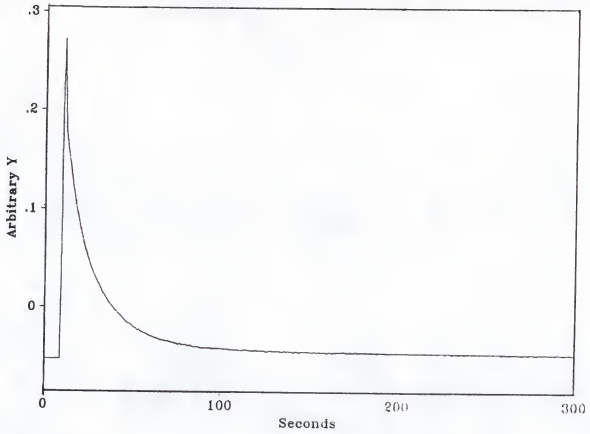

Figure 5-7: The chemiluminescent spectrum (intensity vs. time) of ampicillin.

CHAPTER 6
MECHANISTIC STUDIES

Penicillin G was chosen as an example to investigate the mechanism of the chemiluminescence of β-lactam antibiotics interacting with potassium superoxide. Various experiments were conducted on the aqueous penicillin G sample and the sample containing the products generated by oxidizing penicillin G with potassium superoxide. These experiments include nuclear magnetic resonance (NMR) assay, thin-layer chromatography (TLC), and high performance liquid chromatography (HPLC) using a ultraviolet (UV) spectrophotometer, a photodiode array (PDA) detector, and a mass spectrometry (MS) detector. In all these experiments, solid KO_2 was utilized instead of the saturated KO_2 reagent (KO_2-acetonitrile-18-crown-6-ether) in order to simplify the experiments. A DO_2 experiment was also run to prove the generation of singlet oxygen in the suproxide dismutation reaction.

The Deuteration Experiment

Stauff et al. [104, 105] proposed that the spontaneous disproportion of superoxide generating $^1O_2$, rather than ground state oxygen ($^3O_2$), as shown in equation (1). This proposal had received support from the calculations of Knoppenol [106].

$$O_2^{\cdot-} + O_2^{\cdot-} \xrightarrow[+\,2H^+]{\text{spontaneous}} H_2O_2 + {}^1O_2 \qquad (1)$$

Khan [94, 95] had also proposed that superoxide is a precursor of $^1O_2$, although he believes this occurred by a direct electron transfer reaction [equation (2)].

$$O_2^{\cdot-} \longrightarrow e^- + {}^1O_2 \qquad (2)$$

Nilsson and Kearns [98], however, based on experiments injecting D_2O rather than H_2O into the dry dimethyl sulfoxide (DMSO) containing KO_2, rejected the suggestion that superoxide serves as a direct precursor of $^1O_2$. The major question remaining in their investigation is the fact that even though it can be generated from KO_2 after injection of a small amount of D_2O or H_2O, $^1O_2$ will be mostly surrounded by DMSO, not by D_2O or H_2O because both react with superoxide through the dismutation reaction. Comparing the 30 μsec lifetime of $^1O_2$ in DMSO with its 20 μsec in D_2O and its 2 μsec in H_2O it is not surprising that no difference was observed. Also, whether the trace amounts of singlet oxygen produced in this system is enough to oxidize the $^1O_2$ acceptor tetramethylene (TME) is uncertain, and thus it is possible that no oxidation signal of TME could be detected in the KO_2 system adopted by Khan's experiments.

Since a relatively strong chemiluminescence had been obtained in the reaction of aqueous penicillin G interacting with KO_2, D_2O was used instead of H_2O to dissolve penicillin G, and to examine the deuterium effect on the chemiluminescent intensities. In view of the fact that in D_2O $^1O_2$ has more time to react with penicillin G, an enhancement of chemiluminescence supports the concept that the $^1O_2$ is generated in the superoxide dismutation reaction. 4.0 mg/ml of penicillin G solutions were prepared in pure D_2O, 70% D_2O-30% H_2O, 50% D_2O- 50% H_2O, and pure H_2O. The chemiluminescences of 2

ml of these solutions were tested by injection of 50 μl of KO_2, which is contained in a saturated solution made of 18-crwon-6-ether and acetonitrile. The experimental parameters were set as the following: Gain (PMT/HV) is 8.8, Sensitivity is set at auto, Time Constant is 5, and Suppression Background is set at high. The differently intensified chemiluminescences are described in Table 6-1, and the chemiluminescent profiles of penicillin G in the mixture solvents with varied D_2O to H_2O ratios (from pure D_2O-the top to pure H_2O-the bottom) are demonstrated in Figure 6-1. Inspection of Table 6-1 clearly shows an approximately 9-fold enhancement of chemiluminescent emission of penicillin G by replacing H_2O with D_2O as the solvent. Also lowering the ratio of D_2O to H_2O was correlated with decreased intensities of chemiluminescences. Another observation really attracts attention. When the high voltage of photomultiplier tube (PMT) was adjusted to 980 volts, the time constant was set at 0.25 to catch the weak and short-life emissions. After the first injection of KO_2 into the solution of penicillin G in pure D_2O, the huge numbers of photoelectrons collected by the PMT outscaled the detector. Characteristically, even after a second, or third injection of KO_2 into the same reacting cell, a significant signal was still observed, although their intensities dramatically decreased. This is totally different from the case of the penicillin G in pure H_2O, where a much weaker chemiluminescence from the first injection of KO_2 was detectable, but no signal was observed after the second injection of KO_2. This phenomenon further suggests that $^1O_2$ can be generated in the superoxide dismutation reaction. In this detection system, the syringe needle was connected to a long, curved metal tube, which is immersed in the

center of the cell to prevent the light leakage caused by injection. After injection, KO_2 diffuses radially from the center to the cell wall. Most penicillin G reacts with the KO_2 and the concentration of penicillin G is decreased, especially in the center. KO_2 from the second or third injection has to travel relatively longer distance to react with the remaining penicillin G. The singlet oxygens produced from the second or third injection of KO_2 into the D_2O therefore have more opportunity to react than those in H_2O because of the longer lifetime of $^1O_2$ in D_2O. In the contrast, $^1O_2$ formed in H_2O can not travel far enough to react with penicillin G away from the center. The repeated injections is an advantage of investigations in the static mode.

The results presented in this experiment strongly reinforce that in the contrast of the Haber-Weiss reaction, the $^1O_2$ can be generated by superoxide dismutation reaction, which can occur either spontaneously or when catalyzed by SOD with great rate. It indicates that superoxide maybe must not have time to further react with hydrogen peroxide to produce hydroxyl radicals and cause oxygen toxicity, as described by the Haber-Weiss reaction. Even though it is catalyzed by transition metals, which are available in biological systems, the Haber-Weiss reaction will face competition from the Fenton type reaction [equation (3), (4)].

$$O_2^{\cdot-} + Fe^{III} \longrightarrow Fe^{II} + O_2 \qquad (3)$$

$$Fe^{II} + H_2O_2 \longrightarrow Fe^{III} + {}^{\cdot}OH + OH^- \qquad (4)$$

Equation (4) is consistent with the fact that plenty of H_2O_2 has been generated almost instantly by the superoxide dismutation reaction. It is already claimed that the evidence for the formation of ·OH is overwhelming [107, 108,109, 110]. This does not, of course, preclude the formation of reactive oxygen species in additional to ·OH, for example $^1O_2$ in equation (3). Taking account of the fact that hydroxyl radicals may also come from the Fenton type reaction as well as the Haber-Weiss reaction, and the $^1O_2$ is capable of damaging the same biological components as is superoxide, not all the oxygen toxicity should be rationalized by the Haber-Weiss reaction. The toxic species should be specified in order to better understand the pathology, which causes the diseases, and to develop new therapeutic strategies as well as new antioxidants. In the experiments discussed above, it is strongly suggested that $^1O_2$ well deserves more attention, and it is probably the prime oxidant in various diseases caused by oxygen toxicity.

NMR Consideration

Two sample of 15 mg of penicillin G (or penicillin V) in 0.75 ml deuterium oxide were made, one of them was reacted with 10 mg KO_2. The 300 MHz ^{1}H-NMR, 75 MHz ^{13}C-NMR and Attached Proton Test (APT) were obtained by a GEMINI-300 NMR spectrometer at room temperature. 3-(Trimethylsilyl) propionic-2, 2, 3, 3-d_4 acid, sodium salt (TSP, Aldrich) was used as internal NMR standard and the HDO peak appeared around 4.8 ppm from TSP. These NMR assays are used to detect the structural alternation

before and after the oxidation of penicillin G or penicillin V by KO_2 and to check the purity of these two drugs.

NMR Spectra of Penicillin G

Figure 6-2 is the proton NMR spectrum of potassium penicillin G in D_2O. The interpretation of the spectrum is given below.

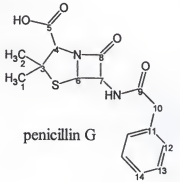

penicillin G

Chemical Shift (ppm)	Position
1.501 (s), 1.570 (s)	1, 2
3.615, 3.630 (ABq, J=14 Hz)	10
4.247 (s)	4
5.430 (d, J=3.9 Hz)	6, 7
5.493 (d, J=3.9 Hz)	6, 7
7.278-7.392 (m)	12, 13, 14

Figure 6-3 depicts the ^{13}C-NMR spectrum of potassium penicillin G in D_2O. The assignments are tabulated below.

Chemical Shift (ppm)	Position
26.594, 30.843	1, 2
42.088	10
58.190	7
64.518	3
66.779	6
73.305	4
127.619	14
129.137, 129.486	12, 13
134.600	11
174.345, 174.497, 174.786	5, 8, 9

The results here of ^{1}H-NMR and ^{13}C-NMR spectra are similar to these presented in a study of penicillins and cephalosporins [111].

Compared with Distortionless Enhancement by Polarization Transfer (DEPT), APT is less sensitive and does not distinguish between CH_3 and CH peaks (both down) or between CH_2 and quaternary C peaks (both up). However, in the case of penicillin G and penicillin V, the partial information obtained by APT is sufficient for interpretations. As shown in Figure 6-4, the CH_3 peaks at position 1, 2 and CH peaks at position 4, 6, 7, 12, 13, 14 are down. Since the stronger peaks at 127.619 ppm, 129.137 ppm, and 129.486 ppm obviously belong to the aromatic carbons, the other down peaks are easily identified. For the up peaks, the peaks at 174.786 ppm, 174.497 ppm, and 174.345 ppm are clearly from carbonyl groups; the peaks at 134.600 ppm and 64.518 ppm refer to the quaternary carbon of aromatic ring and alkanes respectively. Subsequently the peak at 42.008 ppm is identified as CH_2 at position 10.

The degradation products of penicillin G generated by reaction with potassium superoxide were also examined by NMR spectroscopy without isolation as shown in Figure 6-5 (^{1}H-NMR spectrum), and Figure 6-6 (^{13}C-NMR spectrum). The APT spectra of degradation products were not readable and so are not presented. Interestingly, the NMR signal at position 10 in Figure 6-6 seems to have disappeared. Probably penicillin G lost the CH_2 at position 10 after oxidation by KO_2. However, there is a peak at 42.589 ppm close to 42.088 ppm (position 10 in Figure 6-3) in the ^{13}C-NMR spectrum, which may suggest that the electronic environment has changed but CH_2 still exists. More

experiments are needed to clarify the status of the methylene, which is between the carbonyl and benzyl moiety on penicillin G.

Meanwhile the comparison between the NMR spectra of the phenyl ring before and after the oxidation by KO_2 draws attention. If the hydroxyl radical is generated by the interaction between superoxide and hydrogen peroxide, which is produced by the superoxide dismutation reaction, the hydroxylate aromatic compounds should be identified by NMR spectra since the electrophilic hydroxyl radical adds readily to the aromatic nucleus ($K = 3 \sim 8 \times 10^9 M^{-1} S^{-1}$) [112]. No such hydroxylate compounds are demonstrated in Figure 6-5 and Figure 6-6. There is no disubstitution or chemical shift of the aromatic ring to suggest the hydroxylation. Hence, no conclusion can be drawn that the hydroxyl radical is formed by the Haber-Weiss reaction in this superoxide system.

NMR Spectra of Penicillin V

As shown in Figure 5-1, penicillin G emitted the strongest chemiluminescence after the oxidation by KO_2 and surprisingly no chemiluminescent signal was observed with penicillin V under the same reacting conditions. Considering the fact that the only structural difference between penicillin G and penicillin V is the "phenoxyl methyl" moiety of penicillin V, the oxidation of potassium penicillin V in D_2O was examined by NMR spectroscopy by comparing the spectra following the oxidation of penicillin G and penicillin V by KO_2.

The proton NMR spectrum of penicillin V in D_2O is shown in Figure 6-7, and the interpretation is described as below.

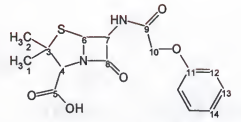

penicillin V

Chemical Shift (ppm)	Position
1.500, 1.513 (s)	1,2
4.260 (s)	4
4.469 (ABq, J=16.2 Hz)	10
5.520 (d, J=4.2 Hz)	6,7
5.569 (d, J=3.9 Hz)	6,7
6.837-7.273 (m)	12, 13, 14

Figure 6-8 is the carbon NMR of penicillin V in D_2O. The peaks are assigned as the followings, which are in agreement with the literature values [113].

Chemical Shift (ppm)	Position
26.548, 31.238	1, 2
57.492	7
64.670	10
66.491[a]	3
66.613[a]	6
73.260	4
114.841	12
122.384	13
130.002	14
156.908	11
170.643	5
174.285[b]	8, 9

[a]the peaks with chemical shifts of 66.491 and 66.613 ppm are overlapping and they are differenciated by APT (Figure 6-9).
[b]the peaks of carbons at position 8 and 9 are overlapping at 174.285 ppm.

In case of penicillin V, APT is very useful to identify carbon 3 at 66.492 ppm (up) and carbon 6 at 66.597 ppm (down) as shown in Figure 6-9. The degradation products of penicillin V after the oxidation by KO_2 were also studied by proton NMR (Figure 6-10) and carbon NMR (Figure 6-11). Both showed no structure alternation on the aromatic ring, and contrary to penicillin G the CH_2 at position 10 remains intact.

Conclusion

As discussed in chapter 1 (equation 7), the quantum yield of chemiluminescence is associated with Φ_R, the yield of product; Φ_{ES} the number of molecules entering the exited states; and Φ_F the fluorescence quantum yield. Therefore, the generation of chemiluminescent products is the first step to emit chemiluminescence. It seems that unlike penicillin G, penicillin V did not carry out this first step and no chemiluminescent signal was observed. The NMR data here suggests that the CH_2 at position 10 be correlated with the chemiluminescent emissions, and no hydroxylate aromatic compound was found to support the possibility that hydroxyl radical was generated by the Haber-Weiss reaction in the current superoxide system.

TLC Analysis

Introduction

The TLC procedures have been used to allow the simple and rapid separation and identification of the different (spontaneous, chemical and enzymatic) degradation products of penicillins and cephalosporins [114]. After testing several spray reagents, Lin

and Kondo [115] found that the iodine-azide reagent was the best for detection of penicillin G, producing a yellow color on the TLC plate; the vanillin-phosphoric acid mixture was the best for the detection of streptomycin (brown) and dihydrostreptomycin (brown); ninhydrin was best for kanamycin (purple) and fradiomycin (purple). Since the NMR spectra had indicated that numerous degradation products of penicillin G were generated after the oxidation by KO_2 (Figure 6-5 and 6-6), these three reagents (iodine-azide, vanillin-phosphoric acid, and ninhydrin) were utilized in the TLC analysis to separate the hydrolysis products from the oxidation products or other derivatives of penicillin G. It is anticipated that sufficient samples would be obtained to conduct experiments using mass spectrometry after separation and purification.

Experimental

TLC plates (1 inch × 3 inches) of silica gel were used for separation. Five different solvent systems were tested: (A) n-butanol-water-ethanol-acetic acid (5:2:1.5:1.5); (B) n-butanol-water-acetic acid (4:1:1); (C) acetone-acetic acid (19:1); (D) acetone-water (17:1); (E) methanol-water (50:50). Among them, solvent system (B) was the best for separating the degradation products of penicillin G. Each TLC plate was sprayed consecutively with the following spray reagents: (a) ninhydrin, (b) iodine-azide, (c) vanillin-phosphoric acid. The iodine-azide reagent was prepared by dissolving 0.5076 g iodine (Sigma) and 58.9 mg sodium azide (Fisher) into 200 ml chloroform to make a solution of 0.01 N iodine-0.02 % azide. Vanillin (Sigma) 0.9992 g was dissolved in 100 ml phosphoric acid and this solution was diluted 1:1 with methanol to form the vanillin-

phosphoric acid reagent. Ninhydrin 0.2010 g was dissolved in 5 ml of 10 % acetic acid, and added to 95 ml of n-butanol to produce the ninhydrin reagent. Since spraying vanillin-phosphoric acid mixture did not mark any new spot, as shown in Table 6-2, this reagent was not used in the separation procedures.

Results and Discussions

Each of the aqueous penicillin G sample (sample PG) 10 mg/ml and the sample containing degradation products of penicillin G (sample $PGKO_2$) was made as in the NMR experiments. Both of them were adjusted to pH 12.00 and were spotted on the same TLC plate. Each spot was dried with pressured air and the spotting was repeated four times to increase the amount of sample in each spot. After the first elution in the solvent system (B), the TLC plate was dried by a hot plate, then ninhydrin and iodine-azide were sprayed consecutively on the TLC plate. Three spots were found originating from sample $PGKO_2$, two spots from sample PG. The colors and the moving distances of these spots were shown in Figure 6-12. Obviously the second spot from sample $PGKO_2$ and the first spot from sample PG have the same R_f value (distance solute moves/distance solvent front moves). After the third elution, three spots of sample $PGKO_2$ were found to have the same R_f values as those of sample PG, as shown in Figure 6-12. This indicates that while it was oxidized by KO_2, the aqueous penicillin G was hydrolyzed as well because of the strong basicity of superoxide in water [116]. Therefore, the first three spots of sample $PGKO_2$ after the third elution were believed to be produced from the reactions other than hydrolysis.

To prepare for the mass spectroscopy experiments, 100 mg/ml of sample $PGKO_2$ was made and put on one of the 36 TLC plates in a line spots. Each spot was dried by pressured air and the spotting was repeated four times. The plate was sprayed after the third elution, 4/5 of the plate was covered by a piece of paper and the other 1/5 was sprayed by ninhydrin and iodine-azide, as shown in Figure 6-13. The invisible three lines on the 4/5 part of the TLC plate was located by the sprayed 1/5 part of the plate, then each line on the 4/5 part was cut off separately. After the three desired block on all the 36 plates were cut off and separated into three samples, each of them was washed by methanol and the silica gel was filtered. The subsequent solution was concentrated into three approximate 1.5 ml solution (solution 1, 2, and 3). Each solution was repeatedly spotted 12 times on a TLC plate (Figure 6-13) and developed in the solvent system (B). After the first elution and the two reagents were sprayed, two spots were found from solution 1, one from solution 2, and none from solution 3. Possibly solution 3 results from the running solvents or from the solvent of sample $PGKO_2$, as its spots were overlapping with the solvent front. These four spots were named 11, 12, 13, and 3. Following the same procedures of mass production as discussed before, four solid sample were finally obtained after filtering, and drying and were analyzed by Fast Atom Bombardment (FAB)-mass spectroscopy. The average lengths of the time consumed during each run are listed in Table 6-3.

One peak of m/z 105 with quite low intensity was found in one of the four samples, as shown in Figure 6-14. This is most likely ph-C=O, however, in the other

three sample spectra it appears that they was enough sodium salts in the samples to suppress other signals. The sodium salts may come from the TLC plates or from other reagents. Although it is consistent with the results of NMR assay, in which the CH_2 seems lost after the aqueous penicillin G was oxidized by KO2, the peak m/z 105 in mass spectrum of spot 13 seems unreliable and better separation methods are needed.

HPLC Detection

HPLC is widely utilized to analyze the degradation products of penicillin G in aqueous solutions because of its specificity, ease of use and high sample capacity. However, no product generated by the oxidation of penicillin G had been studied by HPLC. In this section the products of aqueous penicillin G following the oxidation by potassium superoxide is investigated by HPLC using a C18 column.

Experimental

The HPLC experiments are conducted with the following equipment:

1) Beckman Model 110A pump

   Beckman Model 153 UV detector

   Beckman Instrument Inc., Fullerton, CA.

2) Hewlett-Packard 3392A integrator

   Hewlett-Packard Co., Palo Alto, CA.

3) Waters 501 HPLC pump

   Waters™ 1996 Photodiode Array Detector

Waters™ 717 plus Autosampler

Millipore Corporation, Milford, MA.

4) Exsil® ODS column, 150 by 4.6 mm dimension, 7 μm particle size, 100 A pore size. Keystone Scientific, Inc., Bellefonte, PA.

5) Helium compressed gas, Gainesville Welding Supply, Gainesville, FL.

Various reference compounds were injected and the retention times were measured in order to identify the unknown peaks, which were produced by the degradation of penicillin G following the oxidation by potassium superoxide. Hydrogen peroxide was obtained from Fisher. 3,4-dihydroxybenzoic acid, 2, 4-dihydroxybenzoic acid, 2, 3-dihydroxybenzoic acid, phenylacetic acid, p-hydroxyphenyl acetic acid, and benzaldehyde were bought from Aldrich. Benzoic acid was obtained from Sigma. P-hydroxybenzoic acid was obtained from Eastman (Eastman Organic Chemicals, Rochester, NY). Salicylic acid was obtained from Mallinckroot (Mallinckroot Chemical Works, St. Lois, New York, and Montreal). All the chemicals, including the reference compounds and the samples, were completely dissolved using an ultrasonic cleaner. All the reagents utilized by the HPLC system were filtered and degassed for about 10 minutes. Prior to the experiments, the HPLC setup was washed by water, 50:50 water:methanol, and methanol consecutively, each for half-hour. The UV detector was set at 254 nm, 0.08 absorbance unit full scale. The flow rate was 1.0 ml/min and the pump pressure was kept below 4000 psi. The 2 mg/ml of sample PG and $PGKO_2$ were prepared as in chapter 3.

Results and Discussion

30% MeOH-70% phosphate buffer (pH4.15) is good for the separation of the hydrolysis products of penicillin G in aqueous solutions, but is not good for oxidized sample, which is consistent with the observation of Vadino et al. [117]. Acetonitrile 0.1% in pH 5.66 phosphate buffer was found useful for the detection of the oxidation products of penicillin G as shown in Figure 6-15. Unfortunately, none of the retention times of unknown peaks of sample $PGKO_2$ matched up with that of the reference compounds as shown in table 6-4. Since the same C18 column was not available, the experiments using photodiode array detector (PDA) were conducted on a different Exil^R ODS column. Similar results were obtained as shown in Table 6-4.

Conclusion

1. When the sample $PGKO_2$ stayed overnight huge peaks appeared hours after the injections. Were polymers generated?
2. No benzoic acid or its derivatives were identified by this kind of detection and maybe the amount generated is so small that it is out of the detecting limit of the UV detector.
3. UV detector is not suitable for the detection of the mixture caused by oxidation and hydrolysis. Mass spectrometer is the obvious choice.
4. The HPLC buffer of sodium salts must be replaced by ammonium buffers or other nonmetal-ion solutions since in the TLC analysis vast amounts of sodium salts suppress the signal for mass spectroscopy.

HPLC/ESI-MS and HPLC/APCI-MS Analysis of the Degradation of Penicillin G Following the Oxidation by Potassium Superoxide

Introduction

Electrospray ionization mass spectrometry (ESI-MS) was first introduced by Yamashita and Fenn [118, 119] in 1984. At approximately the same time, a very similar, independent development was reported by Aleksandrov and coworkers [120]. Actually, electrospray as a source of gas-phased ions and their analysis by mass spectrometry was proposed much early by Dole [121], however Dole's experiments were too narrowly focused on the detection of polymeric species, which are not themselves ionized in solution, and the experimental results were not convincing [122].

Since the end of 1980s, ESI-MS has developed at a tremendous pace and established itself as an outstanding method for biochemical applications. It has permitted new possibilities for mass spectrometric analysis of high-molecular-weight compounds of all types, including proteins, nucleotides, and synthetic polymers. Other analytical techniques do not provide the same level of detailed information regarding molecular weights and structures from extremely small amounts of material. Compared to the other mass spectrometric ionization techniques, ESI has three superior features. First, ESI has the truly unique ability to produce extensively multiply charged ions, which may be analyzed on virtually all types of mass spectrometers. Second, the samples analyzed by ESI-MS must be introduced as a liquid phase. This results in a natural compatibility of

ESI with many types of separation techniques. Third, the extreme "softness" of ESI process allows the preservation in the gas phase of noncovalent interaction between molecules as well as the study of three-dimensional conformation. For earlier ionization methods such as fast atom bombardment (FAB) and plasma desorption, abundant energy is applied in a highly localized fashion over a short time. These methods lead not only to ion desolvation but also to fragmentation or even net ionization, that is , the creation of ions from neutrals. As for ESI-MS, in which the desolvation is achieved gradually by thermal energy at a relatively low temperature as it is a far softer technique.

There are three major steps in the production of gas-phase ions from electrolyte ions in solution by electrospray: (1) production of the charged droplets at the ES capillary tip; (2) shrinkage of the charged droplets by solvent evaporation and repeated droplet disintegrations, leading ultimately to very small highly charged droplets capable of producing gas-phase ions; and (3) the actual mechanism by which gas-phase ions are produced from the very small and highly charged droplets. Kebarle and Tang [123] described the first two steps in Figure 6-16. As shown in this schematic representation of the charged-droplet formation, a high voltage of 2-3 KV is supplied to the metal capillary which are typically 0.2 mm o.d. and 0.1 mm i.d. and located 1-3 cm from the counter-electrode. Penetration of an imposed electric field into the liquid leads to formation of an electric double layer in liquid. Enrichment of the surface of the liquid by positive electrolyte ions leads to destabilization of the meniscus and formation of cone and jet

emitting droplets with excess of positive ions. Charged droplets shrink by evaporation and split into smaller droplets and finally gas-phase ions.

More recently, HPLC/ESI-MS has gained widespread recognition as a powerful analytical tools for drug metabolism and pharmacokinetic studies because it permits the separation and ionization of polar nonvolatile or thermally labile compounds, such as drugs, conjugated metabolites, peptides or DNA adducts. In addition, these techniques facilitate qualitative and quantitative studies on the parent compounds and their polar metabolites. Given its attractive advantages such as good sensitivity, reliability, and specificity for a wide variety of compounds with minimal sample handling, HPLC-MS has replaced GC-MS, which requires sample derivatization for polar metabolites.

A series of ionization sources compatible with HPLC is available, which include thermospray ionization (TSP), electron impact (EI) or chemical ionization (CI) with particle beam interface (PB), continuous-flow fast atom ionization (CFFAB) and atmospheric pressure ionization (API) using a heated nebulizer interface (APCI). Most of those methods have their limitations. TSP and APCI require critical control of the vaporizer temperature during analysis, and thermal degradation of labile molecules may occur. CFFAB can only accept low flow rates, and requires the presence of a matrix to assist ionization, thereby affecting the ion-current stability and making the method susceptible to interference from background ions. However, HPLC/ESI-MS is now free of most major technical problems and has become the method of choice for drug metabolism and pharmacokinetic research, as reflected in the impressive number of

applications published in the last few years. More encouragingly, a triple-quadrupole mass spectrometer is capable of performing MS/MS such as neutral-loss scan, parent-ion scan or product-ion scan. Therefore, besides the molecular weight, HPLC/ESI-MS/MS (or MS^n) can give complex mixture analysis, structural elucidation, combinatorial screening, fast chromatography, picogram quantitation and protein sequencing. For example, in addition to MS/MS capabilities, the LCQ LC/ MS^n Detector (octapole-octapole mass spectrometer, Finnigan MAT, San Jose, CA) also provides standard MS/MS/MS.... MS^n (n=1-10) for structural elucidation capability. The selectivity of MS^n means that a compound can be fragmented, and the resulting fragments further isolated and analyzed to yield structural information about complex molecules. The results presented here confirm that HPLC/ESI-MS/MS is an outstanding tool for pharmaceutical analysis.

Experimental

All data were obtained on a Finnigan MAT (San Jose, CA) Benchtop LCQ LC/MS^n Detector (external ionization ion trap) equipped with both an electrospray ionization (ESI) ion source and an atmospheric pressure chemical ionization (APCI) ion source. These sources were interfaced to a Hewlett-Packard (Palo Alto, CA) 1090 (Series II) high pressure liquid chromatograph (HPLC). The effluent from the HPLC column was typically split prior to the ion source.

Chromatographic separation was achieved on a Keystone Scientific (Bellefonte, PA) Exil^R ODS (C-18; 150×4.6 mm dimension; 7 μm particle size; 100 A pore size)

HPLC column utilizing a reverse phase gradient. Two mobile phases were used. Mobile phase A was 0.1% acetic acid in 50:50 water:acetonitrile and mobile phase B was 0.01 M ammonium acetic acid (pH 5.72) with 0.1% acetonitrile in water. The flow rate was 1 ml/min and the loop size is 5 μl. After 1 mg/ml and 0.1 mg/ml penicillin G were oxidized respectively by solid KO_2, the degradation of penicillin G was analyzed via direct infusion between HPLC and ESI-MS at room temperature. A number of different gradients were utilized as described in table 6-5.

Results and Discussion

A number of derivatives and their isomers of penicillin G were separated and identified by HPLC/ESI-MS/MS after the interaction between aqueous penicillin G and solid potassium superoxide. Most of these can be classified into the products of hydrolysis, oxidation, recombination reactions including dimerization, and chemiluminescent reaction.

Among these compounds benzylpenilloic acid (MW 308), benzylpenicillenic acid (MW 334), benzylpenillic acid (MW 334), and benzylpenicilloic acid (MW 352) were found which arise from the base-catalyzed hydrolysis of penicillin G in aqueous solutions. The chromatograms and mass spectra of HPLC/ESI-MS/MS of these four compounds plus penicillin G and the interpretations of mass spectra are presented in appendix A. The existence of these compounds was supported by the degradation pathway of penicillin G proposed by Kessler et al [124].

The oxidation of penicillin G and its derivatives occurred exclusively on the sulfur atom. Derivatives like compound 312 (a product of the oxidation of penicillamine, which is one of the products of hydrolysis of penicillin G), benzylpenilloic acid sulfoxide (MW 324), benzylpenillic acid sulfoxide (MW 350), and benzylpenicilloic acid (MW 368) are examples. Two isomers of penicillin G sulfone were also found and the experimental results and their interpretations are recorded in appendix B.

The recombination of the derivatives of penicillin G resulted in several new compounds, such as the dimer of penicillamine (MW 296), compound 440 (a product of recombining of compound 269 and benzylpenilloaldehyde, one of the hydrolysis products of penicillin G), compound 632 (a product of penicillamine dimer and benzylpenicilloic acid), and compound 642 (a product of benzylpenilloic acid and benzylpenicillenic acid). The HPLC/ESI-MS results and identifications of these compounds are in appendix C. The structures of these compounds and the mechanism of dimerization are summarized in table 6-6. It is believed that the thiol (penicillamine) loses a proton, and then it is oxidized by oxygen to form a free radical and radical coupling generates the dimer [125]. Singlet oxygen is probably involved in this process.

The identification of benzoic acid, compound 336, and compound 511 (a product of compound 336 and benzylpenilloaldehyde) appears to support that a chemiluminescent reaction was involved in the degradation of penicillin G following the oxidation by potassium superoxide. The data of mass spectra of these three compounds and their interpretation are shown in appendix D.

In addition, compound 269 and compound 353 were identified by their mass spectra, as described in appendix E, but their sources are unknown.

Figure 6-17 illustrates the total chromatogram between 0-26 min of HPLC/ESI-MS of sample PG and sample $PGKO_2$ while the HPLC gradient is 100% mobile phase B / 0% mobile phase A. The top chromatogram demonstrates the hydrolysis of penicillin G in the aqueous solution. The peak with the retention time of 22.15 min is most likely penicillin G and the other major peaks at 19.94 min, 20.08 min, 20.91 min, 22.59 min are the derivatives of penicillin G after hydrolysis. All of these were identified by their ESI-MS/MS and verified in the gradient, 100% mobile phase A / 0% mobile phase B. The retention time in different gradients, the structures, the molecular weight, and the mass / charge ratios of the parent ions are listed in table 6-7. The bottom chromatogram was acquired from sample $PGKO_2$ and it clearly shows that during the process of oxidation of penicillin G by potassium superoxide, the hydrolysis of penicillin G occurs as well. This is indicated by the observation that the intensities of the peaks at 19.88 min (the overlapping of peaks at 19.94 min and at 20.08 min in the chromatogram of sample PG) and at 22.59 min increased significantly, however, the peak of penicillin G at 22.15 min seems to have disappeared in the chromatogram of sample $PGKO_2$. The experimental results are consistent with the fact that superoxide is a strong base in aqueous solution [116] and once it entered aqueous solutions, it becomes a catalyst for the hydrolysis of penicillin G; thus, the degradation rate was increased. A close-look at the chromatogram of sample $PGKO_2$, as shown in Figure 6-18, shows that there are two major peaks with

retention times at 20.56 min and 20.81 min, which have no equivalents in the chromatogram of sample PG. The interpretation of the HPLC/ESI-MS of those two peaks suggests that they are benzylpenicillic acid sulfoxide and benzylpenilloic acid sulfoxide, as shown in table 6-8. Actually, by using different HPLC gradients, numerous sulfoxide of the derivatives of penicillin G were found, which were summarized in Figure 6-19, and the pathways of oxidation are specified.

Consider the chemiluminescences of thirteen β-lactam antibiotics. Since there are some sulfur compounds like Martin's sulfurane, which becomes chemiluminescent through sulfoxide or sulfone in the presence of DBA (9, 10-dibromoanthracene) [126], or rubrene [127], perhaps sulfoxide is the right intermediate to give chemiluminescence from β-lactam antibiotics. This is consistent with the fact that no chemiluminscence was observed with the reactions with azetidinone, clavulanic acid, and sulbactam. They either have no sulfur, or the sulfur is already oxidized to sulfone, as shown in table 6-9. This concept is not supported by the fact that as shown in table 6-9, methicillin, penicillin V, and cefotaxime did not emit chemiluminescence, even though they have sulfur in their structures. It is also impossible to rationalize the differently intensified chemiluminescences of penicillin G, dicloxacillin, piperacillin, ampicillin, cephalothin, amoxicillin, and hetacillin in table 6-10 when such a proposal is adopted. Furthermore, the maximum wavelength of chemiluminescence emitted from SO_2 ranges from 260 nm to 480 nm; for S_2, it is 275-425 nm; for HSO, it is 360-380 nm (table 1-4). Obviously, all of them don't match with the 535 nm of penicillin G, as determined in chapter 5.

Therefore, the claim that the chemiluminescence emitted by β-lactam antibiotics came from the oxidation of sulfur is not supported. On the other hand, the existence of benzoic acid, compound 336, and compound 511 in the degradation of penicillin G was proved by their HPLC/ESI (or APCI)-MS/MS and the involvement of singlet oxygen in the chemiluminescent reaction of the penicillin G reaction was verified by the D_2O experiments. It is proposed that the autoxidation initiated by singlet oxygen is the mechanism of the chemiluminescences emitted by β-lactam antibiotics. As shown in Figure 6-20, the dismutation of potassium superoxide generates singlet oxygen ($^1O_2$) and as a strong base in aqueous solutions, superoxide facilitates the removing the α-proton by $^1O_2$ to form dioxetanone and 6-aminopenicillanic acid (6-APA). Dioxetanone then loses carbon dioxide and generates the excited phenylcarbonyl cation, which emits the chemiluminescence at 535 nm by relaxation. Phenylcarbonyl cation can either recombine with 6-APA to produce compound 336, or be further oxidized by $^1O_2$ (or H_2O_2) to produce benzoic acid. Compound 511 is formed when compound 366 reacts with benzylpenilloaldehyde. Compound 336 and compound 511 are found by electrospray ionization (ESI) mass spectrometry. The mass spectra of individual peaks are also obtained to further confirm the structures (MS/MS). The presence of benzoic acid has been proved by negative atmosphere pressure chemical ionization (APCI) mass spectrometry. This type of reaction has two characteristic features: (1) an acidic α-proton whose removal by $^1O_2$ leaves a special stabilized carbon radical, (2) a good leaving group expelled by the attack by peroxide to give a dioxetanone. This proposed mechanism is

applied to rationalize the observations of table 6-9 and table 6-10. In table 6-9, the lack of side chains on azetidinone, sulbactam, and clavulanic acid results in the lack of chemiluminescence; no α-proton on methicillin and cefotaxime results in no chemiluminescence; for penicillin V, the oxygen on the side chain will repels the attack of $^1O_2$ on an α-proton and the chemiluminescence is inhibited. In table 6-10, although penicillin G emits the most intensified chemiluminescence, its chemiluminescent intensity is far lower than luminol, lucigene, luciferin, and other chemiluminescent compound. The conformation of penicillin G determines that the carbonyl and benzyl moiety can not be on the same plane, and the lack of conjugated electron-delocalized structure leads to decreased electron withdrawing ability, thus, the removal of the α-proton is restricted. The variation of the acidity of α-protons also indicates that the chemiluminescent intensities of amoxicillin < ampicillin < piperacillin < penicillin G, which is consistent with their decreased electron-withdrawing abilities. Because $^1O_2$ can works as an oxidizer for the sulfur of cephalothin and as a base to hydrolyze the side chain of hetacillin, whose five-member-ring side chain makes it more susceptible to hydrolysis than that of the other antibiotics, it is not surprising that the chances for chemiluminescence are decreased. The bulky side chain on the hetacillin can block the attack of $^1O_2$ on α-proton, which combined with ring strain facilitate the hydrolysis of the side chain. In an attempt to explain the large chemiluminescent intensity obtained with

dicloxacillin, which does not have an α-proton, a particular mechanism is proposed in which the light is emitted by the dioxetan as shown below:

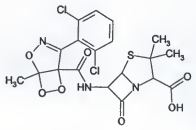

Extensive studies suggested that the most convenient method to produce dioxetans and dioxetanones is following reactions of olefins with singlet oxygen [128-131]. Various dioxetans fall sharply into two classes. Dioxetans with alkyl aryl or other substituents ("simple dioxetans") with little electron donating power yield triple exited carbonyl products, whereas the second type, with strongly electron donating substituents (mainly nitrogen and oxygen) gives very high yields of singlet excitation [132]. Possibly, the dioxetan of dicloxacillin belongs to the second class and further investigations are needed.

Finally, much data acquired from the HPLC-MS, D_2O, NMR, and TLC suggest that the mechanism of chemiluminescence of β-lactam antibiotics is autoxidation initiated by singlet oxygen.

Table 6-1: Effects of deuterium oxide on the intensities of chemiluminescence of penicillin G.

Deuterium Oxide concn, %	Relative integrated chemiluminescent intensity
100	204
70	61
50	22
0	20

Table 6-2: The response of spraying the three reagents on sample $PGKO_2$ and sample KO_2.

	$PGKO_2$		KO_2
	color	# of spots	# of spots
Vanillin	brown	1, L=3.0cm	none
Iodine-Azide	yellow	1, L=3.0cm	none
Ninhydrin	purple	3, L=1.3, 2.5, 3.2cm	none

Table 6-3: The elution time of TLC developments.

	Elution time (min.)					Average elution time (min.)
	Plate 1	Plate 2	Plate 3	Plate 4	Plate 5	
1st elution	41	44	42	44	44	43
2nd elution	39	39	37	40	40	39
3rd elution	40	38	37	39	36	38

Table 6-4: The retention times of the reference compounds and sample $PGKO_2$.

Injection	Concentration	Retention Time (min) with UV at 254 nm	Retention Time (min) with PDA[b]
hydrogen peroxide	0.03%	1.63	1.692
3, 4-dihydroxyl benzoic acid	0.01 mg/ml	2.71	2.795
p-hydroxyl benzoic acid	0.01 mg/ml	4.19	4.192
2, 4-dihydroxyl benzoic acid	0.01 mg/ml	4.20	5.178
2, 3-dihydroxyl benzoic acid	0.01 mg/ml	4.41	5.033
p-hydroxyl phenyl acetic acid	0.01 mg/ml	6.28	6.805
benzaldehyde	1/250[a]	8.95	8.907
benzoic acid	0.01 mg/ml	9.00	8.754
phenyl acetic acid	0.01 mg/ml	13.60	14.464
salicylic acid	0.01 mg/ml	14.35	14.97
major peaks of sample $PGKO_2$	2.0 mg/ml	3.61	4.267
		14.40	14.433
		21.99	25.333

[a]volumn ratio.

[b]on a different Exsil[R] ODS column.

Table 6-5: The operating conditions of HPLC.

File name	Sample	Gradient							Condition
SEQ1924a	mobile phase A	time (min)	0	5	30	50			phase A = 0.1% aqueous acetic acid during this analysis
		%A	50	0	0	50			
		%B	50	100	100	50			
SEQ1924b	sample PG[a]	time (min)	0	5	10	30	40	60	phase A changed to 50:50 water:acetonitrile by adding acetonitrile
		%A	0	0	100	100	0	0	
		%B	100	100	0	0	100	100	
SEQ1924c	sample PG[a]	time (min)	0	5	20	50	60	80	phase A = 0.1% acetic acid in 50:50 water:acetonitrile; phase B = 0.01M ammonium acetate (pH5.72) + 0.1% acetonitrile in water
		%A	0	0	100	100	0	0	
		%B	100	100	0	0	100	100	
SEQ1924d	sample $PGKO_2$[b]	time (min)	0	5	20	50	60	80	phase A = 0.1% acetic acid in 50:50 water:acetonitrile; phase B = 0.01M ammonium acetate (pH5.72) + 0.1% acetonitrile in water
		%A	0	0	100	100	0	0	
		%B	100	100	0	0	100	100	
SEQ1924e	mobile phase B	time (min)	0	15	25	50	60	80	phase A = 0.1% acetic acid in 50:50 water:acetonitrile; phase B = 0.01M ammonium acetate (pH5.72) + 0.1% acetonitrile in water
		%A	0	0	100	100	0	0	
		%B	100	100	0	0	100	100	
SEQ1924f	sample PG[a]	time (min)	0	15	25	50	60	80	phase A = 0.1% acetic acid in 50:50 water:acetonitrile; phase B = 0.01M ammonium acetate (pH5.72) + 0.1% acetonitrile in water
		%A	0	0	100	100	0	0	
		%B	100	100	0	0	100	100	
SEQ1924g	sample $PGKO_2$[b]	time (min)	0	15	25	50	60	80	phase A = 0.1% acetic acid in 50:50 water:acetonitrile; phase B = 0.01M ammonium acetate (pH5.72) + 0.1% acetonitrile in water
		%A	0	0	100	100	0	0	
		%B	100	100	0	0	100	100	

[a]1 mg/ml or 0.1 mg/ml of penicillin G in aqueous solution.

[b]is made from sample PG by reacting with solid potassium superoxide.

Table 6-6: The products of recombination including dimerization after penicillin G reacting with potassium superoxide.

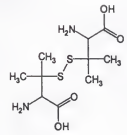

296=149+149
dimer of Penicillamine

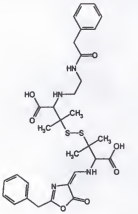

642=308(Benzylpenilloic Acid)+
334(Benzylpenicillenic Acid)

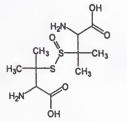

312=296+16

Mechanism:

$$RSH + B^- \rightleftharpoons RS^- + BH$$

$$RS^- + O_2 \longrightarrow RS + O_2^-$$

$$RS^- + O_2^- \longrightarrow RS^- + O_2^{2-}$$

$$2RS^- \longrightarrow RSSR$$

$$BH + O_2^{2-} \longrightarrow OH^- + B^- + O_2$$

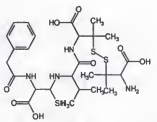

632=296+354(352+2H)-H_2O
352=Benzylpenicilloic Acid

Table 6-7: The major products of hydrolysis of penicillin G after interacting with potassium superoxide.

Mobile Phase A [0.1%HOAc in 50:50 H2O:ACN]	Mobile Phase B [0.01 M NH4OAc (pH 5.72) + 0.1% ACN]	Compound
RT7.79 min	RT19.94 min	benzylpenicilloic acid $C_{16}H_{20}N_2O_5S$, MW352 $[M+H]^+$ = m/z 353.4 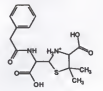
RT9.58 min	RT20.08 min	benzylpenillic acid $C_{16}H_{18}N_2O_4S$, MW334 $[M+H]^+$ = m/z 335.4 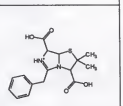
RT10.09 min	RT20.91 min	benzylpenicillenic acid $C_{16}H_{18}N_2O_4S$, MW334 $[M+H]^+$ = m/z 335.4 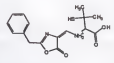
RT11.77 min	RT22.15 min	penicillin G $C_{16}H_{18}N_2O_4S$, MW334 $[M+H]^+$ = m/z335.4 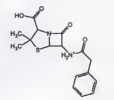
RT12.26 min	RT22.59 min	benzylpenilloic acid $C_{15}H_{20}N_2O_3S$, MW 308 $[M+H]^+$ = m/z 309.4 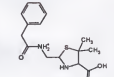

Table 6-8: The major products of oxidation of penicillin G after interacting with potassium superoxide.

Mobile Phase A [0.1%HOAc in 50:50 H2O:ACN]	Mobile Phase B [0.01M NH4OAc(pH5.72) + 0.1%ACN]	Compound
RT11.54 min	RT20.74 min	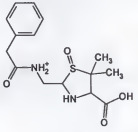 benzylpenilloic acid sulfoxide $C_{15}H_{20}N_2O_4S$, MW324 $[M+H]^+$ = m/z325.40
RT11.57 min	RT20.56 min	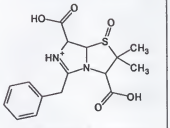 benzylpenillic acid sulfoxide $C_{15}H_{18}N_2O_5S$, MW350 $[M+H]^+$ = m/z351.39

Table 6-9: The six β-lactam antibiotics that emit no chemiluminescence.

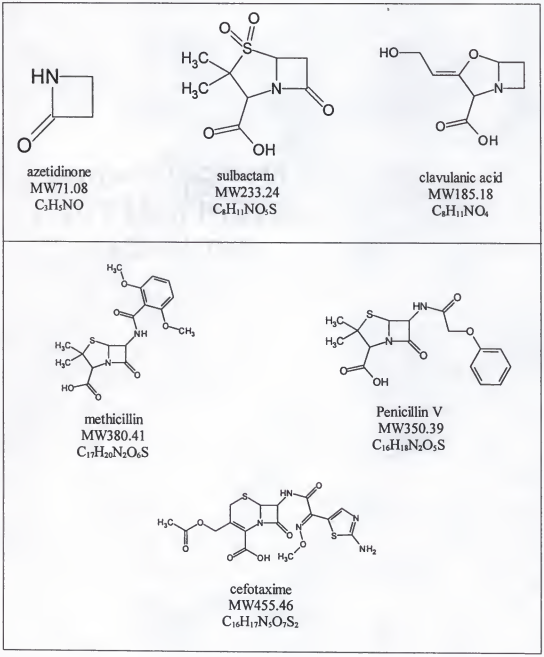

Table 6-10: The seven β-lactam antibiotics that emit chemiluminescences.

Antibiotic	Structure	Relative Intensity
Penicillin G	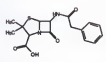	100
Dicloxacillin	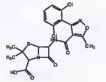	54.4
Piperacillin	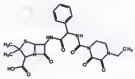	47.9
Ampicillin	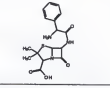	43.3
Cephalothin	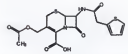	8.3
Amoxicillin	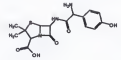	5.6
Hetacillin	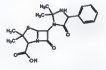	0.6

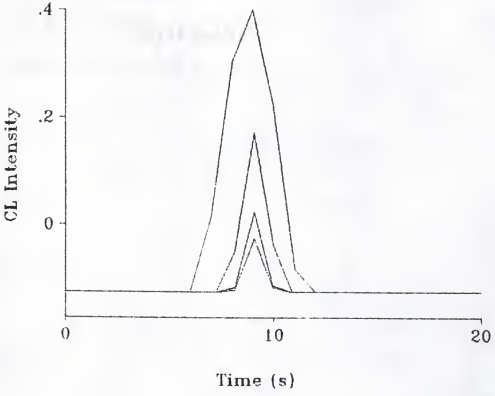

Figure 6-1: The profile of chemiluminescences of penicillin G in different solutions with varied deuterium oxide to water ratios.

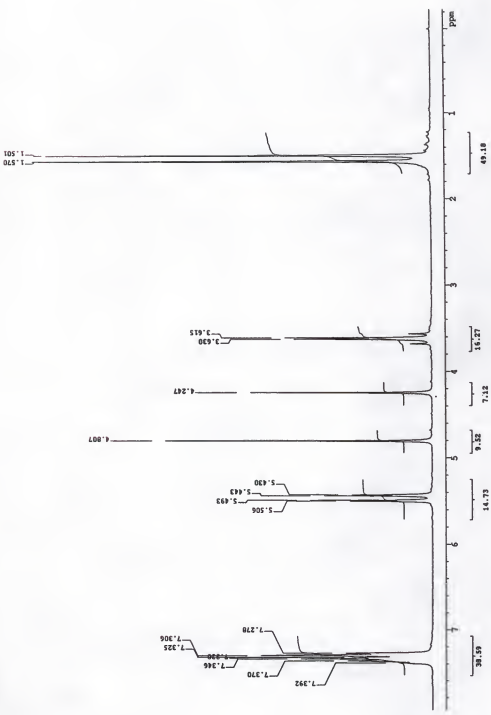

Figure 6-2: ^{1}H-NMR spectrum of potassium penicillin G in D_2O.

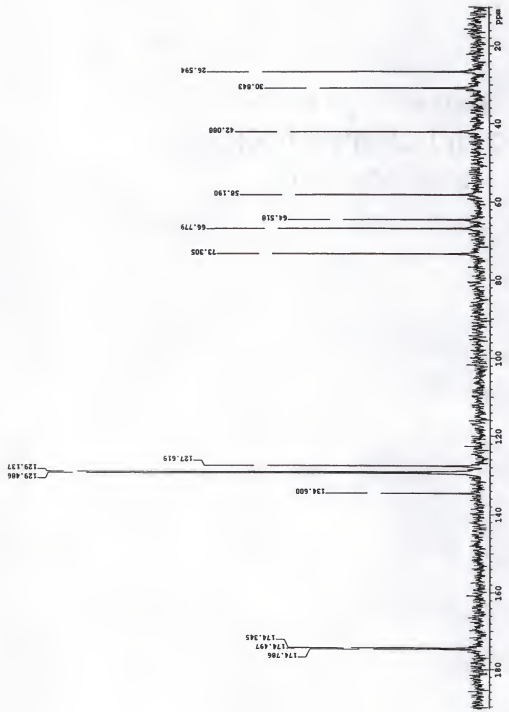

Figure 6-3: ^{13}C-NMR spectrum of potassium penicillin G in D_2O.

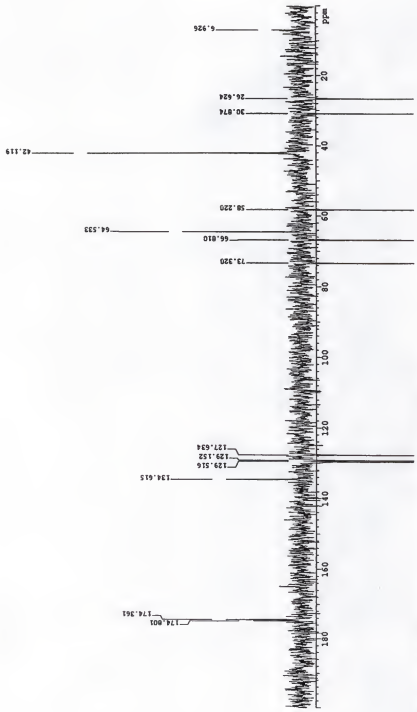

Figure 6-4: APT spectrum of potassium penicillin G in D_2O.

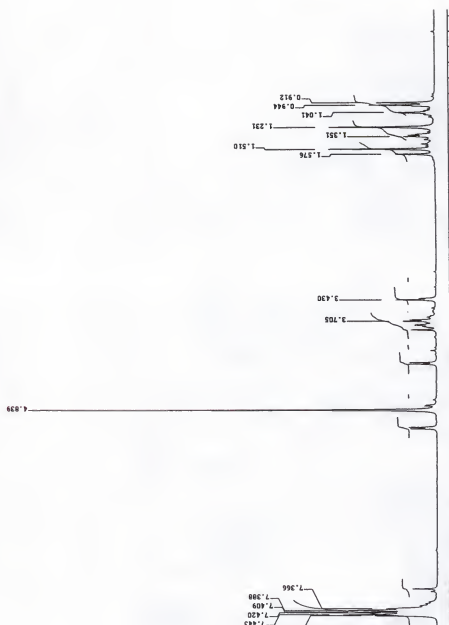

Figure 6-5: ^{1}H-NMR spectrum of the degradation products of potassium penicillin G in D_2O after the oxidation by solid KO_2.

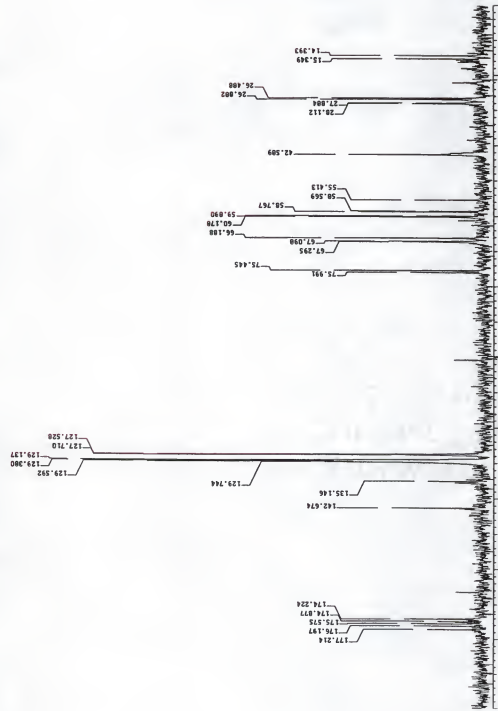

Figure 6-6: ^{13}C-NMR spectrum of the degradation products of potassium penicillin G in D_2O after the oxidation by solid KO_2.

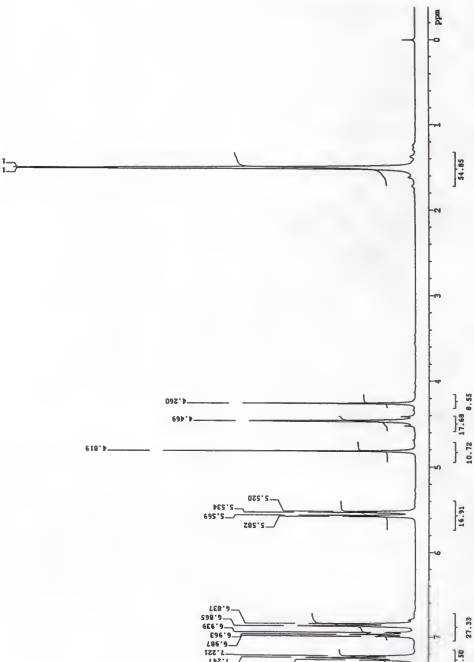

Figure 6-7: ^{1}H-NMR spectrum of potassium penicillin V in D_2O.

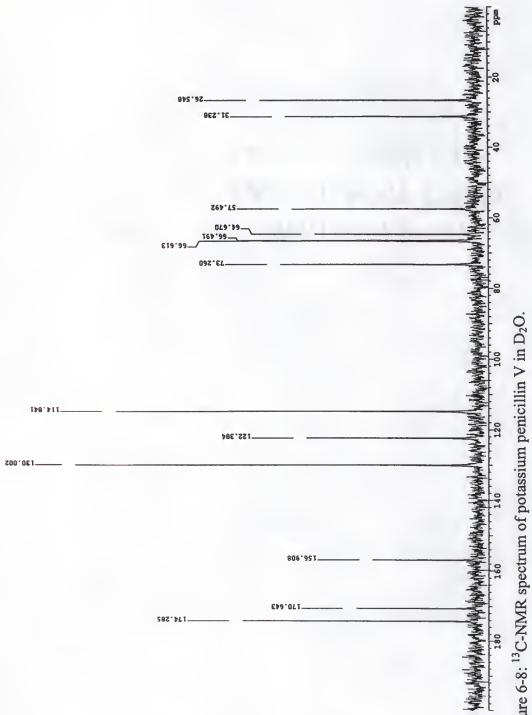

Figure 6-8: ^{13}C-NMR spectrum of potassium penicillin V in D_2O.

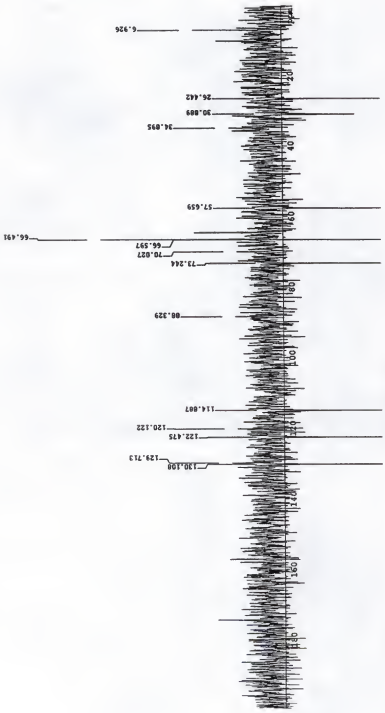

Figure 6-9: APT spectrum of potassium penicillin V in D_2O.

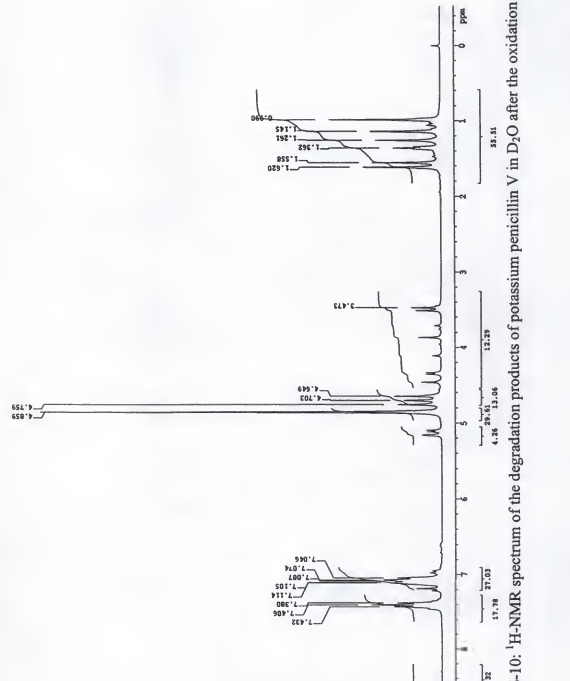

Figure 6-10: ^{1}H-NMR spectrum of the degradation products of potassium penicillin V in D_2O after the oxidation by solid KO_2.

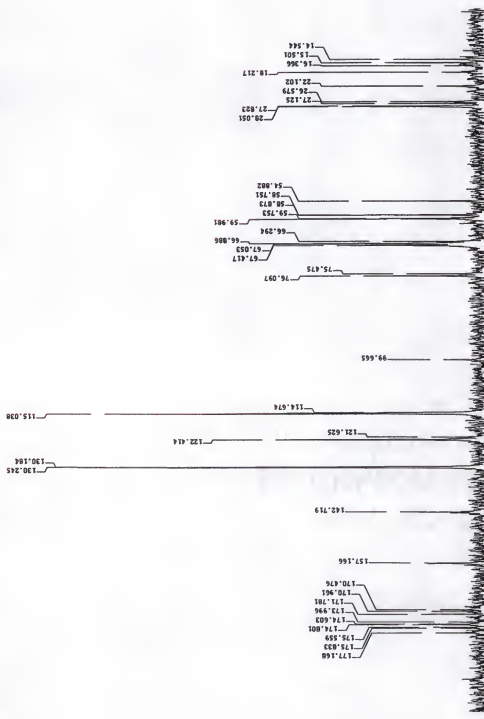

Figure 6-11: ^{13}C-NMR spectrum of the degradation products of potassium penicillin V in D_2O after the oxidation by solid KO_2.

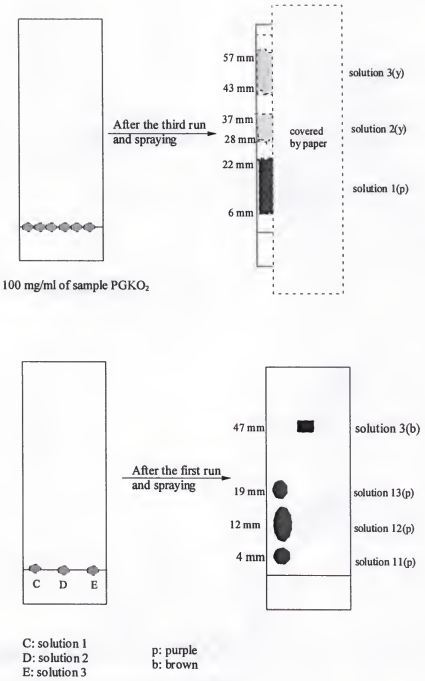

Figure 6-12: The schematic diagrams of TLC assays on sample PG and sample $PGKO_2$.

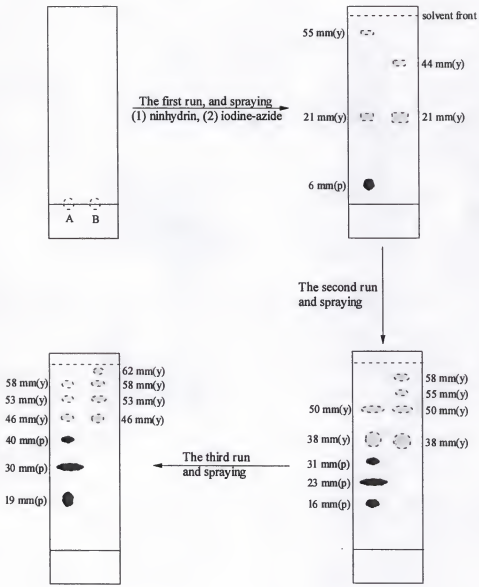

A: 10 mg/ml of sample $PGKO_2$ p: purple
B: 10 mg/ml of sample PG y: yellow

Figure 6-13: the schematic diagrams of preparing the samples for mass spectroscopy by the TLC separations.

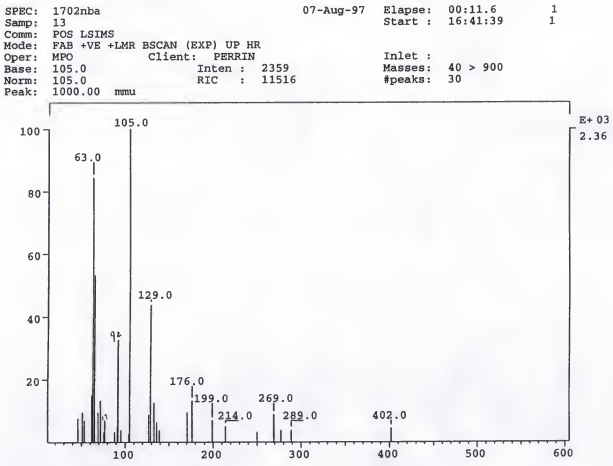

Figure 6-14: The FAB-mass spectrum of the sample from spot 13.

a

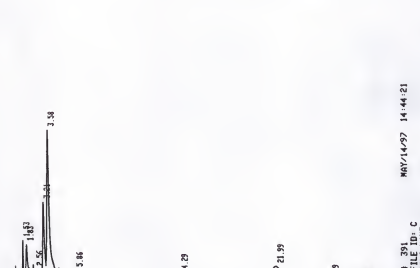

b

Figure 6-15: The chromatograms of sample PG (a) and sample $PGKO_2$ (b). The buffer system: pH5.66 phosphate buffer containing 0.1% acetonitrile.

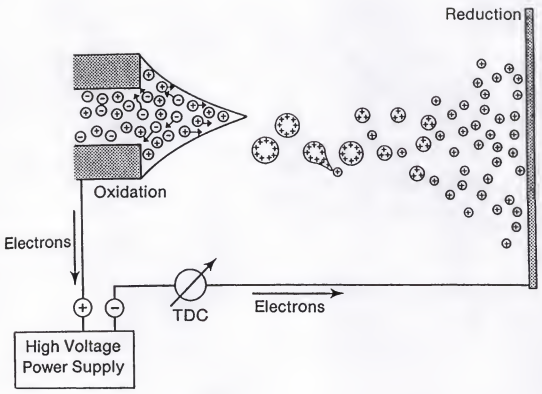

Figure 6-16: Schematic of major processes occurring in electrospray.

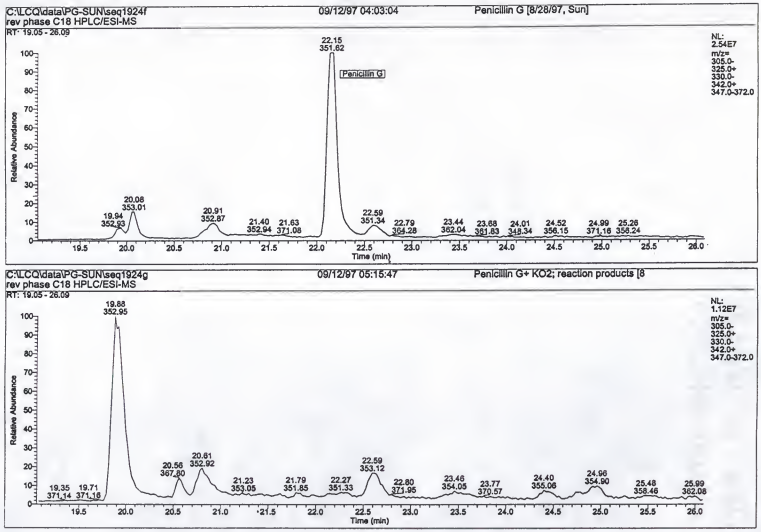

Figure 6-17: The total chromatograms of sample PG and sample $PGKO_2$.

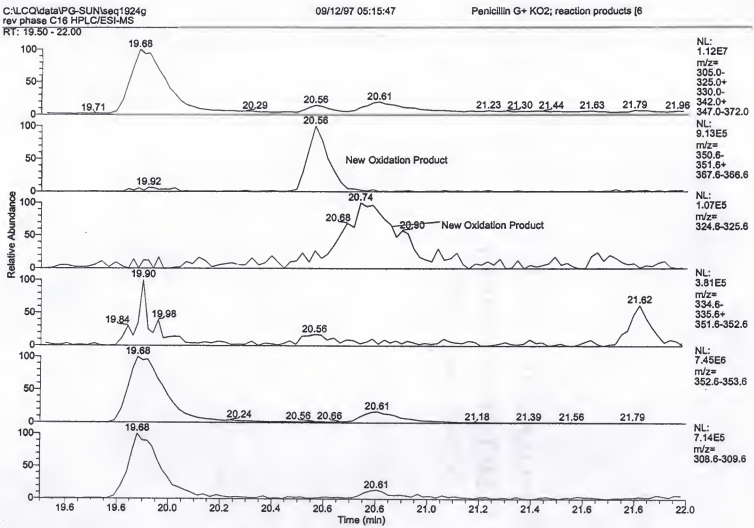

Figure 6-18: The zoom-in chromatograms of the new oxidation products generated by sample $PGKO_2$.

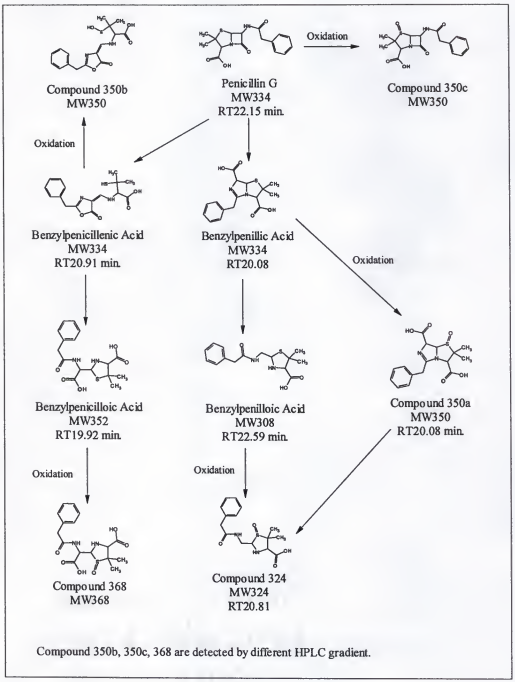

Figure 6-19: The scheme of generation of sulfoxides after penicillin G reacts with potassium superoxide.

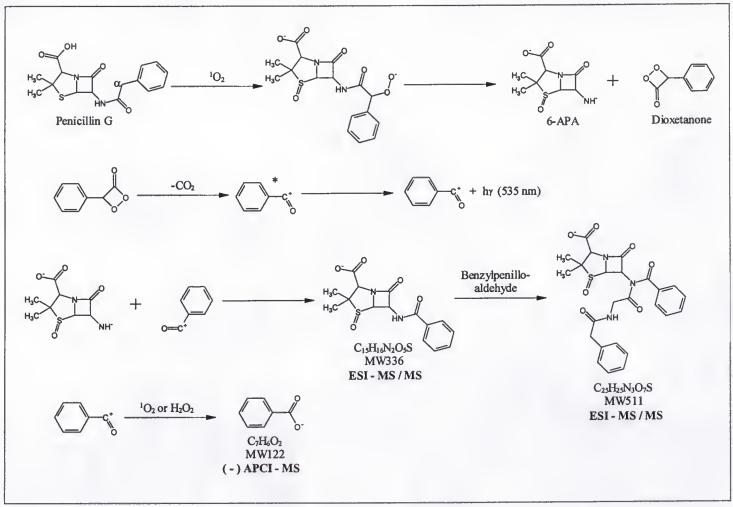

Figure 6-20: The proposed chemiluminescent mechanism of penicillin G following the oxidation by potassium superoxide.

CHAPTER 7
SUMMARY

The conversion mechanism of superoxide anion in aqueous system can be described as the followings:

Superoxide dismutation: $2O_2^{\cdot-} + 2H^+ \longrightarrow H_2O_2 + O_2(^1\Delta_g)$

Haber-Weiss Reactions: $H_2O_2 + O_2^{\cdot-} \longrightarrow O_2(^1\Delta_g) + OH^- + OH^{\cdot}$

$H_2O_2 + OH^{\cdot} \longrightarrow H_2O + HO_2^{\cdot}$

$HO_2^{\cdot} \rightleftharpoons H^+ + O_2^{\cdot-}$

$OH^{\cdot} + O_2^{\cdot-} \longrightarrow O_2(^1\Delta_g) + OH^-$

Quenching reaction: $O_2(^1\Delta_g) + O_2^{\cdot-} \longrightarrow {}^3O_2 + O_2^{\cdot-} + 22\ kcal$

Chemiluminescent reaction: $O_2(^1\Delta_g) \longrightarrow {}^3O_2 + h\gamma\ (1270nm)$

$${}^3O_2 + H_2O \rightleftharpoons 2H_2O_2$$

The superoxide anion has been proved to be relatively unreactive toward most biological components. This is supported by the observations that no chemiluminescence

was detected when superoxide anion in 18-crown-6-ether-acetonitrile was used to oxidize penicillin G in acetonitrile, methanol, butanol, and chloroform. In these solvents superoxide anion will not readily convert into other reactive forms and these observations indicate that superoxide anion itself is not capable of oxidizing penicillin G with the emission of chemiluminescence. However, in aqueous solution, through the superoxide dismutation reaction, superoxide can generate reactive species, for example, hydrogen peroxide and singlet oxygen ($^1O_2$). Hydrogen peroxide is used extensively as a source of $^3O_2$ and it is not reactive enough to oxidize the thirteen β-lactam antibiotics with the resultant emissions of chemiluminescence. This leaves $^1O_2$ as the most probably reactant for the oxidation of penicillin G and the emission of chemiluminescence. The involvement of $^1O_2$ in the chemiluminescent reaction of penicillin G after reacting with potassium superoxide was strongly indicated by the D_2O experiment using deuterium oxide instead of water as the solvent for penicillin G. Meanwhile, no chemiluminescence was measured with penicillin G in phosphate buffer. It is believed that $^1O_2$ is probably quenched by phosphate buffers. The experiments had indicated that pH4.5-7 is the best pH range for the chemiluminescences of β-lactam antibiotics because they are stable in the solutions with pH values close to neutral and the superoxide is easily converted into $^1O_2$ by superoxide dismutation reaction. The degradation studies of penicillin G by HPLC/ESI(or APCI)-MS/MS suggested that the chemiluminescence of β-lactam antibiotics was generated by the autoxidation initiated by $^1O_2$. This type of reactions is

also the pattern of luciferins and many related compounds. The maximum wavelength at 535 nm of chemiluminescent penicillin G is very close to that of Lucifer's at 562 nm. The low efficiency of penicillin G's chemiluminescence is consistent with its chemical structure and the fact that superoxide is a highly efficient $^1O_2$ quencher. The presence of $^1O_2$ was also proved by the characteristic 1268 nm chemiluminescent emission spectrum of $^1O_2$ as discussed in chapter 1. On the contrary, no detectable hydroxyl radical was involved in the degradation of penicillin G, because no aromatic hydroxyl substituted derivatives was observed by NMR and mass spectrometry. Perhaps, the hydroxyl radical can be postulated to be a short-lived transient intermediate, which is produced by the Haber-Weiss reaction, however, the data collected in this dissertation reinforce that $^1O_2$ rather than hydroxyl radical is the prime oxidant in the reaction system. Even though transition metals are available *in vivo*, the metal-catalyzed Haber-Weiss reaction will face competition from Fenton-type reactions, in which H_2O_2 interacts with transition metals or metal complexes to generate hydroxyl radicals. Indeed, The questions arise which is the crucial toxic species, singlet oxygen or the hydroxyl radical, and whether the hydroxyl radical comes from the metal catalyzed Haber-Weiss reaction or from a Fenton-type reaction. The answer to these questions must be specified in order to better understand oxygen toxicity and develop new therapeutic strategies as well as new antioxidants.

GLOSSARY

APCI	Atmospheric pressure chemical ionization
APT	Attached proton test
ATP	Adenosine triphosphate
BHT	Butylated hydroxytoluene
CFFAB	Continuous-flow fast atom bombardment ionization
CI	Chemical ionization
CNS	Central nervous system
DEPT	Distortionless enhancement by polarization transfer
DMSO	Dimethyl sulfoxide
DNA	Deoxyribonucleic acid
EI	Electron impact
ESI	Electospray ionization
ET	Electron transfer (or exited state)
FAB	Fast atom bombardment
FWHM	Full width at half maximum
GC	Gas chromatography
HPLC	High pressure (or performance) liquid chromatography
HV	High voltage
MS	Mass spectrometry
NMR	Nuclear magnetic resonance
ODS	Octadecylsilane
PB	Particle beam
PDA	Photodiode array
PMT	Photomultiplier tube
RSP	Relative standard deviation
SOD	Superoxide dismutation
TLC	Thin-layer chromatography
TME	Tetramethylene
TSP	3-(trimethylsilyl) propionic-2,2,3,3-d4 acid (or thermospray ionization)
UV	Ultraviolet

APPENDIX A
THE PRODUCTS OF HYDROLYSIS OF PENICILLIN G FOLLOWING THE INTERACTION WITH POTASSIUM SUPEROXIDE – THE CHROMATOGRAMS AND MASS SPECTRA OF HPLC/ESI-MS/MS.

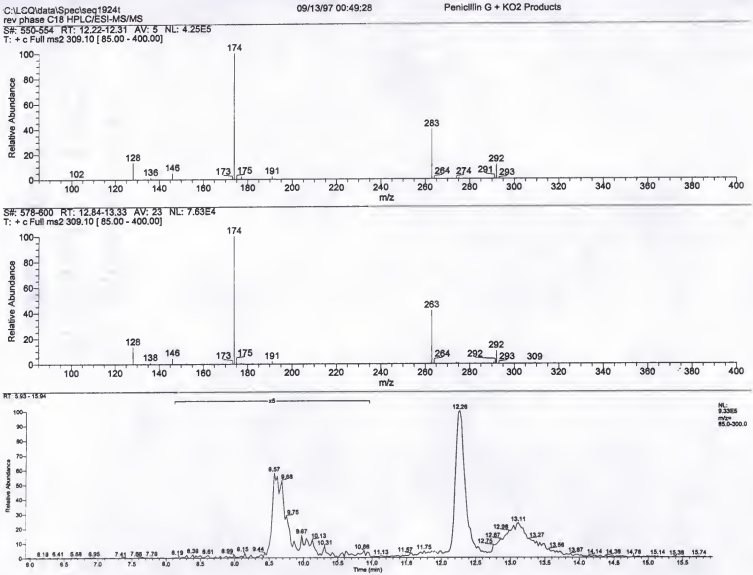

Figure A-1: The positive HPLC/ESI-MS/MS of benzylpenilloic acid.

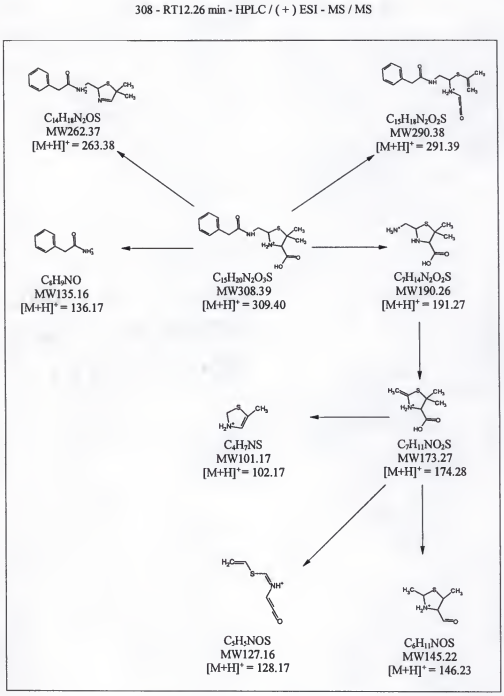

Figure A-2: The interpretation of the positive HPLC/ESI-MS/MS of benzylpenilloic acid.

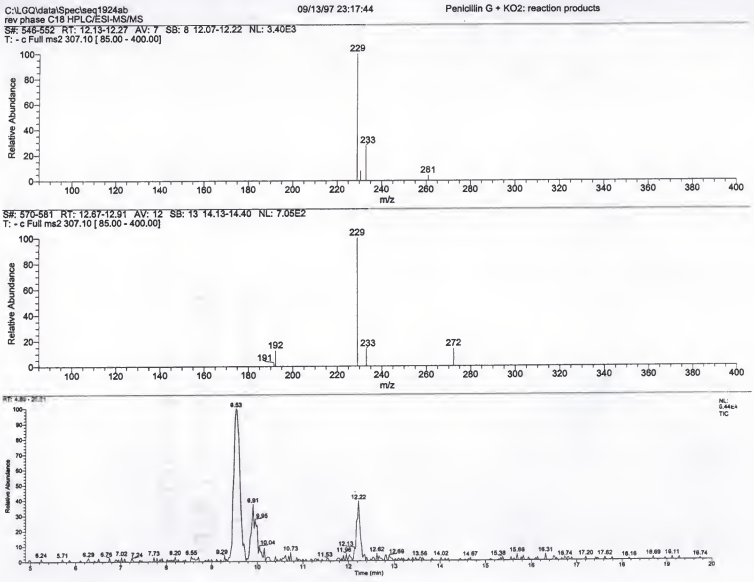
C:\LGC\data\Spec\seq1924ab
09/13/97 23:17:44
Penicillin G + KO2: reaction products
rev phase C18 HPLC/ESI-MS/MS
SF: 545-552 RT: 12.13-12.27 AV: 7 SB: 8 12.07-12.22 NL: 3.40E3
T: - c Full ms2 307.10 [85.00 - 400.00]
Relative Abundance
m/z
SF: 570-581 RT: 12.87-12.91 AV: 12 SB: 13 14.13-14.40 NL: 7.05E2
T: - c Full ms2 307.10 [85.00 - 400.00]
Relative Abundance
m/z
RT: 4.86 - 20.31
NL: 0.44E4 TIC
Relative Abundance
Time (min)

Figure A-3: The negative HPLC/ESI-MS/MS of benzylpenilloic acid.

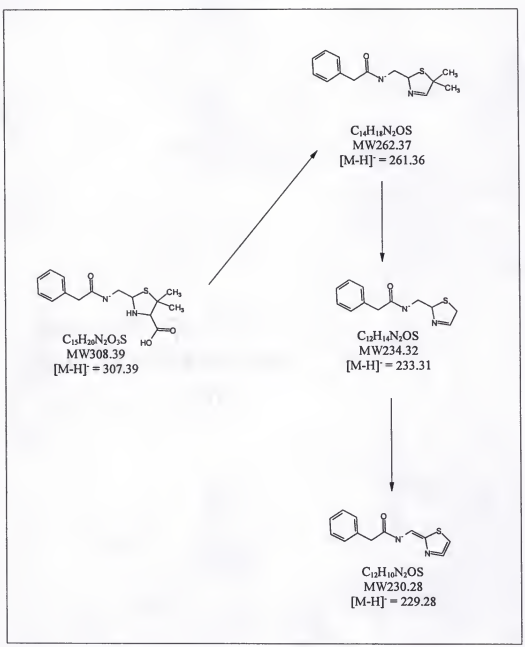

Figure A-4: The interpretation of the negative HPLC/ESI-MS/MS of benzylpenilloic acid.

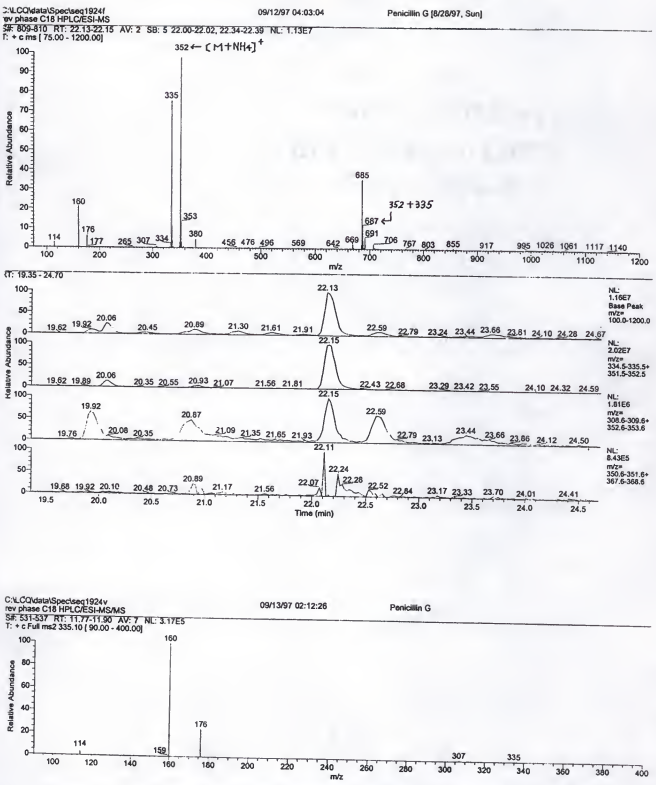

Figure A-5: The positive HPLC/ESI-MS/MS of penicillin G and MS/MS of m/z 335.

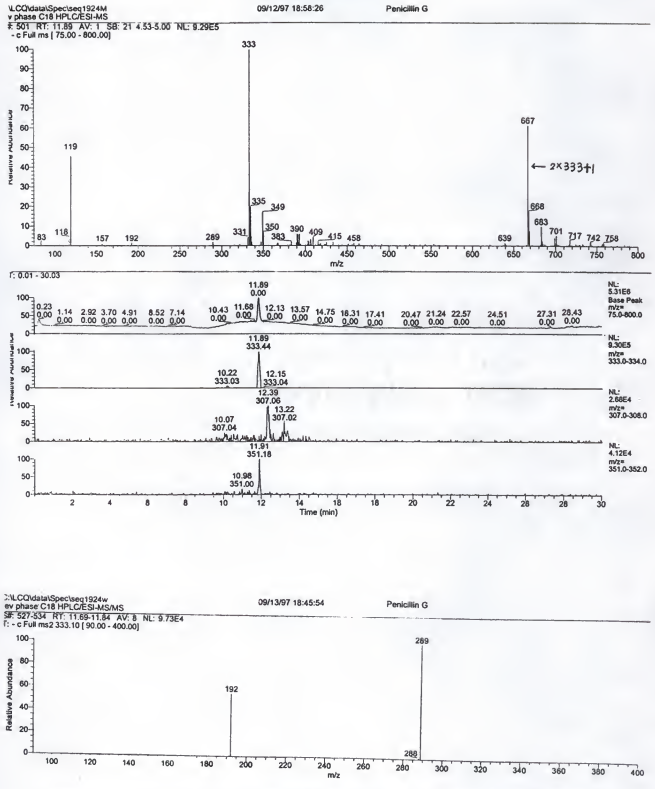

Figure A-6: The negative of HPLC/ESI-MS/MS of penicillin G and MS/MS of m/z 333.

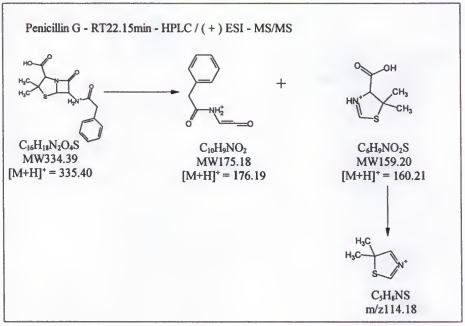

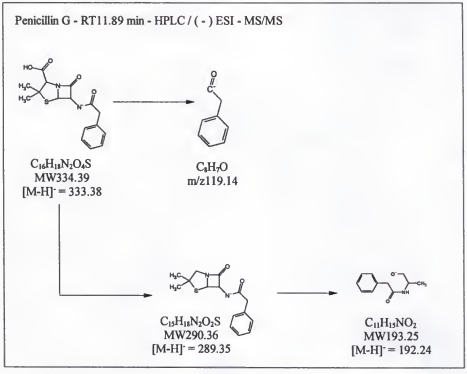

Figure A-7: The interpretations of the positive and negative HPLC/ESI-MS/MS of penicillin G.

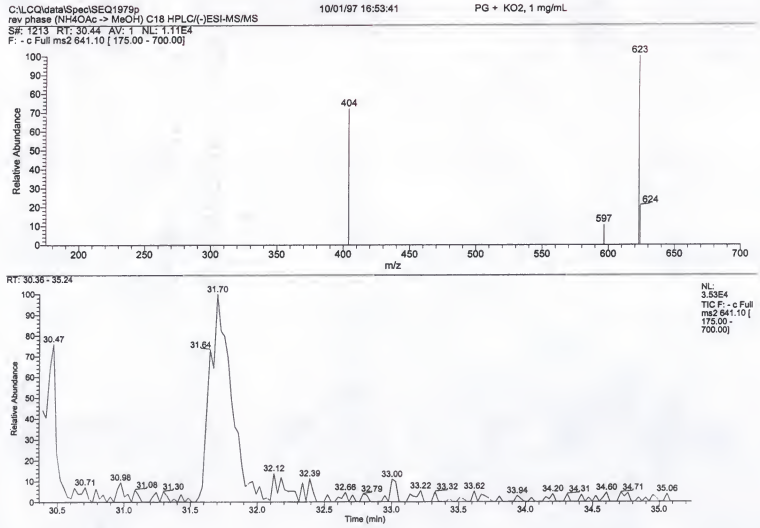

Figure A-8: The positive HPLC/ESI-MS/MS of benzylpenillic acid.

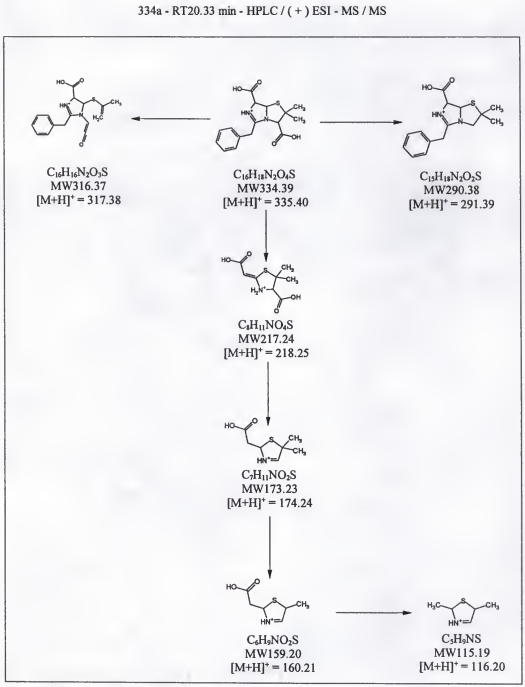

Figure A-9: The interpretation of the positive HPLC/ESI-MS/MS of benzylpenillic acid.

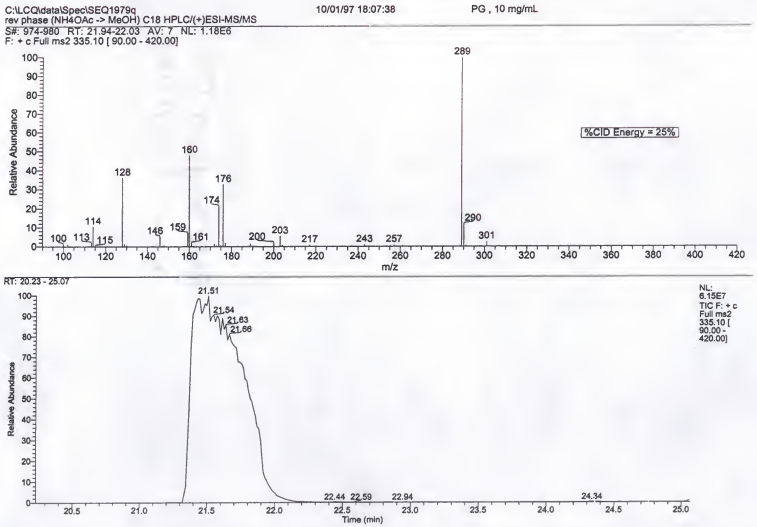

Figure A-10: The positive HPLC/ESI-MS/MS of benzylpenicillenic acid.

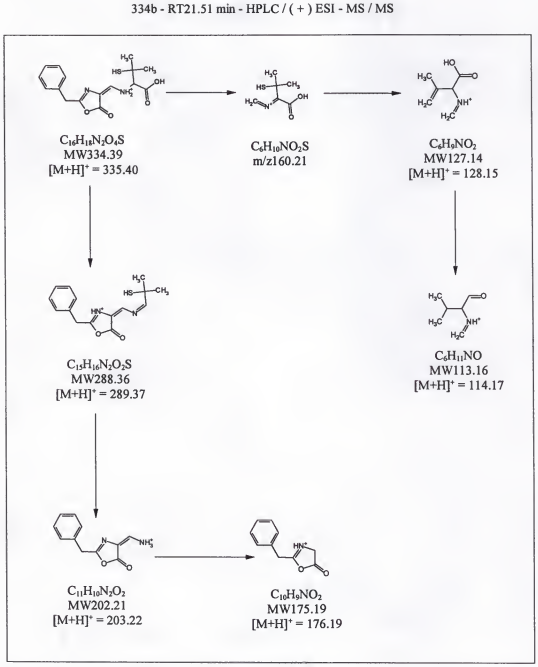

Figure A-11: The interpretation of the positive HPLC/ESI-MS/MS of benzylpenicillenic acid.

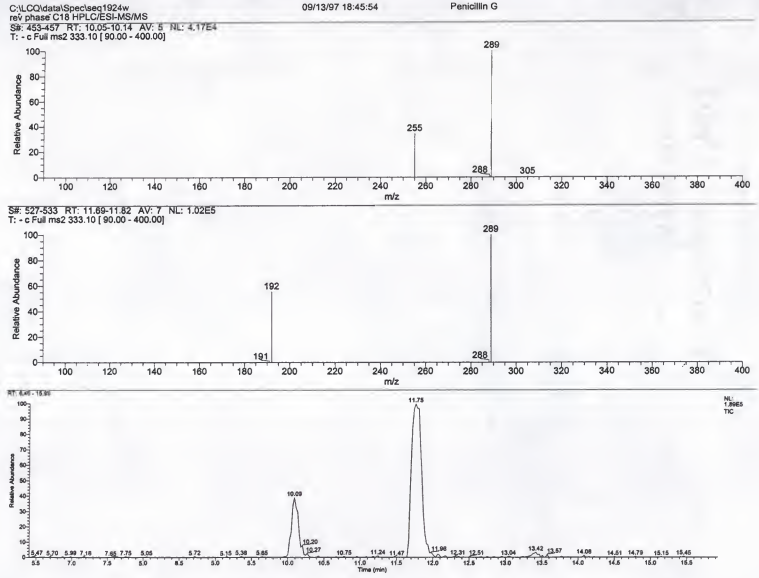

Figure A-12: The negative HPLC/ESI-MS/MS of benzylpenicillenic acid.

334b - RT10.09 min - HPLC / (-) ESI - MS / MS

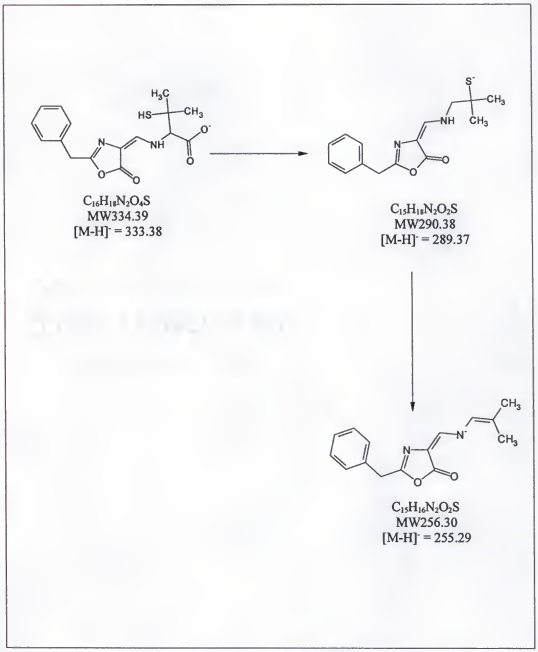

Figure A-13: The interpretation of the negative HPLC/ESI-MS/MS of benzylpenicillenic acid.

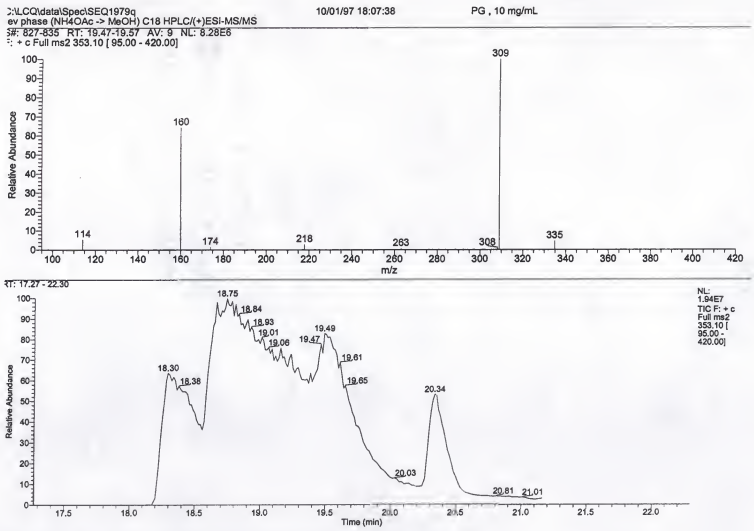

Figure A-14: The positive HPLC/ESI-MS/MS of benzylpenicilloic acid.

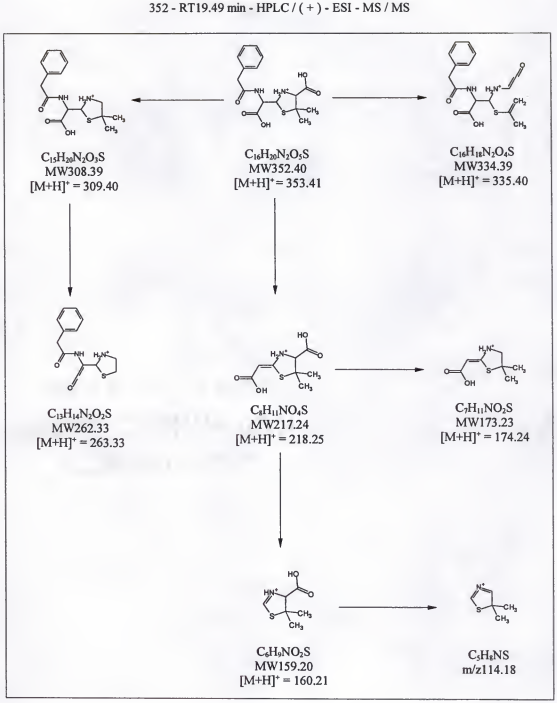

Figure A-15: The interpretation of the positive HPLC/ESI-MS/MS of benzylpenicilloic acid.

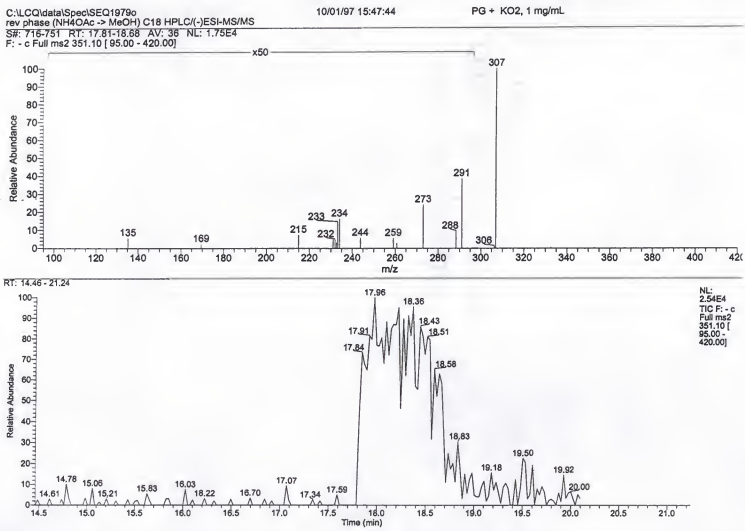

Figure A-16: The negative HPLC/ESI-MS/MS of benzylpenicilloic acid.

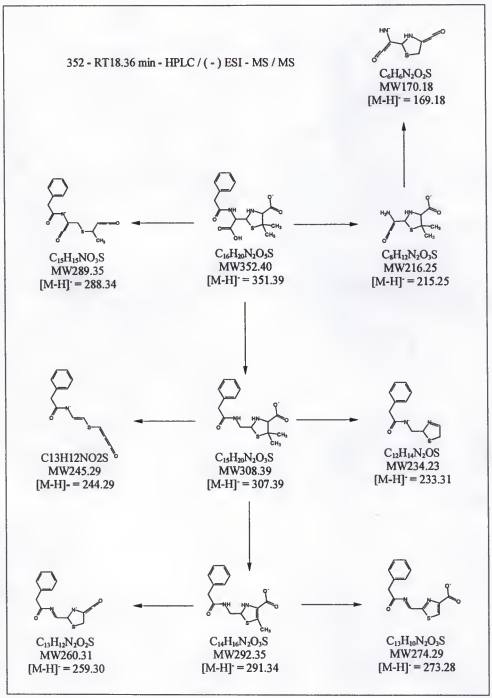

Figure A-17: The interpretation of the negative HPLC/ESI-MS/MS of benzylpenicilloic acid.

APPENDIX B
THE PRODUCTS OF OXIDATION OF PENICILLIN G FOLLOWING THE INTERACTION WITH POTASSIUM SUPEROXIDE – THE CHROMATOGRAMS AND MASS SPECTRA OF HPLC/ESI-MS/MS.

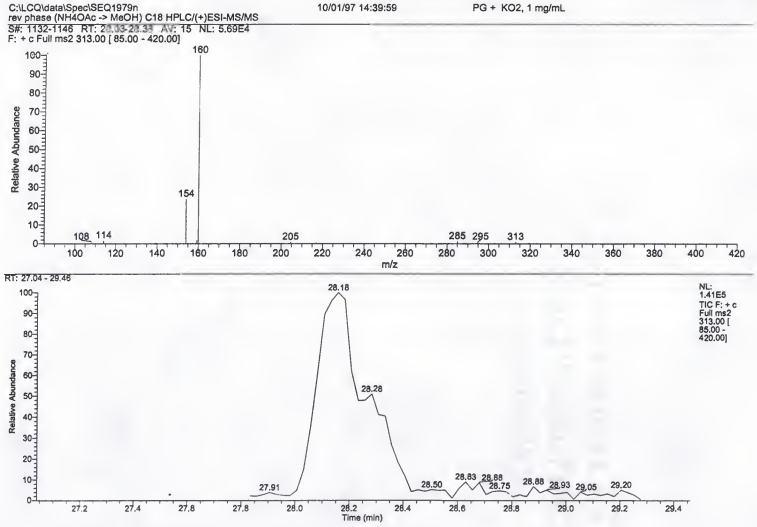

Figure B-1: The positive HPLC/ESI-MS/MS of the sulfoxide of penicillamine dimer.

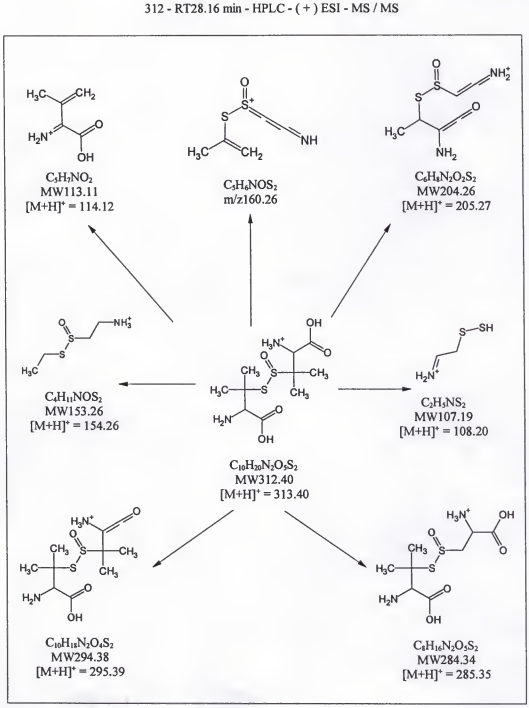

Figure B-2: The interpretation of the positive HPLC/ESI-MS/MS of the sulfoxide of penicillamine dimer.

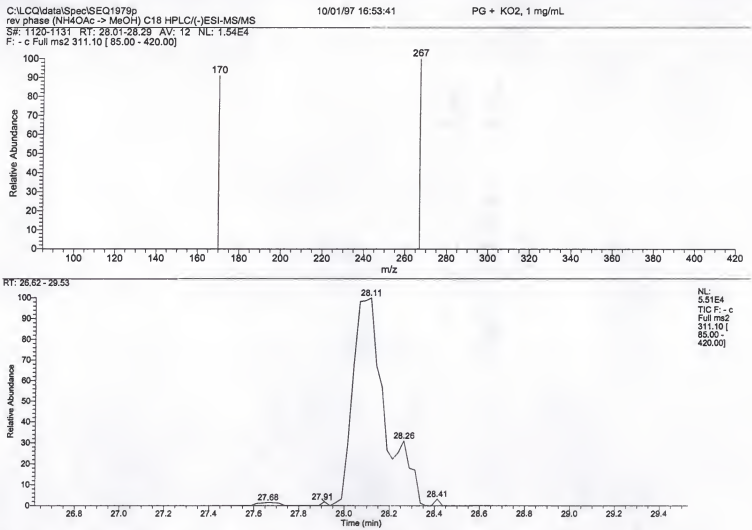

Figure B-3: The negative HPLC/ESI-MS/MS of the sulfoxide of penicillamine dimer.

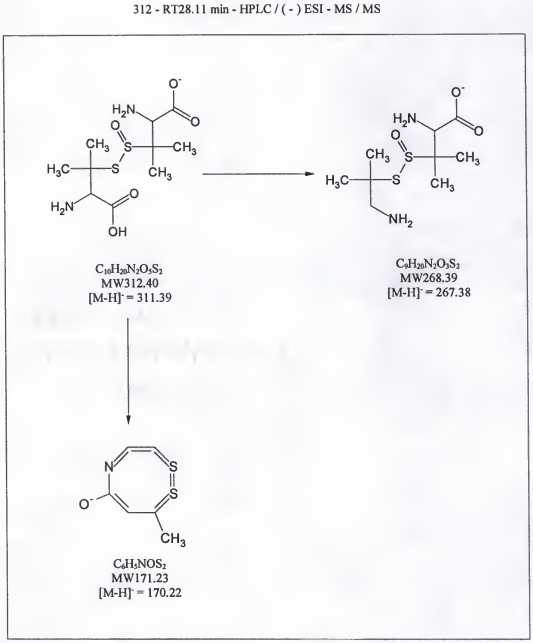

Figure B-4: The interpretation of the negative HPLC/ESI-MS/MS of the sulfoxide of penicillamine dimer.

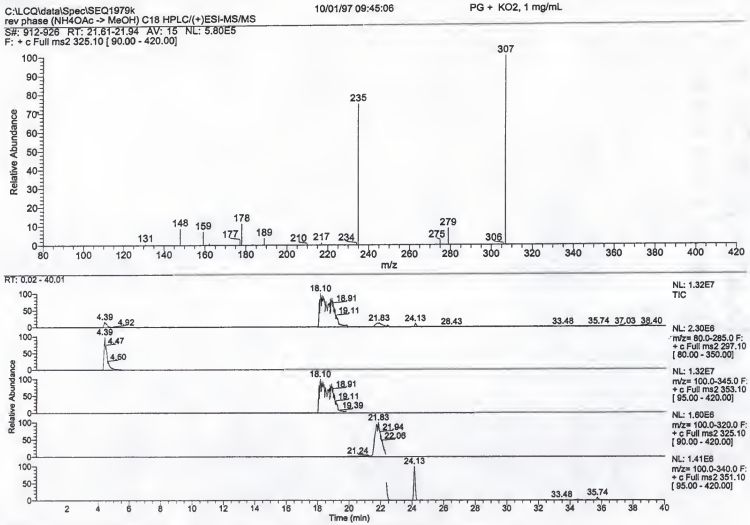

Figure B-5: The positive HPLC/ESI-MS/MS of benzylpenilloic acid sulfoxide.

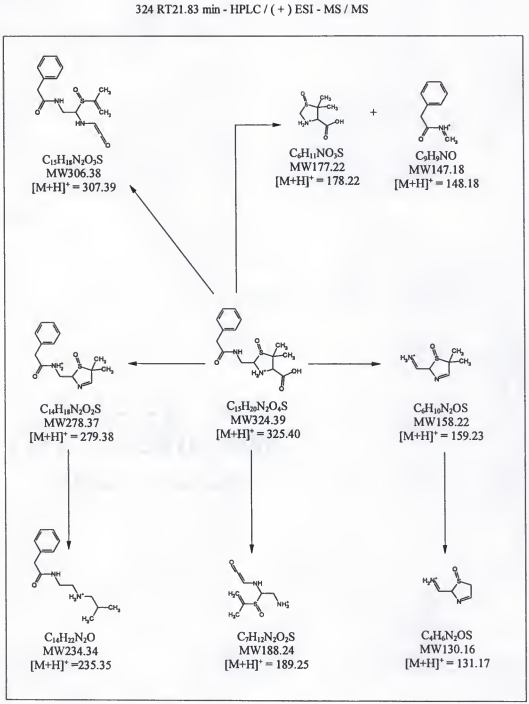

Figure B-6: The interpretation of the positive HPLC/ESI-MS/MS of benzylpenilloic acid sulfoxide.

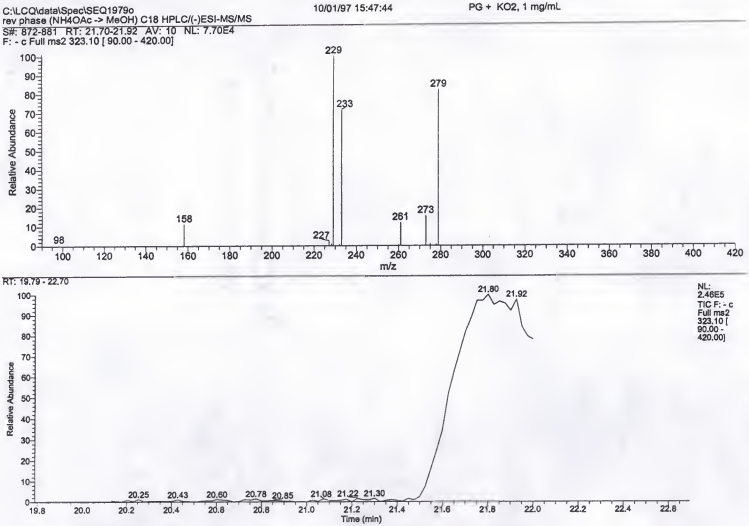

Figure B-7: The negative HPLC/ESI-MS/MS of benzylpenilloic acid sulfoxide.

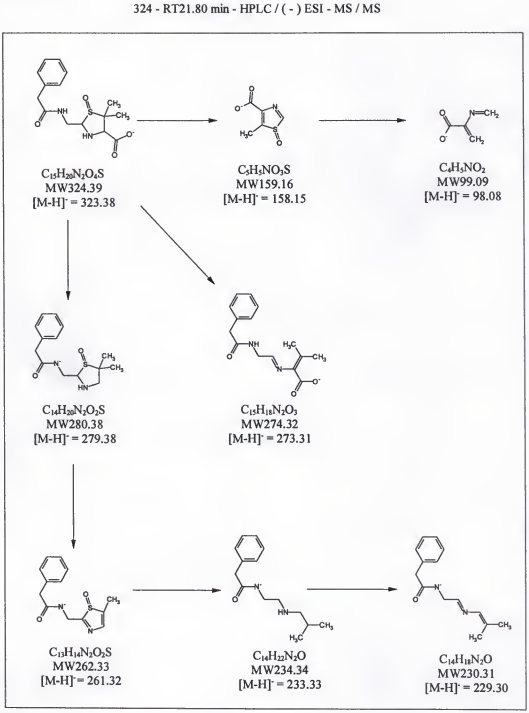

Figure B-8: The interpretation of the negative HPLC/ESI-MS/MS of benzylpenilloic acid sulfoxide.

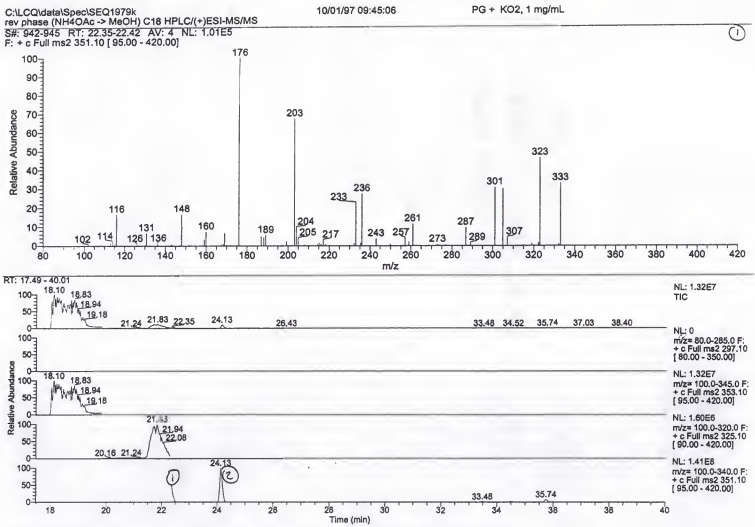

Figure B-9: The positive HPLC/ESI-MS/MS of benzylpenillic acid sulfoxide.

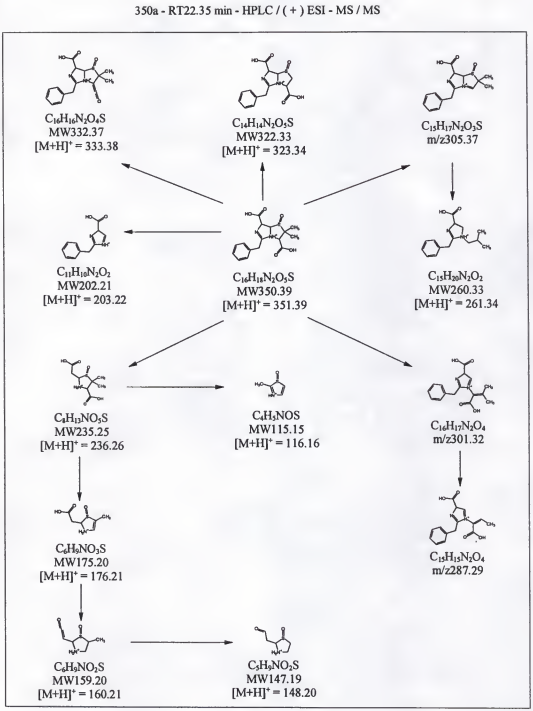

Figure B-10: The interpretation of the positive HPLC/ESI-MS/MS of benzylpenillic acid sulfoxide.

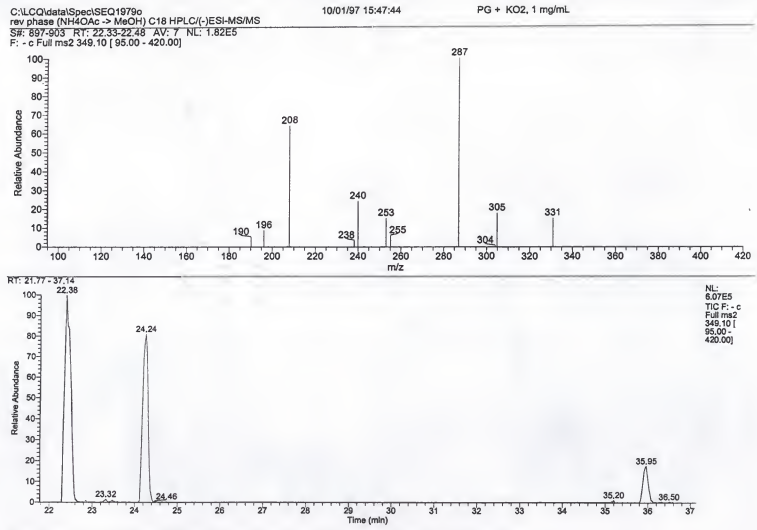

Figure B-11: The negative HPLC/ESI-MS/MS of benzylpenillic acid sulfoxide.

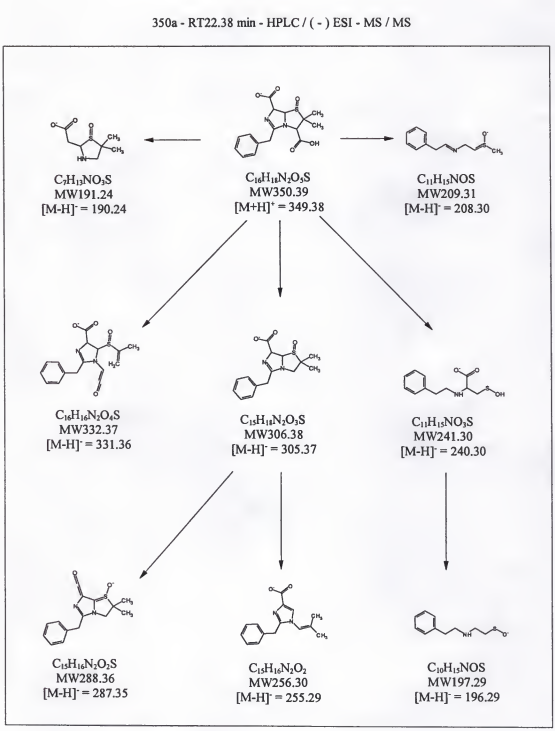

Figure B-12: The interpretation of the negative HPLC/ESI-MS/MS of benzylpenillic acid sulfoxide.

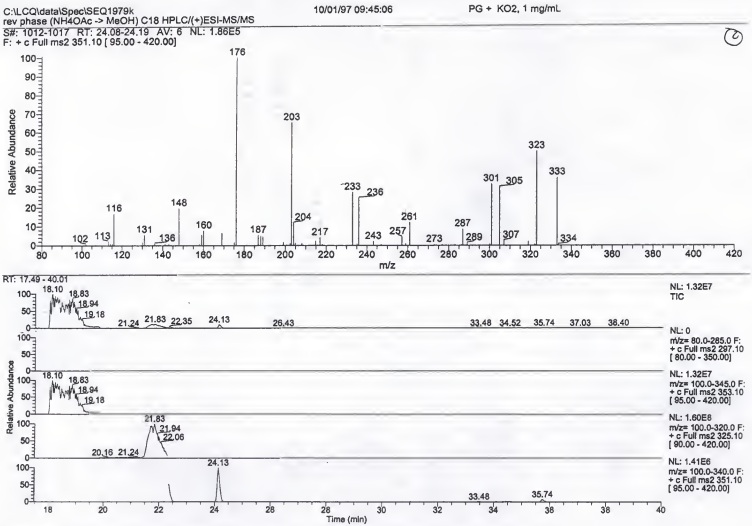

Figure B-13: The positive HPLC/ESI-MS/MS of benzylpenicillenic acid sulfoxide.

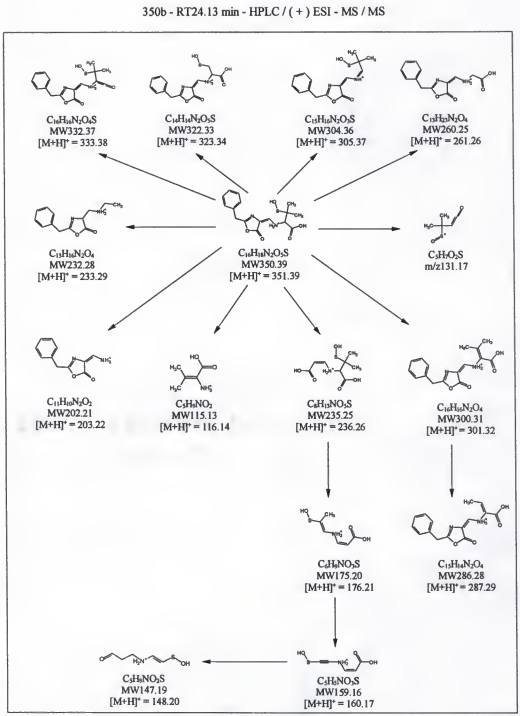

Figure B-14: The interpretation of the positive HPLC/ESI-MS/MS of benzylpenicillenic acid sulfoxide.

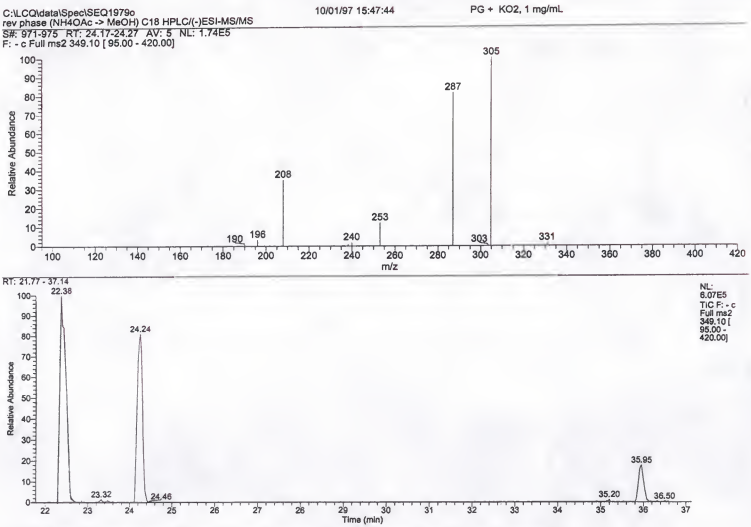

Figure B-15: The negative HPLC/ESI-MS/MS of benzylpenicillenic acid sulfoxide.

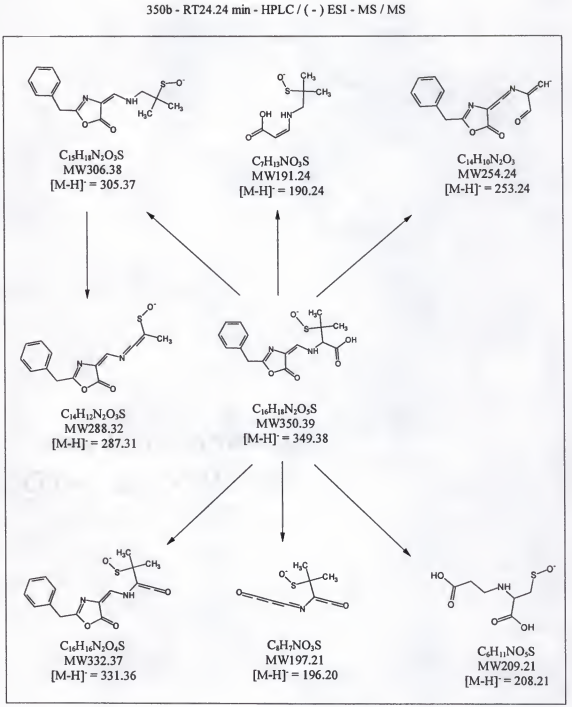

Figure B-16: The interpretation of negative HPLC/ESI-MS/MS of benzylpenicillenic acid sulfoxide.

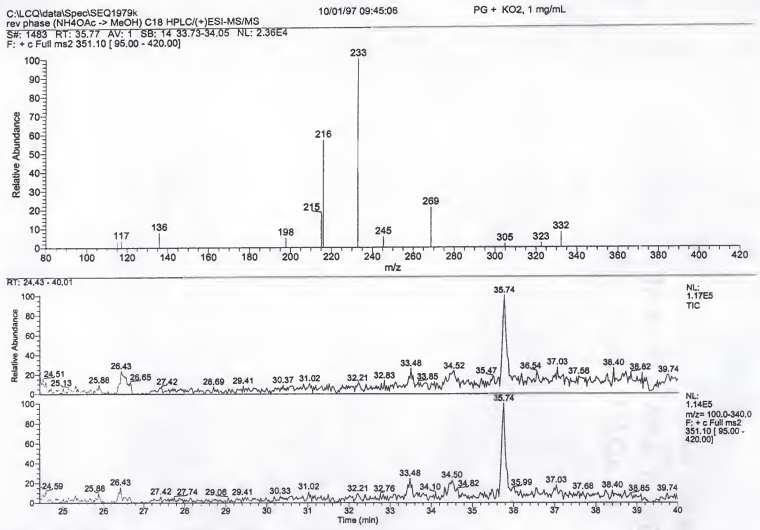

Figure B-17: The positive HPLC/ESI-MS/MS of penicillin G sulfoxide.

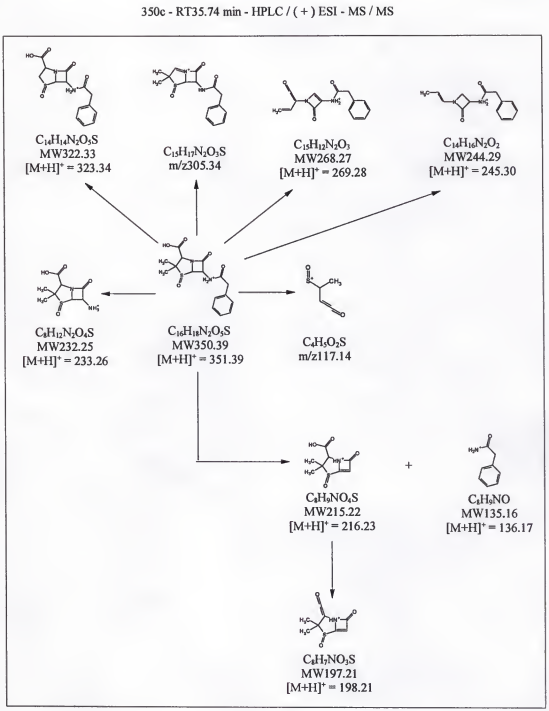

Figure B-18: The interpretation of the positive HPLC/ESI-MS/MS of penicillin G sulfoxide.

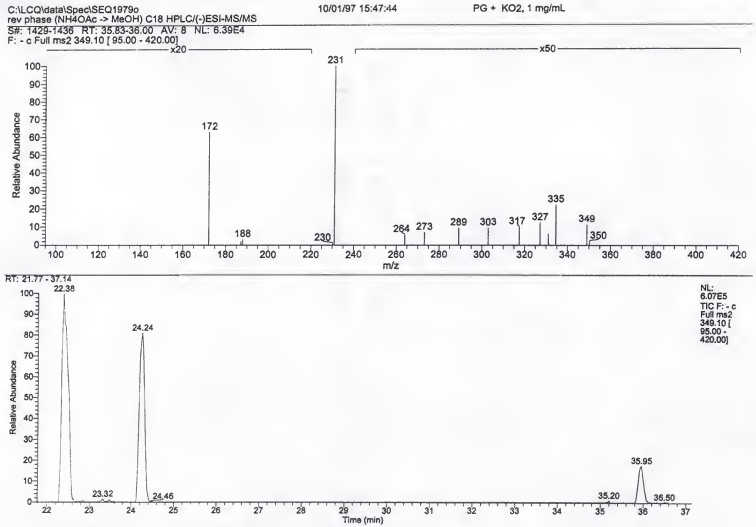

Figure B-19: The negative HPLC/ESI-MS/MS of penicillin G sulfoxide.

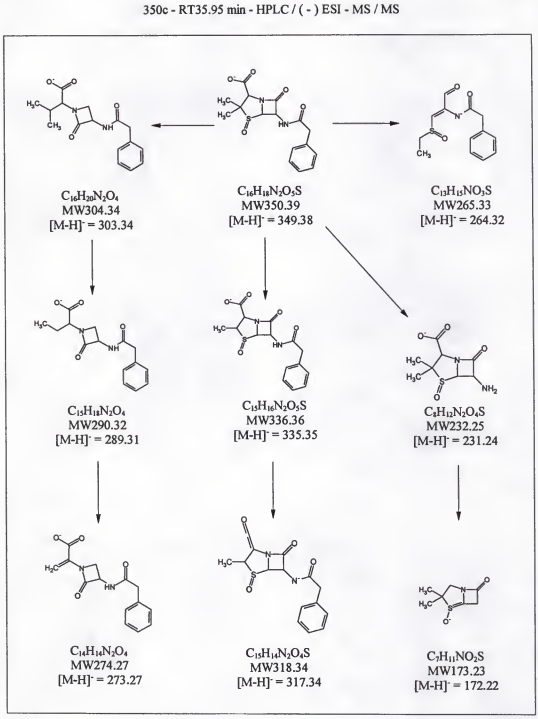

Figure B-20: The interpretation of the negative HPLC/ESI-MS/MS of penicillin G sulfoxide.

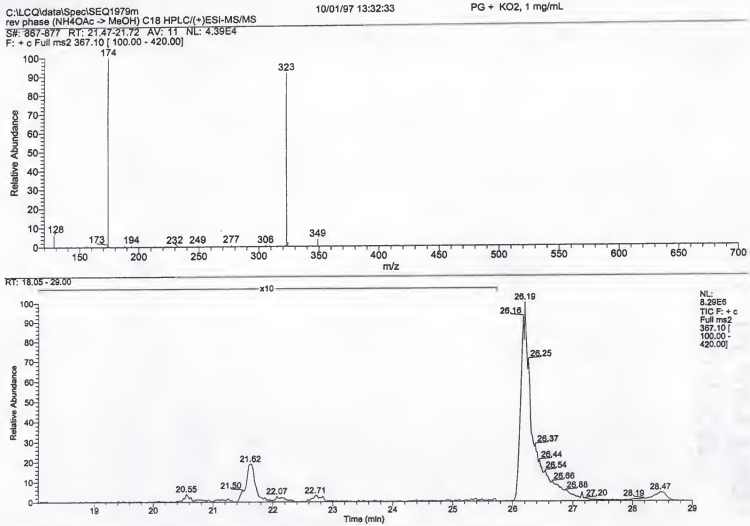
C:\LCQ\data\Spec\SEQ1979m
rev phase (NH4OAc -> MeOH) C18 HPLC/(+)ESI-MS/MS
SM: 367.0/77 RT: 21.47-21.72 AV: 11 NL: 4.39E4
F: + c Full ms2 367.10 [100.00 - 420.00]
10/01/97 13:32:33
PG + KO2, 1 mg/mL
Relative Abundance
m/z
RT: 18.05 - 29.00
x10
Time (min)
NL: 8.29E6 TIC F: + c Full ms2 367.10 [100.00 - 420.00]

Figure B-21: The positive HPLC/ESI-MS/MS of compound 366a-penicillin G sulfone.

366a - RT21.62 min / HPLC - (+) ESI - MS/MS

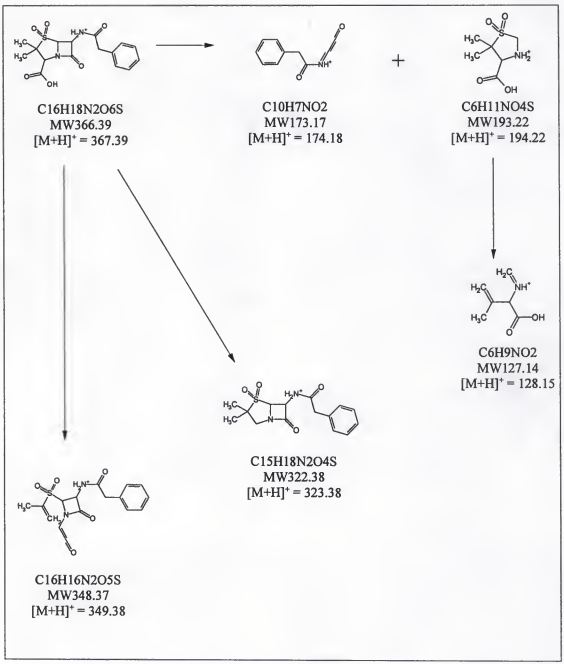

Figure B-22: The interpretation of the positive HPLC/ESI-MS/MS of compound 366a-penicillin G sulfone.

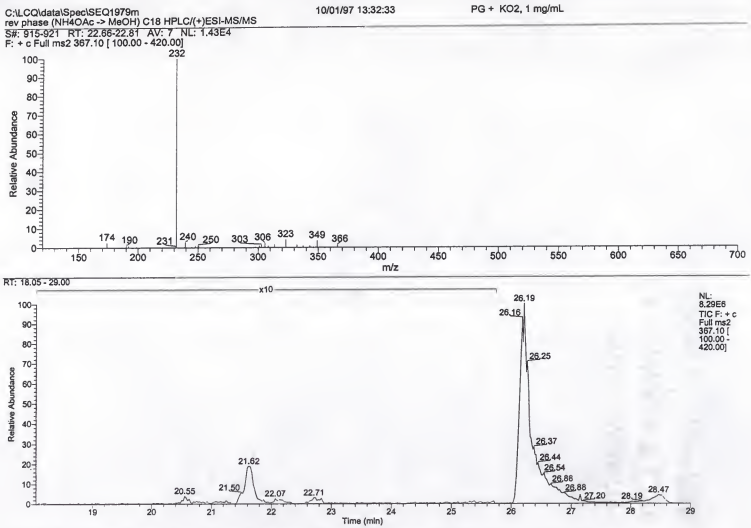

Figure B-23: The positive HPLC/ESI-MS/MS of compound 366b-isomer of penicillin G sulfone.

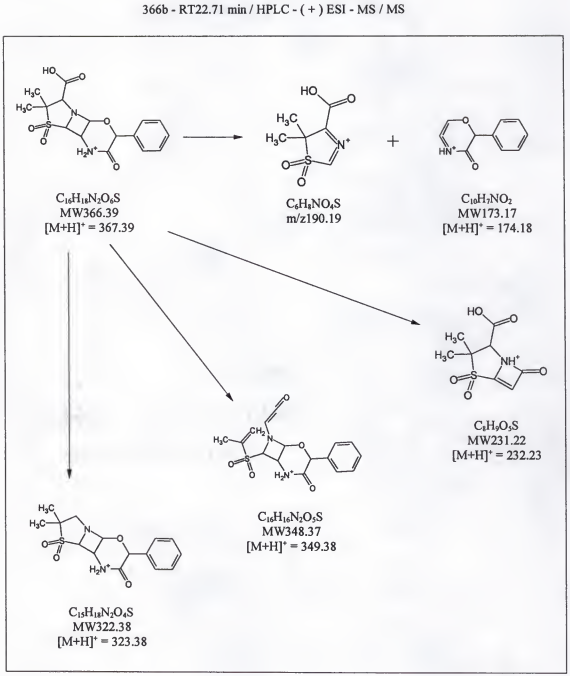

Figure B-24: The interpretation of the positive HPLC/ESI-MS/MS of compound 366b-isomer of penicillin G sulfone.

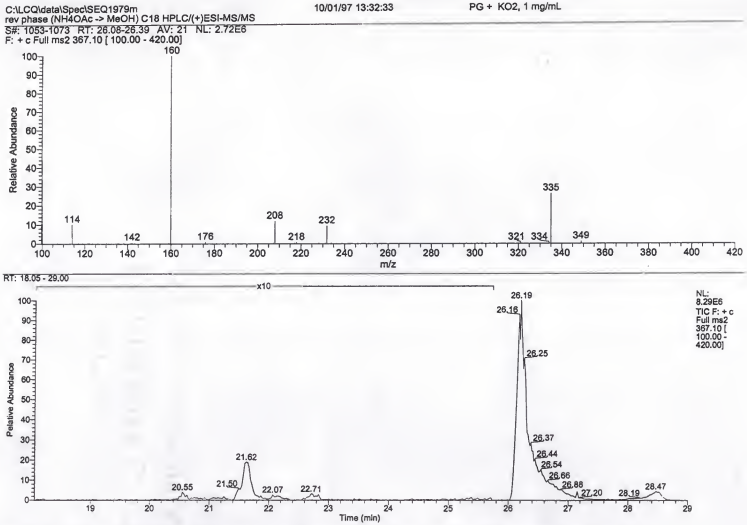

Figure B-25: The positive HPLC/ESI-MS/MS of compound 366c-isomer of penicillin G sulfone.

366c - RT26.19 min / HPLC - (+) - ESI - MS / MS

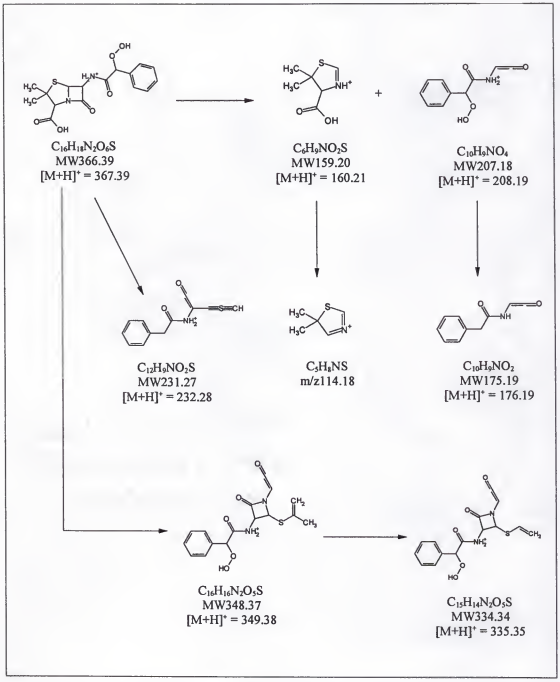

Figure B-26: The interpretation of the positive HPLC/ESI-MS/MS of compound 366c-isomer of penicillin G sulfone.

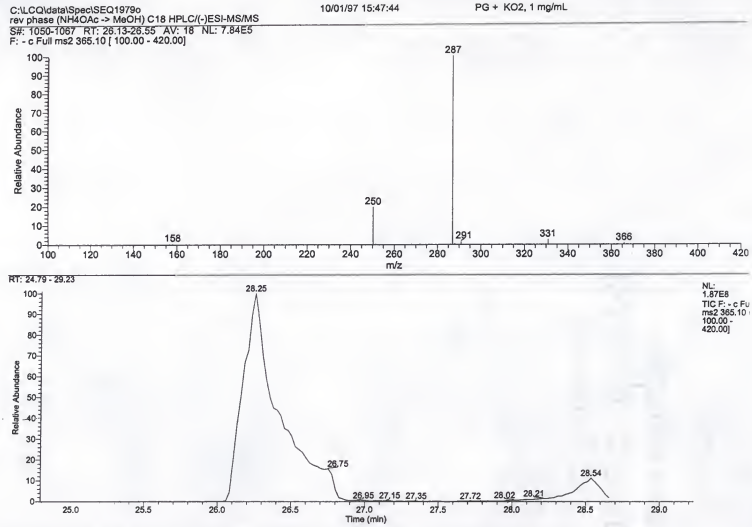

Figure B-27: The negative HPLC/ESI-MS/MS of compound 366c-isomer of penicillin G sulfone.

366c - RT26.25 min / HPLC - (-) ESI - MS / MS

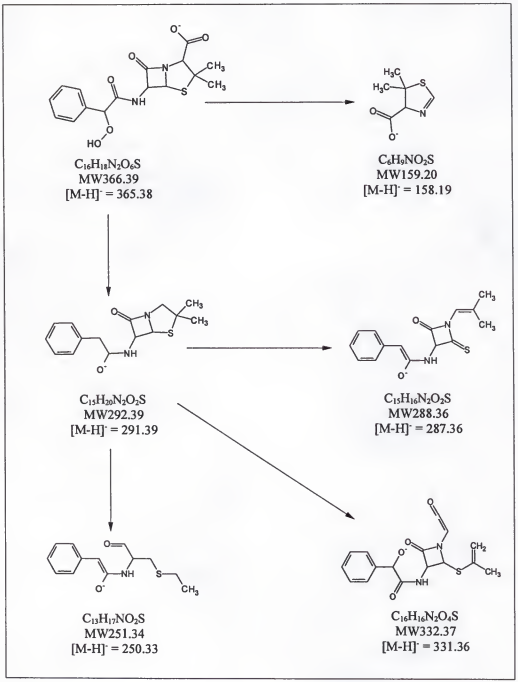

Figure B-28: The interpretation of the negative HPLC/ESI-MS/MS of compound 366c-isomer of penicillin G sulfone.

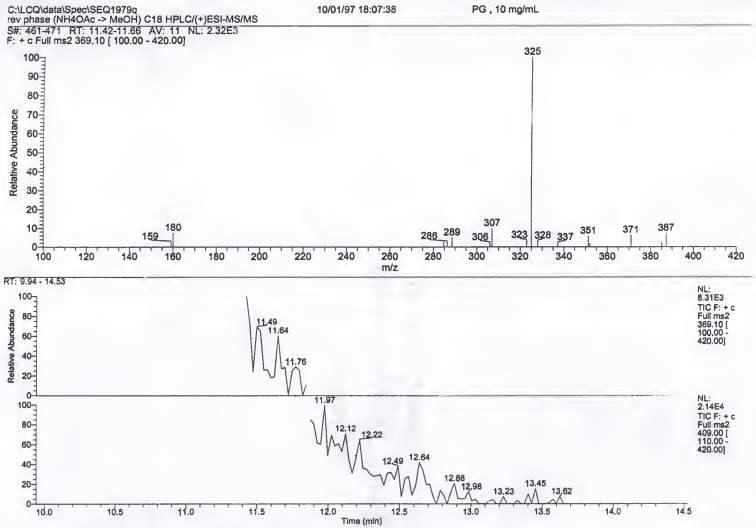
C:\LCQ\data\Spec\SEQ1979c
10/01/97 18:07:38
PG , 10 mg/mL
rev phase (NH4OAc -> MeOH) C18 HPLC/(+)ESI-MS/MS
S#: 461-471 RT: 11.42-11.66 AV: 11 NL: 2.32E3
F: + c Full ms2 369.10 [100.00 - 420.00]
Relative Abundance
m/z
RT: 9.94 - 14.53
NL: 8.31E3 TIC F: + c Full ms2 369.10 [100.00 - 420.00]
NL: 2.14E4 TIC F: + c Full ms2 409.00 [110.00 - 420.00]
Time (min)

Figure B-29: The positive HPLC/ESI-MS/MS of benzylpenicilloic acid sulfoxide.

368 - RT11.64 min - HPLC / (+) ESI - MS / MS

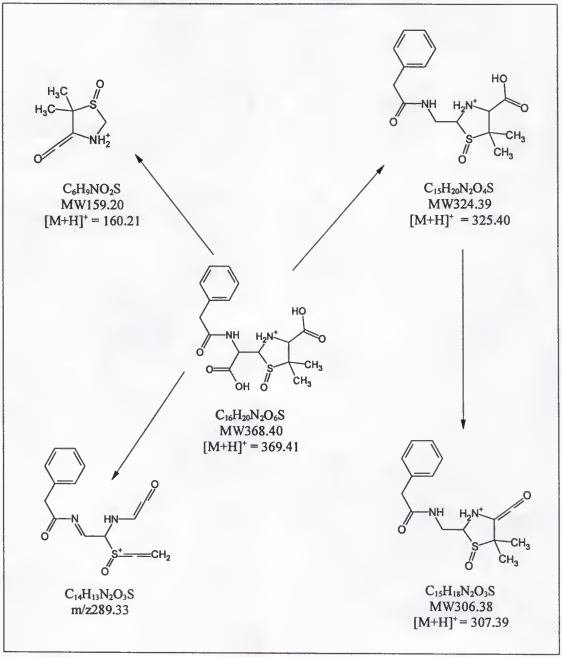

Figure B-30: The interpretation of the positive HPLC/ESI-MS/MS of benzylpenicilloic acid sulfoxide.

APPENDIX C

THE PRODUCTS OF RECOMBINATION REACTIONS OF PENICILLIN G FOLLOWING THE INTERACTION WITH POTASSIUM SUPEROXIDE – THE CHROMATOGRAMS AND MASS SPECTRA OF HPLC/ESI-MS/MS.

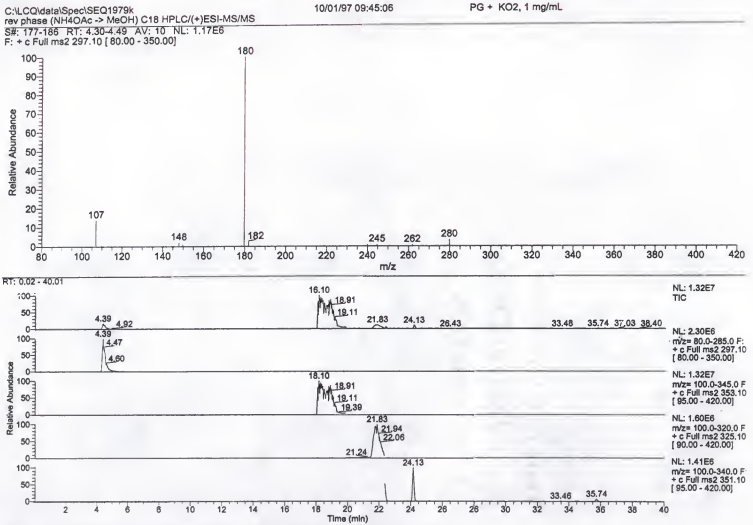

Figure C-1: The positive HPLC/ESI-MS/MS of penicillamine dimer.

296 - RT4.39 min - HPLC / (+) ESI - MS / MS

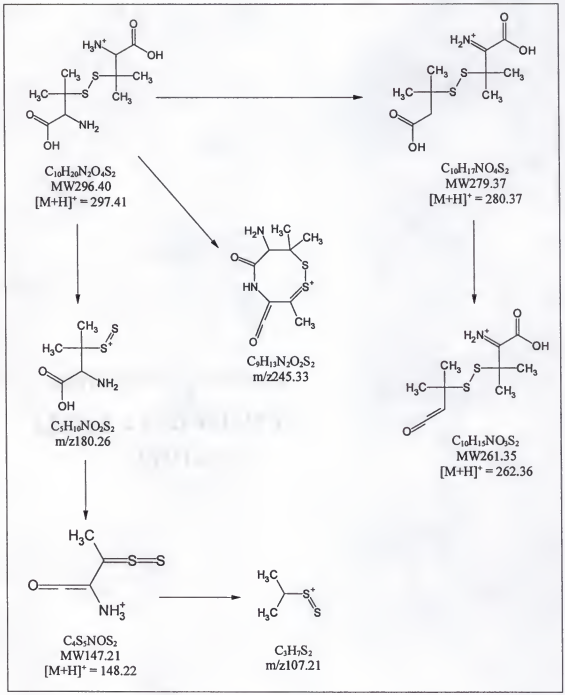

Figure C-2: The interpretation of the positive HPLC/ESI-MS/MS of penicillamine dimer.

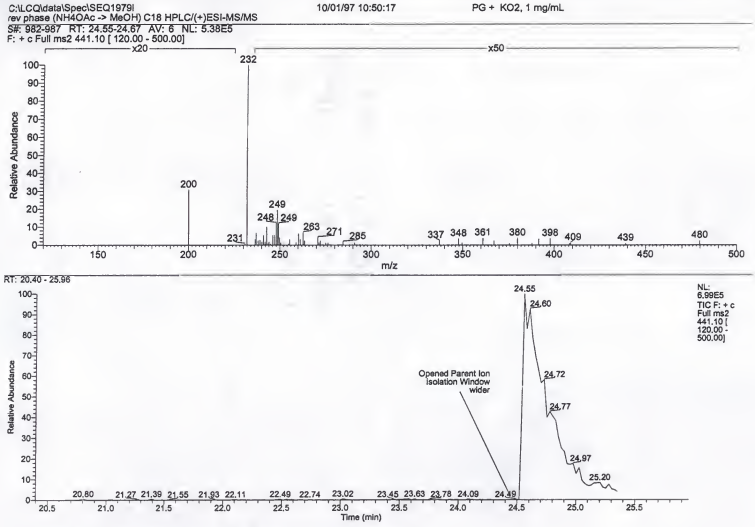
C:\LCQ\data\Spec\SEQ1979I
rev phase (NH4OAc -> MeOH) C18 HPLC/(+)ESI-MS/MS
SR: 982-987 RT: 24.55-24.87 AV: 6 NL: 5.38E5
F: + c Full ms2 441.10 [120.00 - 500.00]
10/01/97 10:50:17
PG + KO2, 1 mg/mL
x20
x50
Relative Abundance
m/z
RT: 20.40 - 25.96
Opened Parent Ion Isolation Window wider
NL: 6.98E5 TIC F: + c Full ms2 441.10 [120.00 - 500.00]
Time (min)

Figure C-3: The positive HPLC/ESI-MS/MS of compound 440.

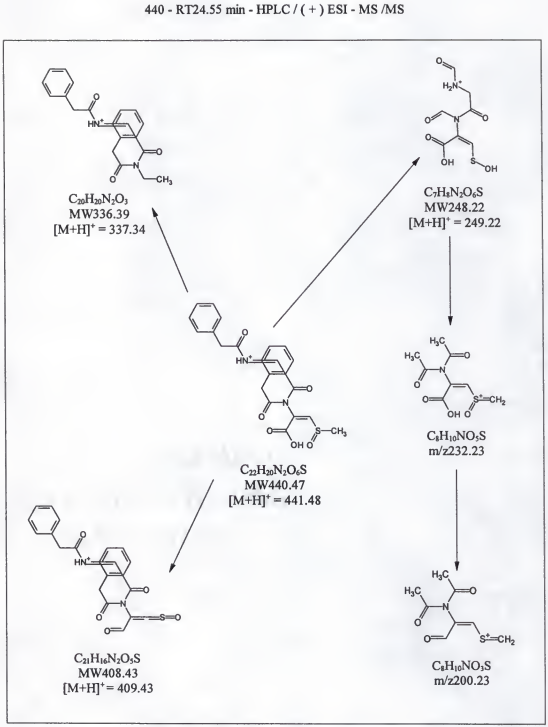

Figure C-4: The interpretation of the positive HPLC/ESI-MS/MS of compound 440.

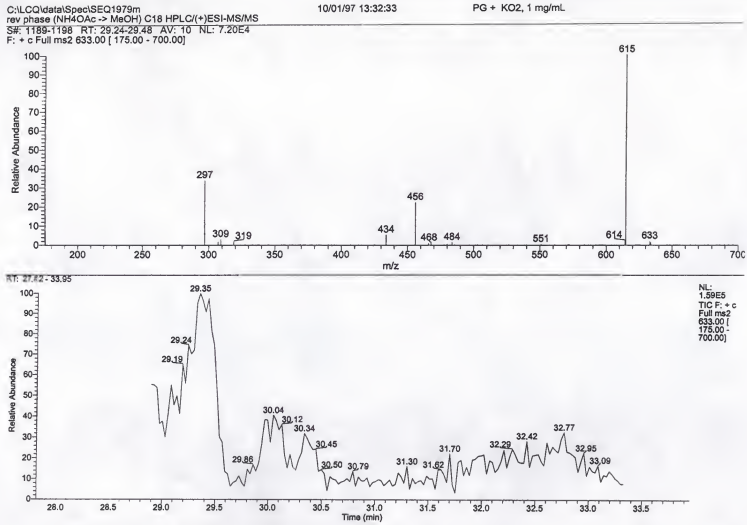

Figure C-5: The positive HPLC/ESI-MS/MS of compound 632.

632 - RT29.35 min - HPLC / (+) ESI - MS / MS

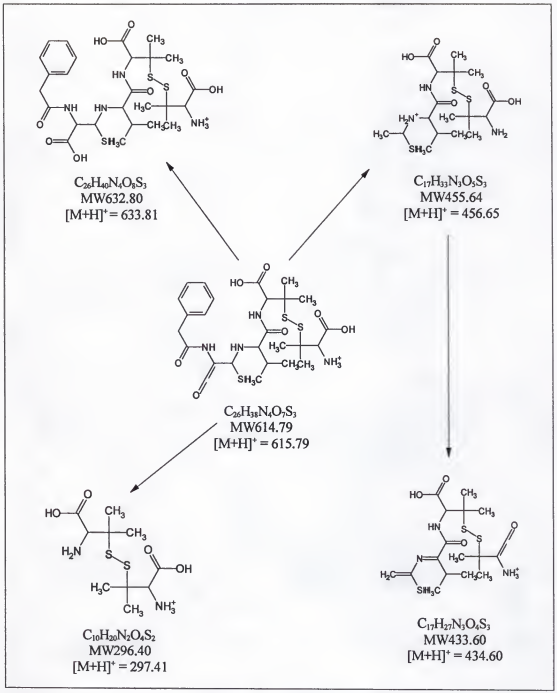

Figure C-6: The interpretation of the positive HPLC/ESI-MS/MS of compound 632.

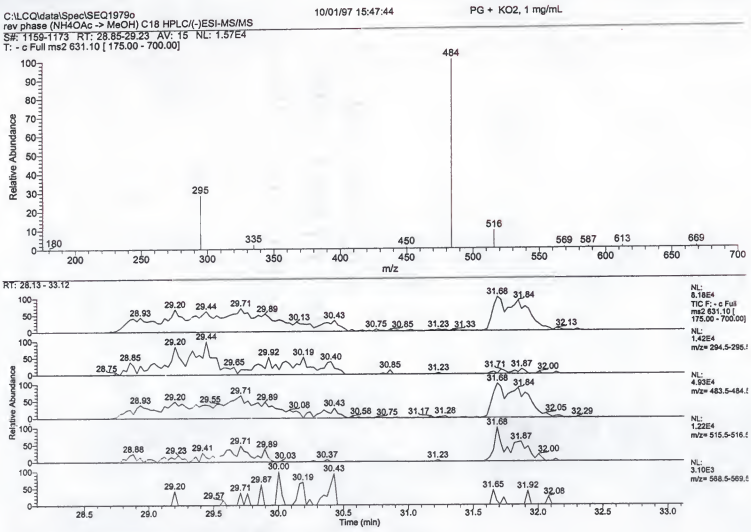
C:\LCQ\data\Spec\SEQ1979o
10/01/97 15:47:44
PG + KO2, 1 mg/mL
rev phase (NH4OAc -> MeOH) C18 HPLC/(-)ESI-MS/MS
S#: 1159-1173 RT: 28.85-29.23 AV: 15 NL: 1.57E4
T: - c Full ms2 631.10 [175.00 - 700.00]
Relative Abundance
m/z
RT: 28.13 - 33.12
Relative Abundance
Time (min)
NL: 8.18E4 TIC F: - c Full ms2 631.10 [175.00 - 700.00]
NL: 1.42E4 m/z= 294.5-295.5
NL: 4.93E4 m/z= 483.5-484.5
NL: 1.22E4 m/z= 515.5-516.5
NL: 3.10E3 m/z= 568.5-569.5

Figure C-7: The negative HPLC/ESI-MS/MS of compound 632.

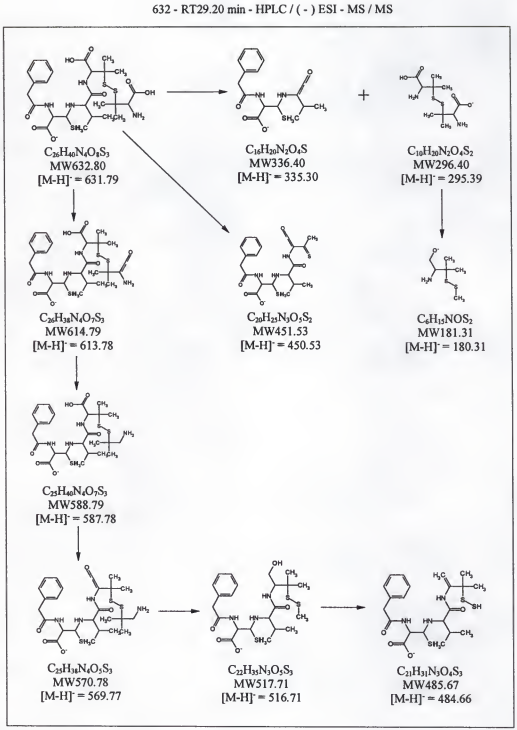

Figure C-8: The interpretation of the negative HPLC/ESI-MS/MS of compound 632.

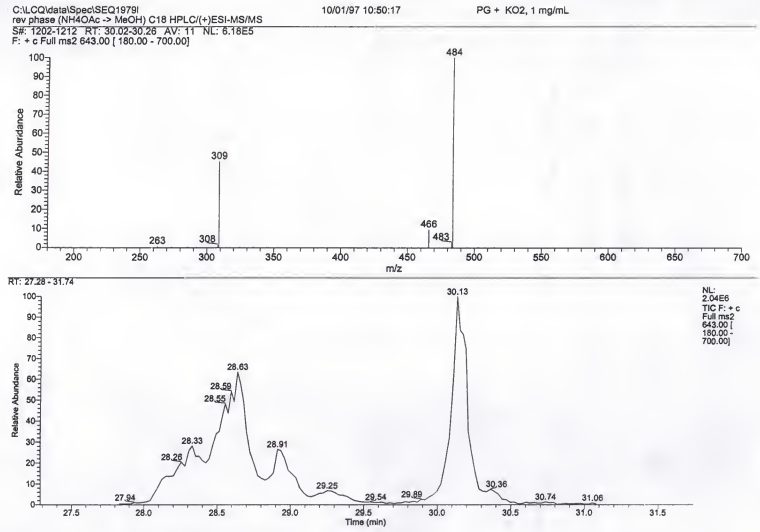

Figure C-9: The positive HPLC/ESI-MS/MS of compound 642.

642 - RT30.13 min - HPLC / (+) ESI - MS / MS

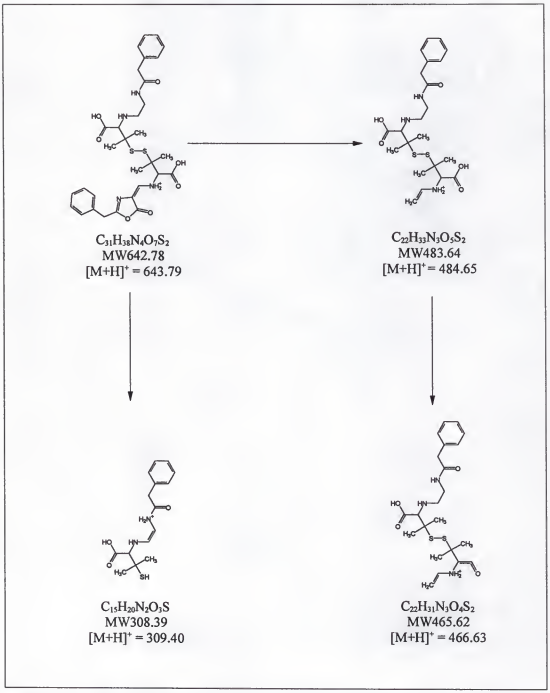

Figure C-10: The interpretation of the positive HPLC/ESI-MS/MS of compound 642.

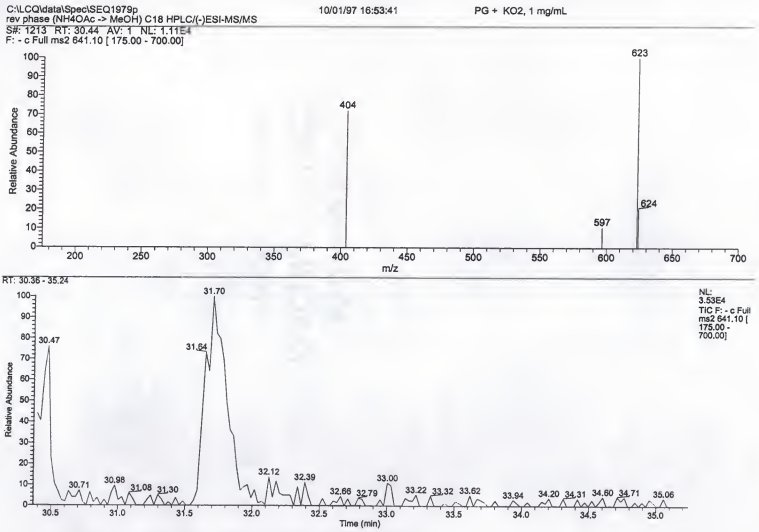

Figure C-11: The negative HPLC/ESI-MS/MS of compound 642.

642 - RT30.44 min - HPLC / (-) ESI - MS / MS

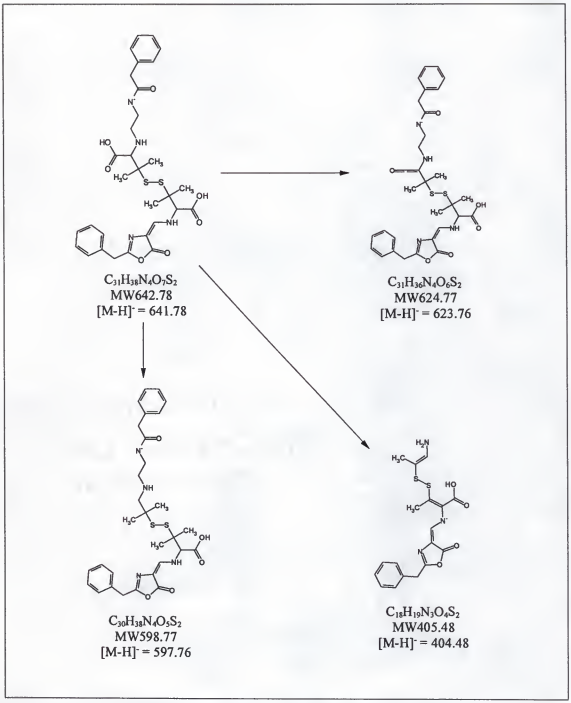

Figure C-12: The interpretation of the negative HPLC/ESI-MS/MS of compound 642.

APPENDIX D
THE PRODUCTS OF CHEMILUMINESCENT REACTION OF PENICILLIN G FOLLOWING THE INTERACTION WITH POTASSIUM SUPEROXIDE – THE CHROMATOGRAMS AND MASS SPECTRA OF HPLC/ESI (OR APCI)-MS/MS.

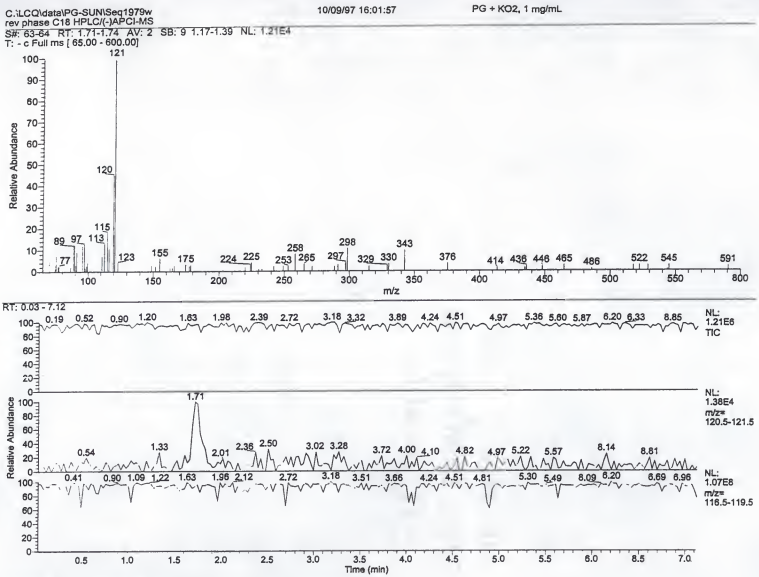
C:\LCQ\data\PG-SUN\Seq1979w
rev phase C18 HPLC/(-)APCI-MS
S#: 63-64 RT: 1.71-1.74 AV: 2 SB: 9 1.17-1.39 NL: 1.21E4
T: - c Full ms [65.00 - 600.00]
10/09/97 16:01:57
PG + KO2, 1 mg/mL
Relative Abundance
m/z
RT: 0.03 - 7.12
NL: 1.21E6 TIC
NL: 1.38E4 m/z= 120.5-121.5
NL: 1.07E6 m/z= 116.5-119.5
Time (min)

Figure D-1: The negative HPLC/APCI-MS of benzoic acid.

122 - RT1.71 min - HPLC / (-) APCI - MS

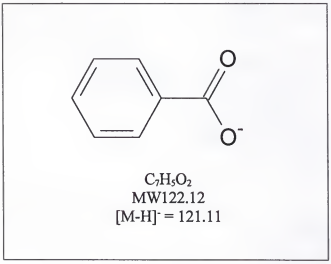

Figure D-2: The interpretation of the negative HPLC/APCI-MS of benzoic acid.

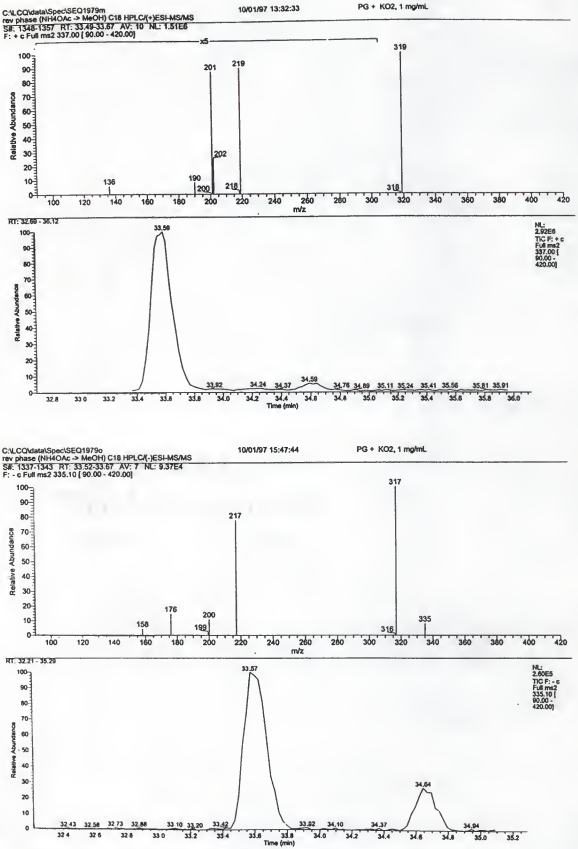

Figure D-3: The positive and negative HPLC/ESI-MS/MS of compound 336.

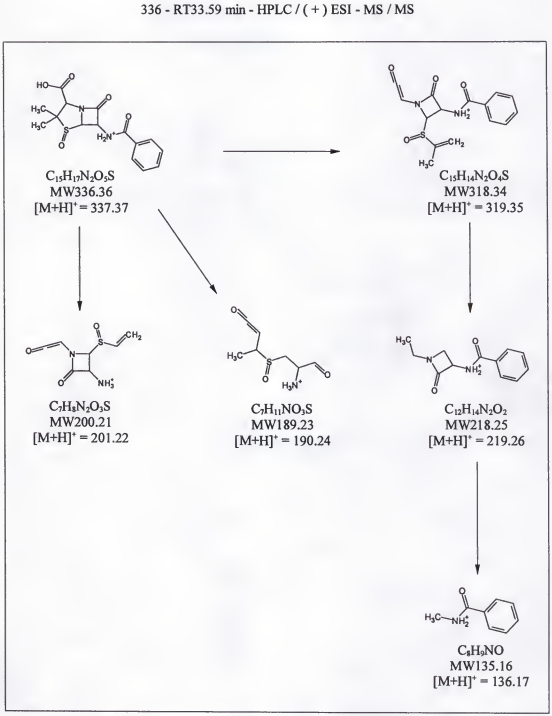

Figure D-4: The interpretation of the positive HPLC/ESI-MS/MS of compound 336.

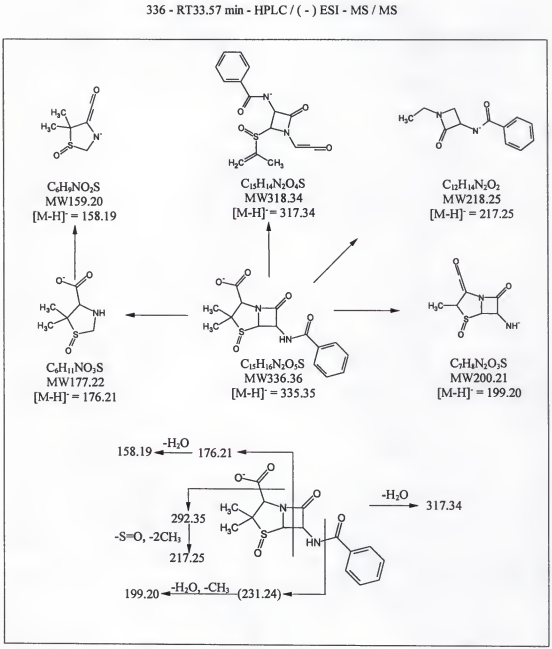

Figure D-5: The interpretation of the negative HPLC/ESI-MS/MS of compound 336.

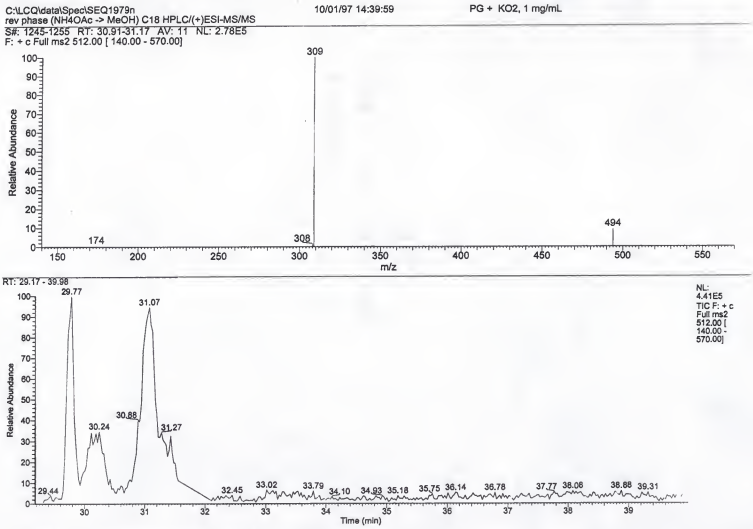

Figure D-6: The positive HPLC/ESI-MS/MS of compound 512.

511 - RT31.07 min - HPLC / (+) ESI - MS / MS

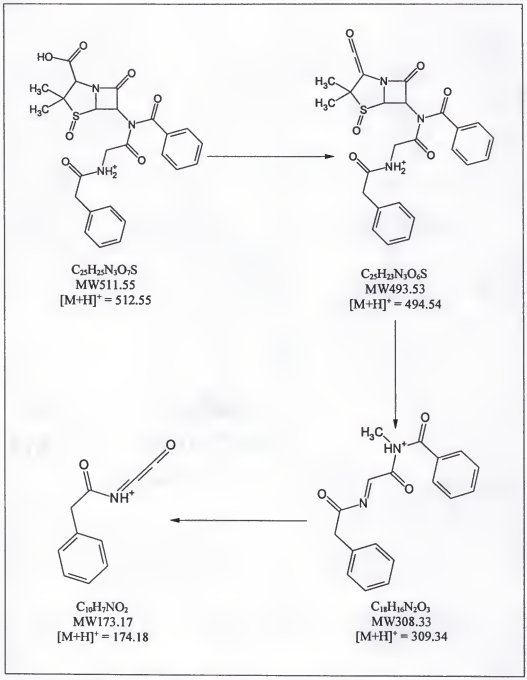

Figure D-7: The interpretation of the positive HPLC/ESI-MS/MS of compound 511.

APPENDIX E
THE PRODUCTS OF UNKNOWN REACTIONS OF PENICILLIN G FOLLOWING THE INTERACTION WITH POTASSIUM SUPEROXIDE – THE CHROMATOGRAMS AND MASS SPECTRA OF HPLC/ESI-MS/MS.

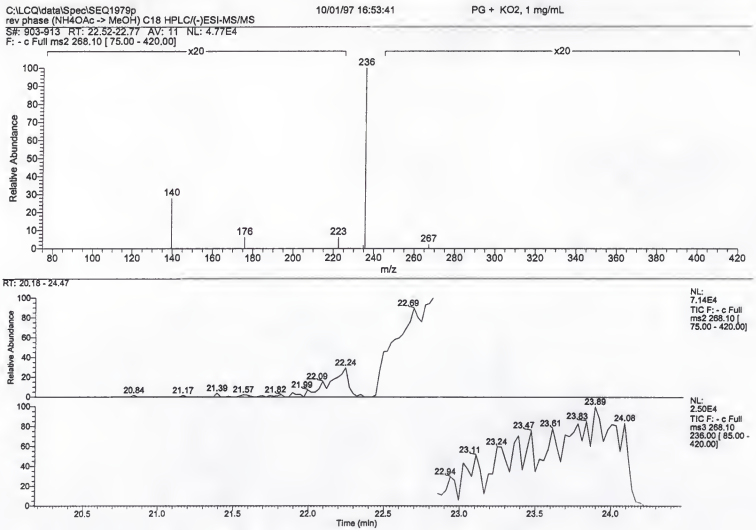

Figure E-1: The negative HPLC/ESI-MS/MS of compound 269.

269 - RT22.69 min. - HPLC / (-) ESI - MS / MS

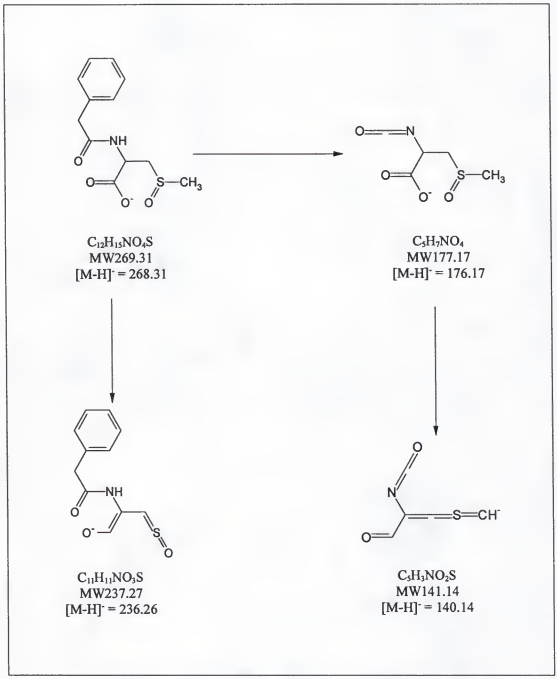

Figure E-2: The interpretation of the negative HPLC/ESI-MS/MS of compound 269.

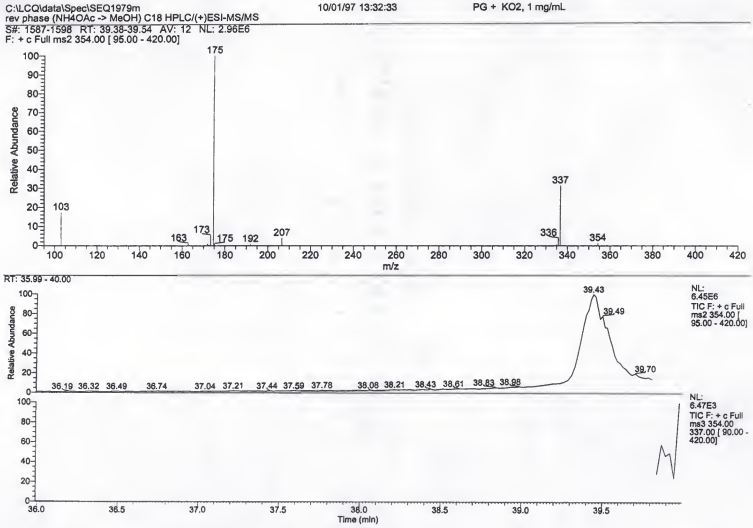
C:\LCQ\data\Spec\SEQ1979m
10/01/97 13:32:33
PG + KO2, 1 mg/mL
rev phase (NH4OAc -> MeOH) C18 HPLC/(+)ESI-MS/MS
S#: 1587-1598 RT: 39.38-39.54 AV: 12 NL: 2.96E6
F: + c Full ms2 354.00 [95.00 - 420.00]
Relative Abundance
m/z
RT: 35.99 - 40.00
NL: 6.45E6 TIC F: + c Full ms2 354.00 [95.00 - 420.00]
NL: 6.47E3 TIC F: + c Full ms3 354.00 337.00 [90.00 - 420.00]
Time (min)

Figure E-3: The positive HPLC/ESI-MS/MS of compound 353.

353 - RT39.43 / HPLC - (+) ESI - MS /MS

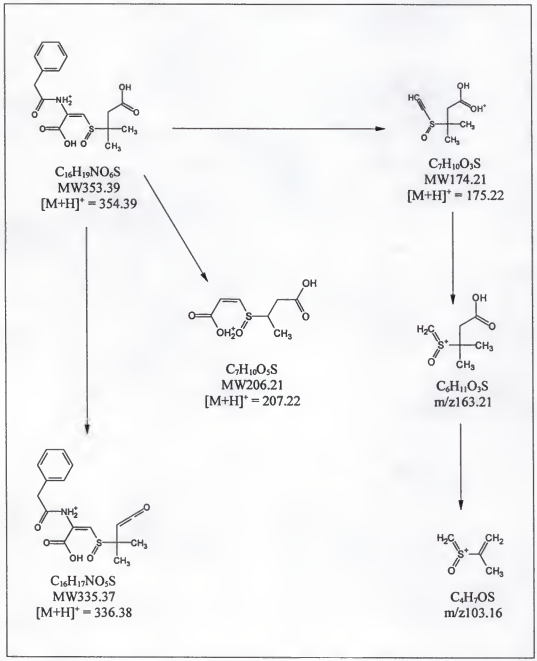

Figure E-4: The interpretation of the positive HPLC/ESI-MS/MS of compound 353.

REFRENCES

1. Childe, W. H. J. and Mecke, R. Z. Physik 68: 344 (1931).

2. Herzberg, G. Nature, Lond. 133: 759 (1934).

3. Straight, R. C. and Spikes, J. D. In Singlet O_2 Chapter 3, CRC Press, Boca Raton, FL (1985).

4. Ashford, R. D. and Ogryzlo, E. A. J. Amer. Chem. Soc. 97: 3604 (1975).

5. Bartlett, P. D. and Schaap, A. P. J. Amer. Chem. Soc. 92: 3223 (1970).

6. Mazur, S. and Foote, C. S. J. Amer. Chem. Soc. 92: 3225 (1970).

7. Kearns, D. R. J. Amer. Chem. Soc. 91: 6554 (1969).

8. Fridovich, I. Annu. Rev. Biochem. 44: 147-159 (1975).

9. Fridovich, I. Science 201: 875-880 (1978).

10. Halliwell, B. In Age Pigments pp1-62, Elsevier/North-Holland, Amsterda (1981).

11. Frimer, A. A. In Superoxide Dismutase vol.2, pp 83-125, CRC press, Boca Raton, FL (1982).

12. Sawyer, D.T. and Valentine, J. S. Acc. Chem. Res. 14: 393-400 (1981).

13. Corey, E. J. and Mehrotra, M. M., Khan A. U. Biochemical and Biophysical Research Communication 145: 842-846 (1987).

14. Halliwell, B. In Chloroplast Metabolism: the Structure and Function of Chloroplasts in Green Leaf Cells Oxford University Press, Oxford (1981).

15. Fridovich, I. Annu. Rev. Pharmacol. Toxicol. 23: 239-257 (1983).

16. Halliwell, B. and Gutteridge, J. H. C. Biochem. J. 219: 1-14 (1984).

17. Gartuer, A. and Weser, U. Top. Curr. Chem. 132: 1-61 (1986).

18. Diguiseppi, J. and Fridovich, I. J. Biol. Chem. 257: 4046-4051 (1982).

19. Khan, A. U. and Kasha, M. Proc. Natl. Acad. Sci. USA 92: 12365 – 12367 (1994).

20. Kallogg, E. W. and Fridovich, I. J. Biol. Chem. 252: 6721 – 6728 (1977).

21. Greenward, R. A. and Moy, W.W. Arthritis Rheum. 23: 445 – 463 (1980).

22. Lunec, J., Halloran, S. P., White, A. G., Dormandy, T. L. J. Rheumatol. 8: 233-245 (1981).

23. Snider, G. L. Am. Rer. Respir. Dis. 124: 321-324 (1981).

24. Church, D. F. and Pryor, W.A. Environ. Health Perspect. 64: 111 – 126 (1985).

25. Pryor, W. A. and Dooley, M. M. Am. Rev. Respir. Dis. 131: 941-943 (1985).

26. Weisiger, R. A. Gastroenterology 90: 494-496 (1986).

27. Parks, D. A., Bulkley, G. B., Granger, D. N. Surgery 94: 428-432 (1983).

28. Granger, D. N., Rutili, G., McCord, J. M. Gastroenterology 81: 22 – 29 (1981).

29. McCord, J. M. and Roy, R. S. Can. J. Physiol. Pharmacol. 60: 1346-1352 (1982).

30. Cerutti, P. A. Science 227: 375 – 381 (1985).

31. Zimmerman, R. and Cerutti, P. Proc. Natl. Acad. Sci. USA 81: 2085-2087 (1984).

32. Weitzman, S. A. and Stossel, T. P. J. Immunol. 128: 2770-2087 (1982).

33. Harman, D. J. Gerontol. 11: 298-300 (1956).

34. Kalous, M. and Drahota, Z. Physiol. Res. 45 (5): 351 – 359 (1996).

35. Ames, B. N. Prog. Clin. Biol. Res. 206: 3-32 (1986).

36. Shohal, R. S. In Age pigments pp 303-316, Amsterdam, Elsevier/North-Holland Biomedical Press (1981).

37. Tolmasoff, J. M.; Ono, T.; Cutler, R. G. Proc. Natl. Acad. Sci. USA 77: 2777-2781 (1980).

38. Blackett, A. D. and Hall, D. A. Age Aging 10: 191-195 (1981).

39. Clapp, N. K., Satterfield, L. C., Bowles, N. D. J. Gerontol. 34: 497-501 (1979).

40. Enstrom, J. E. and Pauling, L. Proc. Natl. Acad. Sci. USA 79: 6023-6027 (1982).

41. Knight, J. A. Annals Clinical and Laboratory Science 27 (1): 11-25 (1997).

42. Rosen, D. R., Siddique, T., Patterson, D. Nature 362: 59-62 (1993).

43. Beckman, J. S., Carson, M., Smith, C. D., Koppenol, W. H. Nature 364: 584 (1993).

44. Hensley, K., Carney, J. M., Mattson, M. P., Aksenova, M., Harris, M., Wu, J. F., Floyd, R. A., Butterfield, D. A. Proc. Natl. Acad. Sci. USA 91: 3270-4 (1994).

45. McNamara, J. O., Fridovich, I. Nature 363: 20-1 (1993).

46. Behl, C., Davis, J., Cole, G. M., Schubert, D. Biochem. Biophys. Res. Comm. 186: 944-50 (1992).

47. Jeandel, C., Nicolas, M. B., Dubois, F., Nabet-Belleville, F., Penin, F., Cuny, G. Gerontology 35: 275-82 (1989).

48. Sinet, P. M. Ann. NY Acad. Sci. 396: 83-94 (1982).

49. McCord, J. M. N. Engl. J. Med. 312: 159-63 (1985).

50. Johns, D. R. N. Engl. J. Med. 333: 638-44 (1995).

51. Wallace, D. C. Science 256: 628-32 (1992).

52. LeVine, S. M. Med. Hypotheses 39: 271-4 (1992).

53. Korpela, H., Kinnunen, E., Juntunen, J., Kumpulainen, J., Koskenvuo, M. J. Neurol. Sci. 91: 79-84 (1989).

54. Dexter, D. T., Carter, C. J., Wells, F. R., Javoy-Agid, F., Agid, Y., Lees, A. J. J. Neurochem. 52: 381-9 (1989).

55. Cohen, G. FASEB 130-5 (1988).

56. Halliwell, B. Acta. Neurol Scand. 126: 23-33 (1989).

57. Dexter, D. T., Wells, F. R., Lees, A. J., Agid, F., Agid, Y., Jenner, P., Marsden, C. D. J. Neurochem. 52: 1830-6 (1989).

58. Spina, M. B., Cohen, G. Proc. Natl. Acad. Sci. USA 86: 1398-1400 (1989).

59. Langston, J. W., Ballard, P., Tetrud, J. W., Irwin, I. Science 219: 979-80 (1983).

60. Huber, W. Eur. J. Rheumatol. Inflamm. 4: 173-182 (1981).

61. Goebel, K. M. and Storck, U. Am. J. Med. 74: 124-128 (1983).

62. Goebel, K. M., Storck, U., Neurath, F. Lancet 1: 1015-1017 (1981).

63. Stern, L. Z., Ringel, S. P., Ziter, F. A., Menander-Hber, K. B., Ionasescu, V., Pellegrino, R. J., Snyder, R. D. Arch. Neurol. 39: 342-346 (1982).

64. Greenwald, R. A. J. Free Radic. Biol. Med. 1: 173-177 (1985).

65. Southorn, P. A. and Garth, D. Mayo Clin. Proc. 63: 381-389 (1988).

66. Dormandy, T. L. Proc. R. Soc. Med. 70: 91-93 (1977).

67. Crary, E. J. and McCarty, M. F. Med. Hypotheses 13: 77-98 (1984).

68. Hall, E. J. In Radiobiology for the Radiologist Hagerstown, Maryland, Harper & Row Publishers (1973).

69. Powis, G. In Metabolism and Action of Anti-Cancer Drugs pp 211-260, London, Taylor and Francis (1987).

70. Lazo, J. S., Sebi, S. M., Filderman, A. E. In Metabolism and Action of Anti-Cancer Drugs pp 194-210, London, Taylor and Francis (1987).

71. Cunningham, M. L., Ringrose, P. S., Lokesh, B. R. Cancer Lett. 21: 149-153 (1983).

72. Abraham. E. P. In Beta-Lactam Antibiotics pp 3-11, Japan Scientific Societies Press, Tokyo, Springer-Verlag, Berlin Heidelberg New York (1981).

73. Sheehan, J. C. In β-Lactam Antibiotic-Mode of Action, New Developments, and Future Prospects pp 5-12, Academic Press (1981).

74. Noguchi, H. and Mitsuhashi, S. In Beta-Lactam Antibiotics pp 59-81, Japan Scientific Societies Press, Tokyo, Springer-Verlag, Berlin Heidelberg New York (1981).

75. Kirschbaum, J. In Analytical Profiles of Drug Substances vol. 15, pp 427-507 (1986).

76. Schulman, S. G., Perrin, J. H., Yan, G. F., Chen, S. Analytica Chimica Acta 255: 383-385 (1991).

77. White and Roswell. In Chemiluminescence and Bioluminescence p 215, Marcel Dekker, New York (1985).

78. Glinski, R. J. J. Am. Chem. Soc. 108: 531 (1986).

79. Sutton, D. G., Westberg, K. R., Melzer, J. E. Anal. Chem. 51: 1399 (1979).

80. Glinski, R. J., Mishalanie, E. A., Birks, J. W. J. Photochem. 37: 217-231 (1987).

81. Finlayson, B. J., Pitts, J. N., and Atkinson, R. J. Am.Chem.Soc. 96: 5356 (1974).

82. Toby, S. Chem. Rev. 84: 277-285. (1984).

83. Getty, R. H. and Birks, J. W. Anal. Lett. 12(5A): 469-476 (1979).

84. Totter, J. R. Photochem. Photobiol. 22: 203-211 (1975).

85. Gough, T. A., Webb, K. S. and Eaton, R. F. J. Chromatogr. 137: 293 (1977).

86. Greaves, J. C. and Gavin, D. J. Chem. Physics. 30: 348-9 (1959).

87. Seitz, W. R. Crc Crit. Rev. Anal. Chem. 13: 1 (1981).

88. Rubinstein, I., Martin, C. R., Bard, A. J. Anal. Chem. 55: 1580 (1983).

89. Spurlin, S. R. and Yeung, E. S. Anal. Chem. 54: 318 (1982).

90. Glinski, R. J. and Taylor, C. D. Chem. Phys. Lett. 155: 511-2 (1989).

91. Kenner and Ogryzlo. In Chemiluminescence and Bioluminescence P 139, Marcel Dekker, New York (1985).

92. Garcia Campana, A. M., Baeyens, W. R. G., and Zhao, Y. Analytical Chemistry News & Features February 1 (1997).

93. Mao, J., Zang, L., and Shi, X. Biochem. Mol. Biol. Int. 36: 227-32 (1995).

94. Khan, A. U. and Kasha, M. J. Am. Chem. Soc. 92: 3239-3300 (1970).

95. Khan, A.U. J. Phys. Chem. 80: 2219-2228 (1976).

96. Khan, A. U. and Kasha, M. J. Am. Chem. Soc. 103: 6516-6517 (1981).

97. Corey, E. J., Mehrotra, M. M., and Khan, A. U. Biochem. Biophys. Res. Commun. 145: 842-846 (1987).

98. Nilsson, R. and Kearns, D. R. J. Phys. Chem. 78: 1681-1683 (1974).

99. Kukreja, R. C. and Hess, M. L. Cardiovas. Res. 26: 641-655 (1992).

100. Chen, S., Yan, G., Schwartz, M. A., Perrin, J. P., and Schulman, S. G. J. Pharm. Sci. 80: 1017 (1991).

101. Nakashima, K., Kawaguchi, S., Akiyama, S., and Shulman, S. G. Biomed. Chromatogr. 7: 217 (1993).

102. Vidon, D. J., Andre, P., Baaj, D., Gryczka, C., and Philipp, P. FEMS Microbiol. Lett. 120: 225 (1994).

103. Brodersen, R. Trans. Faraday Soc. 43: 351 (1947).

104. Stuff, J., Schmidkunz, H., and Hartmann, G. Nature (London) 198: 281-282 (1963).

105. Sander, U., and Stauff, J. An. Asoc. Quim. Argent. 59: 149-155 (1971).

106. Koppwnol, W.H. Nature (London) 262: 420-421 (1976).

107. Halliwell, B. and Gutteridge, J. M. C. Meth. Enzymol. 186: 1-85 (1990).

108. Halliwell, B. and Gutteridge, J. M. C. Arch. Biochem. Biophysics. 200: 1-8 (1990).

109. Halliwell, B. and Gutteridge, J. M. C. FEBS Lett. 300: 108-112 (1992).

110. Burkitt, M. J. Free Radical Res. Commun. 18: 43-57 (1993). Halliwell, B. and Gutteridge, J. M. C. Meth. Enzymol. 186: 1-85 (1990).

111. Wilson, W. L., Avdovich, H. W., and Huges, D.W. J. Off. Agr. Chem. 57: 1300 (1974).

112. Fossey, J., Lefort, D., and Sorba, J. In Free Radicals in Organic Chemistry pp 166-180, John Wiley & Sons, New York (1995).

113. Chang, C. J. and Hem, S. J. Pharm. Sci. 68: 64-69 (1979).

114. Vandamme, E. J. and Voets, J. P. J. Chromatogr. 71: 141 (1972).

115. Lin, S-Y. and Kondo, F. Microbios 77: 223-229 (1994).

116. Fossey, J., Lefort, D., and Sorba, J. In Free Radicals in Organic Chemistry pp 185, John Wiley & Sons, New York (1995).

117. Vadino, W. A., Sugita, E. T., Schnaare, R. L., Ando, N. Y., Niebergall, P. J. J. Pharm. Sci. 68: 1316-1318 (1979).

118. Yamashita, M., Fenn, J. B. J. Phys. Chem. 88: 4451 (1984).

119. Yamashita, M., Fenn, J. B. J. Phys. Chem. 88: 4671 (1984).

120. Aleksandrov, M. L., Gall, L. N., Krasnov, V. N., Nikolaev, V. I., Pavlenko, V. A., Shkurov, V. A. Dokl. Akad. Nauk. SSSR 227: 379 (1984).

121. Dole, M., Mack, L. L., Hines, R. L., Mobley, R. C., Ferguson, L. D., Alice, M. B. J. Chem. Phys. 49: 2240 (1968).

122. Kebarle, P. and Ho, Y. In Electrospray Ionization Mass Spectrometry, Fundamentals, Instrumentation & Applications, pp 6, edited by Cole, R. B., John Wiley & Sons, INC., New York, Chichester, Weinheim, Rrisbane, Singapore, Toronto (1997).

123. Kebarle, P. and Tang, L. Anal. Chem. 65: 972A (1993).

124. Kessler, D. P., Ghebre-Sellassie, I., Knevel, A. M., and Lem, S. L. J. Chem. Soc., Perkin Trans II 1247 (1981).

125. March, J. In Advanced Organic Chemistry pp 1199-1205, John Willey & Sons (1992).

126. Martin, J. C., Frary, J. A., and Arhart, J. R. J. Am. Chem. Soc. 96: 4606 (1974).

127. Bartlett, P. D., Aida, T., Chu, H.-K., and Fang, T.-S. ibid. 102: 3515 (1980).

128. McCapra, F. and Hann, R. A. Chem. Commun. 443 (1969).

129. Lee, K., Singer, L. A., and Legg, K. D. J. Org. Chem. 41: 2685 (1976).

130. Bartlett, P. D. and Schaap, A. P. J. Am. Chem. Soc. 92: 3232, 6055 (1970).

131. Mazur, S. and Foote, C. S. ibid 92: 3225 (1970).

132. Gundermann, K.-D. and McCapra, F. In Chemiluminescence in Organic Chemistry pp 55, Springer-Verlag, Berlin, Heidelberg, New York, London, Paris, Tokyo (1987).

BIOGRAPHICAL SKETCH

Jingshun Sun was born in Jilin, China on October 7, 1967. After finishing his high school in 1986, he went on to undergraduate studies at Fuzhou University. He spent the next seven years of studying and researching in the field of Analytical Chemistry and received a Bachelor and Master of Science degree. Shortly after being employed in Fuzhou as a versatile employee learning about life, he was given the opportunity to join Dr. John H. Perrin's laboratory where he carried out the work described in this dissertation. In August of 1998, he will receive a Ph.D. in Medicinal Chemistry and move on to another challenging hurdle in life.

I certify that I have read this study and that in my opinion it conforms to acceptable standards of scholarly presentation and is fully adequate, in scope and quality, as a dissertation for the degree of Doctor of Philosophy.

John H. Perrin, Chair
Professor of Medicinal Chemistry

I certify that I have read this study and that in my opinion it conforms to acceptable standards of scholarly presentation and is fully adequate, in scope and quality, as a dissertation for the degree of Doctor of Philosophy.

Stephen G. Schulman
Professor of Medicinal Chemistry

I certify that I have read this study and that in my opinion it conforms to acceptable standards of scholarly presentation and is fully adequate, in scope and quality, as a dissertation for the degree of Doctor of Philosophy.

Kenneth B. Sloan
Professor of Medicinal Chemistry

I certify that I have read this study and that in my opinion it conforms to acceptable standards of scholarly presentation and is fully adequate, in scope and quality, as a dissertation for the degree of Doctor of Philosophy.

Ian R. Tebbett
Associate Professor of Medicinal Chemistry

I certify that I have read this study and that in my opinion it conforms to acceptable standards of scholarly presentation and is fully adequate, in scope and quality, as a dissertation for the degree of Doctor of Philosophy.

James D. Winefordner
Graduate Research Professor of
Chemistry

This dissertation was submitted to the Graduate Faculty of the College of Pharmacy and to the Graduate School and was accepted as partial fulfillment of the requirements for the degree of Doctor of Philosophy.

August 1998

Dean, College of Pharmacy

Dean, Graduate School

UNIVERSITY OF FLORIDA
3 1262 08555 3047